Cellular signalling of adrenomedullin regulating
Endothelial barrier function and granulocyte extravasation

Inaugural-Dissertation

zur

Erlangung des Doktorgrades

der Mathematisch-Naturwissenschaftlichen Fakultät

der Universität zu Köln

vorgelegt von

Qian Mao

aus Jinan (V.R.China)

Berichterstatter: Prof. Dr. Angar Büschges

(Gutachter)   Prof. Dr. Stefan Herzig

                        PD. Dr. Ingo Flamme

Tag der mündlichen Prüfung: 19. Oktober. 2012

TABLE OF CONTENTS

LIST OF FIGURES

LIST OF TABLES

ABBREVIATIONS

AC	Adenylate cyclase
ADM	Adrenomedullin
AJ	Adherens junction
ALI	Acute lung injury
AMBP-1	Adrenomedullin binding protein-1
ARDS	Adult respiratory distress syndrome
AUC	Area under the curve
BAL	Bronchoalveolar lavage
bEnd.5	Brain microvascular endothelial cells
BCA	Bicinchoninic acid
BSA	Bovine serum albumin
BW	Body weight
C5a	Complement factor 5a
Ca^{2+}	Calcium
CAFTY	Ca^{2+}-free Tyrode solution
cAMP	Cyclic adenosine monophosphate
cAPK	cAMP-dependent protein kinase
CB	Cytochalasin B
CBD	cAMP-binding domain (CBD)
CCRL	Chemokine C-C motified receptor like
CD	Cytochalasin D
cDNA	Complementary DNA
cGMP	Cyclic guanosine monophosphate
CGRP	Calcitonin gene-related peptide
CHO	Chinese hamster ovary
CLP	Coecum ligation and puncture
CNG	cyclic nucleotide-gated ion channels
CRE	cyclic AMP response element
CREB	cyclic AMP response element (CRE)-binding protein
CRLR	Calcitonin receptor like receptor
CTR	Calcitonin receptor
Da	Dalton
DAG	Diacylglycerol
DMEM	Dulbecco's modified Eagle's medium
DMSO	Dimethyl sulfoxide
DNA	Deoxyribonucleic acid

DTT	Dithiothreitol
EC50	Half-maximal effective concentrations
ECIS	Electrical cell-substrate impedance sensing
ECL	Enhanced chemiluminescence
EDTA	Ethylendiamintetra essig acid
ELISA	Enzyme-linked immunosorbent assay
Epac	Exchange protein activated by cAMP
ERK	Extracellular-signal regulated kinases
ESAM	Endothelial cell-selective adhesion molecule
et al.	Et alii
FACS	Fluorescence activated cell sorter
FBS	Fetal bovine serum
FCS	Fetal calf serum
FITC	Fluorescein isothiocyanate
fMLP	N-Formyl-L-methionyl-L-leucyl-L-phenylalanine
FSK	Forskolin
g	Gram
GEF	Guanine exchange factor
GFP	Green fluorescence protein
GPCR	G-protein coupled receptor
h	Hour(s)
HBSS	Hanks balanced salt solution
HEPES	N-[2-Hydroxyethyl]-piperazin-N'-[2-Ethansulfonsäure]
HLMEC	Human lung microvessel endothelial cell
HOCL	Hypochlorous acid
HRPO	Horseradish peroxidase
HUVEC	Human umbilical vein endothelial cell
ICAM	Intercellular adhesion molecule
Ig	Immunglobulin
IgG	Immunoglobulin G; isotype control antibody
IL-1α/1β	Interleukin 1α/1β
IP	Immunoprecipitation
i.v.	Intravenously
JAM	Junction adhesion molecule
kDa	Kilodalton
kg	Kilogram
LDS	Lithium dodecyl sulfate
LFA	Lymphocyte function-associated antigen
LPS	Lipopolysaccharid

LSM	Laser scanning microscop
MAC	Membrane-activation complex
MAM	Migration assay medium
MAP	P38 mitogen-activated protein
MAPK	P38 mitogen-activated protein kinase
MBS	Myosin–binding subunit
MEM	Minimal essential medium
MES	2-(N-morpholino)ethanesulfonic acid
Min	Minute(s)
MLC	Myosin light chain
MLCK	Myosin light chain kinase
MLCP	Myosin light chain phosphatase
MMP	Matrix metallopeptidase
MOPS	3-(N-morpholino)propanesulfonic acid
MPO	Myeloperoxidase
mRNA	Messenger ribonucleic acid
NEAA	Non-essential amino acids
NFκB	Nuclear factor κB
NO	Nitric oxide
NOS	Nitric oxide synthase
PAF	Platelet-activating factor
PAM	Peptidylglycine alpha-amidating monooxygenase
PAMP	ProADM N-terminal 20 peptide
PAR	Protease-activated receptor
PBS	Phosphate buffered saline
PCR	Polymerase chain reaction
PDE	Phosphodiesterase
PE	Phycoerythrin
PECAM	Platelet and endothelial cell adhesion molecule-1
PFA	Paraformaldehyd
PG	Prostaglandine
PI3K	Phosphatidylinositol-3 Kinase
PKA	Protein kinase A
PKC	Protein kinase C
PMNs	polymorphonuclear neutrophils
PO	Peroxidase
pTyr	Phospho-Tyrosine
p-value	Probability
PVDF	Polyvinylidenefluoride

RAMP	Receptor activity modifying proteins
RNA	Ribonucleic acid
RND 1	Rho family GTPase 1
ROS	Reactive oxygen species
rpm	Rounds per minute
RT	Room temperature
RT-PCR	Reverse transcriptase polymerase chain reaction
SD	Standard derivation
SDS	Sodium dodecyl sulfate
SDS-PAGE	Sodium dodecyl sulfate polyacrylamide gel electrophoresis
SEM	Standard error of mean
Ser	Serine
SiRNA	Small interfering ribonucleic acid
S1P	Sphingosine-1-phosphate
TBS	Tris buffered saline
TCEP	Tris(2-carboxyethyl)phosphine
TEER	Transendothelial electrical resistance
TEM	Transendothelial migration
TGFβ	transforming growth factor-β
Tie-2	Angiopoietin-1 receptor
TNFα/β	Tumor necrosis factor α/β
TJ	Tight junction
TLR	Toll like receptor
TMB	3,3′,5,5′-Tetramethylbenzidine
Tris	Tris(hydroxymethyl)aminomethane
Tyr	Tyrosine
VASP	Vasodilator stimulated phosphoprotein
VCAM	Vascular adhesion molecule
VE-cadherin	Vascular endothelial cadherin
VEGF	Vascular endothelial growth factor
VE-PTP	Vascular endothelial protein tyrosine phosphatase
WB	Western blot analysis
WBC	White blood cell
w/v	Weight/volume
ZO-	Zonular occludings-
% (v/v)	Volume percent
% (w/v)	Weight percent

1. ABSTRACT

Background: Disturbed endothelial barrier function is a hallmark of inflammation. Effusion of protein rich plasma fluid leading to edema formation and overshooting transmigration of leukocytes contribute to severe organ dysfunction under conditions of generalized inflammation, e.g. acute lung injury and sepsis. The peptide hormone Adrenomedullin (ADM) and its receptor (CRLR/RAMP2/3) constitute an important signaling system for the protection of endothelial barrier function. Although elevation of cAMP in endothelial cells was identified as signaling pathway of ADM responsible for barrier protection, it was speculated that other mechanisms are involved and precise intracellular signaling routes have not been explored, yet.

Main findings and conclusions: ADM was confirmed to be a strong stabilizer of the endothelial barrier function *in vitro*, preventing and reversing hyperpermeability independent of the inflammatory stimulus (as determined by electrical impedance and FITC-dextran permeability measurements after stimulation with thrombin, TNFα, histamine, VEGF). Moreover, it was shown for the first time that ADM inhibited TNFα-induced granulocyte transmigration which was solely due to effects of ADM on endothelial cells. These *in vitro*-findings could be translated to animal models of vascular permeability and inflammation: ADM dose-dependently reduced vascular permeability in the skin of mice and rats (Miles assay; stimulus histamine). In a murine lipopolysaccharide (LPS)-induced lung injury model, ADM reduced lung edema and leukocyte extravasation.

In endothelial cells, barrier protection could solely be reduced to cAMP signaling via the protein kinase A (PKA) and Epac-Rap1 pathways (dose response comparison with Forskolin). Dissection of the downstream cascade by means of cAMP analogs, specific for PKA and Epac-Rap1 signaling (benz-cAMP and "007", respectively), demonstrated that both pathways are with respect to their efficacy equally involved in effects on permeability probably addressing independent effector mechanisms as suggested by enhanced efficacy of combination of both. Consistently, both pathway activators prevented vascular

hyper-permeability *in vivo*. PKA activation and inhibition of MLC phosphorylation downstream of ADM diminish stimulus induced actin stressfiber formation and contraction of endothelial cells thus counteracting intercellular gap formation and hyperpermeability. Most notably, also effects independent of the contractile apparatus were demonstrated: ADM stabilized barrier function even in the absence of a functional actin cytosceletton after treatment with Cytochalasin D and knockdown of cortactin. ADM induced stabilization of VE-cadherin at the cell borders and increased the amount of detectable VE-cadherin/VE-PTP complex which is important for the regular function of VE-cadherin.

In contrast, granulocyte transmigration was only reduced by PKA activation and ADM effects were lost after knockdown of cortactin. In line with this finding, a PKA inhibitor abolished the effect of ADM. As PKA activation reduces myosin light chain phosphorylation these data collectively link leukocyte extravasation to the contractile apparatus of the endothelial cell. As "007" was fully active with respect to TNFα induced hyperpermeability but had no effect with respect to granulocyte transmigration, endothelial hyperpermeability per se is not a prerequisite for granulocyte transmigration.

2. ZUSAMMENFASSUNG

Hintergrund: Die Störung der endothelialen Schrankenfunktion ist ein Haupkennzeichen der Entzündung: Die Bildung von Ödemen durch den Austritt Protein-reicher Plasamaflüssigkeit und überschießende Auswanderung weißer Blutzellen ins Gewebe tragen zu schwerer Organfehlfunktion bei generalisierten Entzündungszuständen bei, wie z.B. im akuten Lungenversagen und der Sepsis. Das Peptidhormon Adrenomedullin (ADM) und sein Rezeptor (CRLR/RAMP2/3) stellen ein wichtiges Singalsystem dar, das die endotheliale Schrankenfunktion stabilisiert. Einer Erhöhung des cAMP-Spiegels wurde hierfür als Signalweg von ADM in Endothelzellen identifiziert. Daneben wurde aber auch die Existenz andere Mechanismen vermutet. Bislang sind die intrazellulären Signalwege von ADM in der endothelialen Schrankenfunktion noch nicht präzise untersucht worden.

Hauptbefunde und Schlußfolgerungen: Es konnte bestätigt werden, dass ADM *in vitro* als starker Stabilisator der endothelialen Schrankenfunktion wirkt, indem es unabhängig vom verwendeten Entzündungsstimulus Hyperpemeabilität verhindert bzw. aufhebt (detektiert als elektrische Impedanz und Permeabilität für FITC-Dextran nach Stimulation mit Thrombin, TNFα, Histamin und VEGF). Darüber hinaus konnte erstmals gezeigt werden, dass ADM auch die durch TNFα-induzierte Transmigration von Granulozyten verhindert – ein Effekt der ausschließlich durch Wirkung von ADM auf das Endothel zustande kommt. Diese *In vitro*-Ergebnisse konnten auch in Tiermodellen für vaskuläre Permeabilität und Entzündung abgebildet werden. Mit ADM vorbehandelte Mäuse und Ratten zeigten dosisabhängig eine reduzierte Gefäßpermeabilität in der Haut (Miles-Assay mit Histamin als Stimulus). Darüber hinaus konnte eine Verringerung der Ödembildung und der Rekrutierung neutrophiler Granolozyten in der Lunge in einem murinen Lipopolysaccharid (LPS)-induzierten Lungenschädigungs-Modell gezeigt werden.

In Endothelzellen konnte der die Schrankenfunktion steigernde Effekt von ADM ausschließlich auf den cAMP-Signalweg zurückgeführt werden, und gezeigt

werden, dass sowohl der Protein-Kinase A als auch der Epac/Rap1 Signalweg aktiviert werden (Dosis-Wirkungs-Vergleich mit Forskolin). Mit Hilfe von cAMP-Analoga die spezifische Aktivatoren der Proteinkinase A (PKA) bzw. Epac/Rap1-Signalwege sind (benz-cAMP bzw. "007") wurde die funktionelle Bedeutung der Signalwege analysiert. Die maximalen Effekte beider Signalwege in der Regulation der endothelialen Permeabilität sind zwar vergleichbar stark, laufen aber wahrscheinlich über unterschiedliche Effektormechanismen ab, da die Kombination beider Wege zur Verstärkung führt. Übereinstimmend mit dem *in vitro*-Befund verhinderten beide cAMP-Analoga die Gefäß-Hyperpermeabilität *in vivo*. Durch Aktivierung des PKA Signalweges und Hemmung der MLC Phosphorylierung reduziert ADM die Stimulus-induzierte Bildung von Aktin *Stressfibers* und die Kontraktion von Endothelzellen und wirkt so der Bildung interzellulärer Lücken und der daraus folgenden Hyperpermeabilität entgegen. Bemerkenswerter Weise konnten auch Effekte, die unabhängig vom kontraktilen Apparat waren, gezeigt werden: ADM stabilisiert die Schrankenfunktion sogar in der Abwesenheit eines funktionellen Aktin-Cytoskeletts nach Behandlung mit Cytochalasin D und *Knockdown* von Cortactin. ADM induziert die Stabilisierung von VE-Cadherin an den Zell-Zell Kontakten und die Menge des nachweisbaren VE-cadherin/VE-PTP Komplexes, der wesentlich für die korrekte Funktion von VE-Cadherin ist.

Im Gegensatz dazu wurde die Granulozytentransmigration nur durch die PKA-Aktivierung gehemmt – ein Effekt der nach *Knockdown* von Cortactin aufgehoben war. Im Einklang mit diesem Befund hebt die Inhibition von PKA die Wirkung von ADM auf die Granulozytentransmigration auf. Da PKA-Aktivierung die Phosphorylierung der MLC hemmt, wird durch diese Befunde insgesamt die Abhängigkeit der Granulozytentransmigration vom kontraktilen Apparat der Endothelzelle deutlich. Da andererseits "007" die gestörte Schrankenfunktion aufhebt aber keinen Effekt auf die Transmigartion ausübt, ist eine gestörte Schrankenfunktion an sich (Hyperpermeabilitä) keine Voraussetzung für die Granulozytentransmigration.

3. INTRODUCTION

The vascular endothelium represents a semipermeable barrier between blood and tissue which is important for tissue homeostasis by regulating the exchange of plasma fluid, electrolytes, proteins and cells. Endothelial barrier dysfunction is a hallmark of acute and severe inflammatory conditions associated with trauma, thrombosis, stroke, ischemia–reperfusion injury, sepsis, and acute lung injury (ALI/ARDS), but also relevant in the course of more chronic conditions such as diabetes and cancer. Increased microvascular permeability leads to plasma effusion and leukocyte extravasation, giving rise to tissue edema formation and eventually fatal organ dysfunction. Although the pathophysiology is well known for many years, a causative therapy to directly improve endothelial barrier function in inflammation is still not available (Temmesfeld-Wollbrück et al., 2007).

Adrenomedullin (ADM) was first discovered as a 52-amino-acid peptide from phaeochromocytoma that increased cAMP levels in a thrombocyte assay and was vasorelaxant when administered to rats (Kitamura et al., 1993). ADM is a multifunctional peptide which is able to act as an autocrine, paracrine, or endocrine mediator in many important and interrelated biological functions, such as in vascular tone regulation, fluid and electrolyte homeostasis and regulation of the reproductive system (Brain & Grant, 2004). More recent studies reveal the importance of ADM in systemic inflammatory response, particularly by improving endothelial barrier function thus establishing an organ protective effect in animal models of sepsis (Allaker et al. 2005; Zudaire et al., 2006).

In the following three chapters, the present knowledge from literature is briefly summarized with respect to the biological function and regulatory effects of ADM in pathological conditions, particularly direct effects on endothelium in response to inflammation. Under this focus the knowledge is further reviewed with respect to the regulation of endothelial permeability as well as transendothelial migration of leukocytes.

3.1. Adrenomedullin (ADM)

3.1.1. Structure and distribution of ADM

Adrenomedullin was first discovered as a peptide from the lysate of an adrenal phaeochromocytoma that increased cyclic adenosine monophosphate (cAMP) levels in a thrombocyte assay and was vasorelaxant when administered to rats (Kitamura et al., 1993). The 52-amino-acid peptide belongs to the calcitonin superfamily of peptides, which also includes calcitonin, calcitonin gene-related peptide (CGRP), amylin, and intermedin (Muff et al., 1995; Wimalawansa, 1997). The amidation at the C-terminus by peptidylglycine alpha-amidating monooxygenase (PAM) and the 6-amino acid ring structure formed by an intramolecular disulphide bond between residues 16 and 21 are essential for the receptor binding of ADM and for its biological activity (Eguchi et al., 1994). ADM_{22-52} lacking the intramolecular disulphide ring can only bind to ADM receptor without biological activity and is used as ADM receptor antagonist (Eguchi et al., 1994).

The ADM gene encodes a 185-amino acid preproADM (**Figure 1**). After cleavage of a 21-residue N-terminal signaling peptide, preproADM is converted into a 164-amino acid proADM peptide, which is a precursor of two biologically active peptides, namely ADM and proADM N-terminal 20 peptide (PAMP) (Kitamura et al., 1994; Kitamura et al., 2002). Under normal healthy conditions, ADM circulates at low picomolar concentrations (2-10 pM) (Kitamura et al., 1994; Suzuki et al., 2004) in the plasma in two forms, a mature 52-amino acid peptide (mADM) and an immature glycine-extended 53-amino acid peptide (iADM), which is subsequently converted to mADM after enzymatic amidation (Kitamura et al., 1998; Asakawa et al., 2001).). iADM represents 85% of total plasma ADM (Yamaga et al., 2003).

Figure 1 Structure of ADM and post-translational processing of preproADM gene (Modified from Hamid & Baxter, 2005)

After cleavage of a 21-residue N-terminal signaling peptide from the initial 185-amino acid preproADM peptide, the 164-amino acid proADM peptide is converted, which is a precursor of two biologically active peptides, namely ADM and PAMP. Further degradation products derived from the ADM precursor or ADM are also listed.
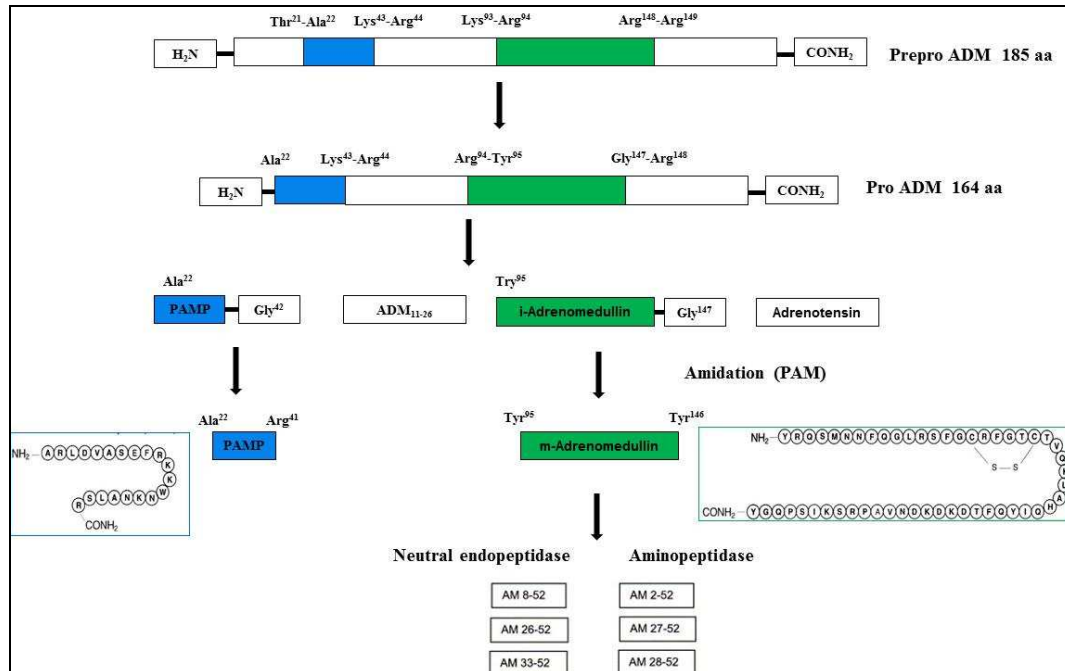
In the blood circulation, ADM is bound to ADM binding protein 1 (AMBP-1; also called complement factor H) which stabilizes the peptide (Elsasser et al., 1999; Pio et al., 2001). It is also reported that via its binding to AMBP-1 the receptor-mediated effects of ADM are increased, while its receptor-independent antimicrobial activity is suppressed (Beltoeski & Jamroz, 2004). In addition, the inhibitory effect of factor H in alternative pathway of complement activation is enhanced via its binding to ADM. It is noteworthy that, neither CGRP nor PAMP binds complement factor H from plasma (Beltoeski & Jamroz, 2004).

In humans and rats, circulating ADM is rapidly metabolized with the elimination half-life ($T_{1/2}$) of about 20 min. However, little is known about its precise metabolism and clearance. ADM is metabolized by neutral endopeptidase and cleared in the pulmonary circulation (Lisy et al., 1998; Dupuis et al., 2005). Studies using intravenous administration of radioactively labeled ADM derivatives demonstrate a high first pass effect during the passage through the

lung vasculature, where 36% of a bolus is captured in dogs (Dschietzig et al., 2002; Dupuis et al., 2005). Studies in rats show that more than 25% of the lung bound ADM can be displaced by non-labeled ADM, which proportion is therefore likely to be receptor bound. Moreover, ADM is present in human urine with about six-fold higher concentration than in human plasma, suggesting that a renal clearance may be also relevant in addition to pulmonary clearance (Sato et al., 1995). However, circulating ADM is cleared by neutral endopeptidase in kidney, located in the tubular brush border system, and the subsequent urinary excretion of ADM may be derived from renal production rather than from glomerular filtration (Lisy et al. 1998, Nishikimi, 2007).

3.1.2. Receptors and intracellular signalling of ADM

ADM exerts its biological actions through binding to the heterodimeric G-protein coupled receptor complex (GPCR) composed of the calcitonin receptor-like receptor (CRLR) associated with RAMP-2 (ADM-1 receptor) or RAMP-3 (ADM-2 receptor). RAMPs bind to the receptor molecule in the endoplasmic reticulum and facilitate their translocation to the plasma membrane. Additionally, RAMPs regulate the degree of receptor glycosylation and play an important role in receptor specificity, ligand affinity, and receptor desensitization (McLatchie et al., 1998). Although the three isoforms of RAMPs show a differential tissue distribution, a pharmacological difference of ADM-1 and-2 receptor is not established yet (Chakravarty et al., 2000; Hagner et al., 2002). Besides ADM-1 and -2 receptors, ADM can also mediate its effects via CGRP-1 receptor, especially in the vascular system (Dennis et al., 1990; Chiba et al., 1989). Indeed, ADM can bind to some regions in the brain where actually CRLR is not expressed, suggesting the existence of specific ADM receptors with a different molecular structure (Hinson et al., 2000).

The cellular signaling mechanisms through which ADM mediates its biological effects vary among species, vascular beds and cell types, but mainly involve cAMP, nitric oxide (NO) and calcium-dependent mechanisms (Lopez & Martinez., 2002). Moreover, activation of different kinases, such as protein kinase A (PKA), Src, protein kinase C (PKC), p38 mitogen-activated protein

kinase (MAPK), and extracellular-signal regulated kinases (ERK), have been reported to be involved in ADM signaling. The combinations of various signaling may be responsible for numerous biological functions of ADM in different cell types (reviewed by Gibbons et al., 2007).

3.1.3. Biological actions of ADM in response to inflammation

The ADM gene is broadly expressed throughout most organs during embryonic development and adulthood, especially in endothelial cells, vascular smooth muscle cells, cardiac myocytes, and human leucocytes (Garayoa et al., 2002; Hinson et al., 2000). Moreover, in highly vascularized tissues, such as placenta, lung, heart, and kidney, levels of ADM tend to be relatively higher. Experimental data from literature underscore a role of ADM in a variety of functions, including blood pressure regulation, broncho-dilatation, renal function, hormone secretion, cell growth, differentiation, neurotransmission, and modulation of the immune response. Moreover, ADM plays a crucial role as autocrine factor during proliferation and regeneration of endothelial cells (reviewed by Ishimitsu et al., 2006; Gibbons et al., 2007). However, data from targeted deletion in mice of ADM or its receptor gene, point to another dominant function of this peptide in regulating vascular permeability. While heterozygous littermates show a mild hypertension (Shindo et al., 2000) and exhibit a more pronounced inflammatory response to endotoxin-induced septic shock (Dackor and Caron, 2007), homozygous knockout mice develop a strong and lethal hydrops fetalis (Caron and Smithies, 2001). A similar phenotype is further substantiated by data from knockout mice lacking CRLR or PAM genes (Dackor et al., 2006; Czyzyk et al., 2005). Conversely, mice overexpressing ADM show moderate hypotension and are largely resistant to LPS induced shock (Shindo et al., 2000).

Transcription of the ADM gene is stress sensitive. A variety of stimuli such as hypoxia, inflammatory stimuli (e.g. LPS), as well as pro-inflammatory cytokines (e.g. IL-1α, IL-1β, TNFα, and TNFβ) are shown to induce the expression of ADM (reviewed by Tammesfeld-Wollbrück et al., 2007). Accordingly, elevated plasma ADM levels have been detected in a wide variety of physiological and pathological conditions, including normal pregnancy and pregnancy with

complications, cardiovascular and pulmonary diseases, diabetes, endocrine disorders, hepatic and renal failure, cancer, and sepsis (reviewed by Gibbons et al., 2007). In their analysis, based on published human clinical data, Gibbons and colleagues compared *fold change* of plasma ADM in a variety of human conditions. One of the highest increases in plasma ADM levels occurred during sepsis, which evidences the importance of ADM under inflammatory conditions. Moreover, in animal studies, high expression of ADM was observed in the lung in endotoxaemia (Cheung et al., 2004) and in acute lung injury induced by hyperoxia and LPS (Agorreta et al., 2005). In a model of cecal ligation and puncture in rats, the small intestine was demonstrated to be an important source of ADM release during polymicrobial sepsis (Zhou et al., 2001). These observations raised the question as to whether elevated ADM levels reflect a protective defense mechanism rather than being of pathological significance.

Meanwhile, there is strong evidence from the literature that administration of ADM to supra-physiological levels exerts strong anti-edematous effects:

In vitro, using measurement of physiological hydrostatic pressure as indictor of endothelial permeability, ADM was shown to dose-dependently reduce hyperpermeability induced by different stimuli, such as thrombin, hydrogen peroxide, *E. coli* hemolysin, or *S. aureus* alpha-toxin, in endothelial cells from different species (human, rat, porcine) and different vasculatures (umbilical vein, lung pulmonary artery) (Hippenstiel et al., 2002; Hocker et al., 2006). The measurable increase of intracellular cAMP levels was supposed to be the key mechanism of action of ADM signaling. Inhibition of MLC phosphorylation via PKA activation was hypothesized to counteract and reduce endothelial contractility and to further stabilize endothelial barrier function (Hippenstiel et al., 2002). Moreover, ADM was shown to tighten blood brain barrier in terms of increased transendothelial electrical resistance (Kis et al., 2001; Kis et al., 2003; Honda et al., 2006). In *ex vivo*-models using hydrogen peroxide-exposed rabbit lungs and *S. aureus* α-toxin-infused rat ileums, ADM showed protective effects in those isolated organs (Hippenstiel et al., 2002; Brell et al., 2005; Hocke et al., 2006).

Further *in vivo*- studies were in line with the results obtained *in vitro* and in isolated organs. ADM reduced the ovalbumin-induced airway microvascular leakage in an ovalbumin-sensitized guinea pig model (Ohbayashi et al., 1999). Intravenous infusion of ADM in rats protected against endotoxemia induced lung injury (Itoh et al. 2007). In a sheep model of endotoxemia induced lung injury, ADM reduced pulmonary hypertension and prevented hypodynamic circulation (Ertmer et al., 2007). ADM was shown to protect lung function significantly in models of oxygen and ventilator induced lung injury (Müller et al., 2010; Tao et al, 2012).

In a rodent model of Gram positive sepsis and in the severe model of coecum ligation and puncture (CLP) induced polymicrobial sepsis, ADM reduced vascular leakage and secondary lung damage, and prolonged survival (Hocke, et al, 2006; Temmesfeld-Wollbrück et al., 2007; Wu et al, 2008). In further models of polymicrobial sepsis (Wang, 2001; Yang et al., 2010; Gonzalez-Rey et al., 2006), endotoxin-related shock (Gonzalez-Rey et al., 2006) and hemorrhage (Cui et al., 2005) ADM showed beneficial effects on survival.

In severe sepsis a loss of plasma ADM coincides with loss of AMBP (the complement factor-H) at the transition from the phase of hyperdynamic to hypodynamic circulation due to increased consumption of components of the complement system (Yang et al., 2002). A decrease of ADM plasma level in sepsis was believed to facilitate generalized edema formation and deterioration of cardiac function (Westphal et al., 2006). In the CLP-induced sepsis model, administration of ADM together with human complement factor-H significantly could halt transition to hypodynamic circulatory failure (Yang et al., 2002), while infusion of ADM stabilized cardiac output in endotoxemic sheep (Ertmer et al., 2007).

3.2. Regulation of vascular permeability

Endothelial permeability is described as a passage through either one of two different routes: one transcellular (cross cells), via caveolae-mediated vesicular transport, and the other paracellular (between cells), through interendothelial

junctions. Although transcytosis plays an important role in the basal permeability of the endothelium, paracellular flux of plasma fluid and proteins through endothelial cell–cell junction is more dominant in the development of vascular inflammation under pathophysiological conditions (Komarova & Malik, 2010; Mehta & Malik, 2006).

3.2.1. Endothelial cell-cell junctions and vascular integrity

Although endothelial cell-cell junctions are differently structured in different organs, the general constituent of endothelial cell–cell junctional structures, with major impact on cell-to-cell adhesion and barrier properties, are tight junctions (TJs) and adherens junctions (AJs). AJs represent the predominant type of junctions within the endothelial barrier, whereas TJs predominate in the epithelium (Vandenbroucke et al., 2008). In the endothelium, the TJs are interwoven with AJs over the lateral intercellular space differing from the structure in epithelium (**Figure 2**). The molecular structure of AJ as well as TJ is based on the homophilic interaction of transmembrane proteins between two adjacent cells. Specific cytosolic proteins link to the adhesion proteins anchoring them to the cell cytoskeleton and transducing cellular signaling. By way of this protein complex, cell-cell junctions influence the important cellular process, such as proliferation, polarity, protein expression, and permeability (Bazzoni & Dejana, 2004).

Figure 2 Endothelial cell-cell junctions

In the endothelium, the tight junctions and adherence junctions are interwoven with each other over the lateral intercellular space. The tight junction proteins, claudins, occludins and JAMs, are linked to the intracellular actin cytoskeleton via zonular occludins (ZOs). The primary molecular structure of adherence junction is VE-cadherin-catenin complex linking directly or indirectly to actin cytoskeleton.
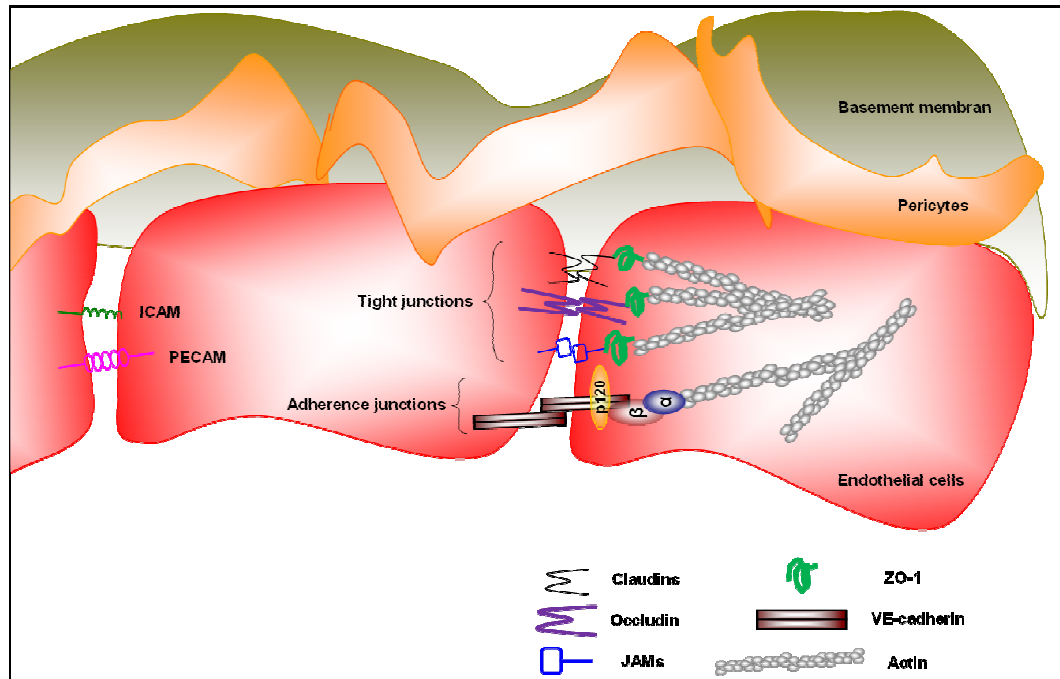
Tight junctions are primarily found in blood-brain, blood-retinal, or blood-testis barrier microvasculature (Mehta & Malik, 2006; Hawkins & Davis, 2005). Tight junction resembles a zipper-like structure formed by homophilic interactions of transmembrane proteins, including occludin, claudins, and junction adhesion molecule (JAMs). These three TJ proteins represent the backbone for TJs. They are intracellularly connected to the actin cytoskeleton via zonular occludins (ZO-1; 2) (Bazzoni, 2006). Complex tight junctions as found e.g. in the blood brain barrier are responsible for a high transendothelial electrical resistance and are exclusively impermeable to the passage of solutes (Crone & Olesen, 1982). Although TJs are well developed in large artery endothelial cells that are exposed to high flow rates, TJs are less complex in capillaries than in arterioles, and even less in venules within the microvasculature (Wallez & Huber, 2008).

Adherens Junctions have been recognized as a critical component in regulating paracellular permeability of microvascular endothelium, with the exception of blood-brain barrier and blood-retinal barrier endothelium (Mehta & Malik, 2006). AJs have been identified in nearly all types of vascular beds, especially in the peripheral microvasculature. In the postcapillary venules, where leukocyte adhesion and inflammatory hyperpermeability selectively occur, beside AJs other types of junctions are poorly developed. The primary molecular structure of AJ is based on homophilic interactions of vascular endothelial cadherin (VE-cadherin) (**Figure 3**). VE-cadherin is a transmembrane protein composed of five extracellular calcium–binding domains, one transmembrane domain and a cytoplasmatic tail domain (Vestweber, 2008).   The hemophilic interaction of extracellular domains is calcium dependent. The intracellular domain is anchored to the cell cytoskeleton through binding with catenins (α, β, γ and p120) (Djana, 2004; Vestweber, 2008). This cytosolic connection to the cytoskleton is of importance for maintaining junctional strength and for the regulation of paracellular permeability (Yuan, 2002). It is hypothesized that through these junction-cytoskeleton connections, endothelial cytoskeletal contractile forces can be transmitted to cell–cell junctions and thus dynamically regulate endothelial permeability. Antibodies that inhibit the adhesion function of VE-cadherin cause dissociation of endothelial cell layers *in vitro,* enhanced accumulation of neutrophils in a peritonitis mouse model and lead to subcutaneous hemorrhage and death of mice (Vestweber et al., 2009).

The stability and composition of the VE-cadherin-catenin complex is dependent on the status of cell contacts and regulated by tyrosine phosphorylation (Vestweber, 2008). In subconfluent cell culture where the endothelial cells are weakly connected to each other, β-catenin and p120 are infirmly linked to VE-cadherin, and the protein components of this complex are highly phosphorylated. In contrast, in confluent cell culture where endothelial cells are strongly connected to each other, γ-catenins are predominant over β-catenins in VE-cadherin-catenin complex, and the phosphorylation of the components is reduced (Lampugnani et al., 1997; Lampugnani et al., 1995). The destabilization of cell contacts is accompanied by a decreased association with

γ-catenin and increased association with β-catenin (Lampugnani et al., 1995). The underlying mechanism is still not fully understood (Vestweber, 2008).

Furthermore, there is correlation between tyrosine phosphorylation of various components of the VE-cadherin-catenin complex and the decrease of VE-cadherin-mediated adhesion. Many vasoactive stimuli, such as histamine, thrombin, VEGF and TNFα, have in common that they induce phosphorylation of the VE-cadherin-catenin components and thus destabilize the complex (Angelini et al., 2006; Vestweber, 2008). Thrombin is shown to cause disassembly of AJs via PKC-induced modification of VE-cadherin and β-catenin phosphorylation (Konstantoulaki et al., 2003). Vascular endothelial growth factor (VEGF) stimulation induces activation of Src-kinase and thus phosphorylation of VE-cadherin on the residue Serine 665, leading to α-arrestin-2 regulated internalization and loss of endothelial barrier function (Gavard & Gutkind, 2006).

An important counteracting regulator of this phosphorylation is the vascular endothelial protein tyrosine phosphatase (VE-PTP), which is associated with tyrosine kinase receptor (Tie 2) and VE-cadherin. Docking of neutrophil granulocytes or lymphocytes on tumor necrosis factor (TNFα)-stimulated endothelial cells leads to dissociation of VE-PTP from VE-cadherin, (Nottebaum et al., 2008). Down-regulation of VE-PTP expression increases endothelial cell permeability, enhances leukocyte transmigration, and inhibits VE-cadherin-mediated adhesion (Nottebaum et al., 2008).

Figure 3 Structure of VE-cadherin-catenin complex in endothelial cells

The primary molecular structure of adherence junction is based on the homophilic interactions of VE-cadherin. This transmembrane protein VE-cadherin consists from five extracellular domains, one transmembrane domain and a cytoplasmatic tail domain interactingwith catenins (α, β, γ and p120). VE-cadherin is anchored to the cell cytoskeleton, whereas through binding its extracellular domains, VE-cadherin can interact with other binding partners, such as VE-PTP.
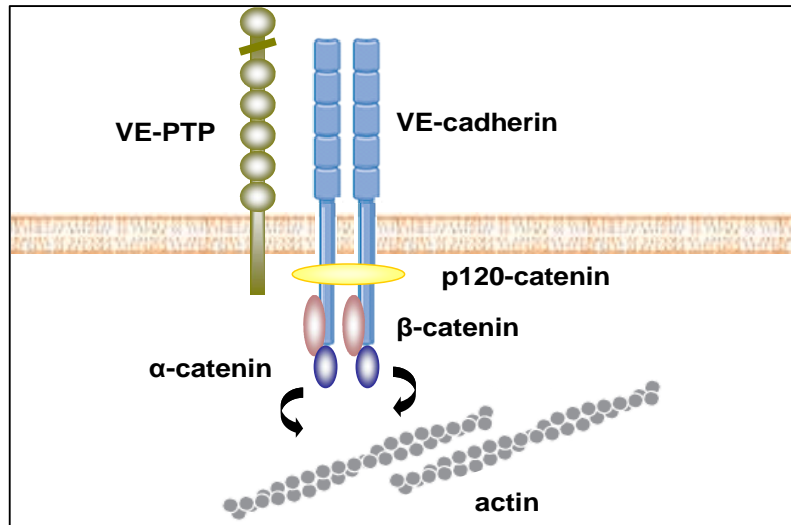
3.2.2. Endothelial cytoskeleton and vascular permeability

3.2.2.1. Dynamic functions of cytoskeleton and vascular permeability

Similar to smooth muscle cells vascular endothelial cells are contractile cells developing forces driven by a mechanochemical interaction between actin and myosin (**Figure 4**). The increased actomyosin contractility is characterized by the formation of stress fibers, which are bundles of actin filaments associated with nonmuscle myosin II (Wojciak-stothard & Ridley, 2002). The key signal to trigger endothelial contraction is the phosphorylation of the regulatory part of myosin, the myosin light chain (MLC) (Dudek & Garcia, 2001; Tiruppathi, 2002). Phosphorylation of MLC induces conformational change of myosin, interacting with actin, sliding along actin filaments, subsequently causing contraction (Tiruppathi, 2002; Sandoval et al., 2001). This myosin-actin cross-bridge cycling provides a mechanical basis to develop contractile force in response to physiological and pathological stimulation and is the cause for generating and maintaining a centripetal tension (Yuan, 2002).

In vascular endothelial cells, the phosphorylation status of MLC results from the balance of MLC kinase (MLCK) and MLC phosphatase (MLCP) (Garcia et al., 1995). Firstly, MLCK phosphorylates MLC at Ser-19 and subsequently at Thr-18, starting actomyosin-interaction thus generating centripetal forces which ultimately may be responsible for dissociation of cell-cell contacts and formation of interendothelial gaps (Moy et al., 1996). MLCK is activated in a Ca^{2+}/calmodulin dependent manner and by tyrosine kinase-mediated phosphorylation at Tyr-464 and Tyr-471 (Goeckeler & Wysolmerski, 1995; Garcia et al., 1995). Secondly, MLCP dephosphorylates MLC as opposed to MLCK, decreases contractile forces, and subsequently relaxes the endothelial cytoskeleton (Verin et al., 1995). Finally, small GTPases of the Rho family are also involved in regulating the phosphorylation status of MLC (van Nieuw Amerongen & van Hinsbergh, 2001). RhoA, a member of the Rho family of small GTPases, can increase MLC phosphorylation indirectly by activating its downstream effector, Rho C-terminal kinase (ROCK), which subsequently phosphorylates and inhibits MLCP (Noda et al., 1995; Yoshioka et al., 2007). Besides the formation of actin stress fibers and the induction of contractile forces, activation of Rho and ROCK directly affects the destabilization of cell contacts (Wojciak-Stozhard & Ridley, 2002). In addition to RhoA, additional small GTPases of the Rho superfamiliy, Rac and Cdc42, are also implicated in actomyosin contractility, since their downstream effector, p21-activated kinase (PAK), phosphorylates MLC on Ser-19 (Goeckeler et al., 2000).

MLC phosphorylation is involved in modulating endothelial barrier dysfunction in response to cellular mediators (e.g. activated neutrophils), as well as inflammatory agonists (e.g. thrombin, histamine, cytokines, oxygen radicals). Inhibition of MLCK by specific inhibitors (ML7 and ML9), prevents phosphorylation of MLC and stabilizes vascular permeability. Using fluorescence microscopic approaches, endothelial cells exposed to inflammatory stimuli present a morphological change characterized by increased staining of MLC phosphorylation accompanied with formation of stress fiber and intercellular gaps (reviewed by Yuan, 2002).

Figure 4 Contractile machinery and actin cytoskeleton in endothelial cells

In vascular endothelial cells, the balance of MLCK and MLCP results in the phosphorylation status of MLC, inducing conformational change of myosin, subsequently interacting with actin, sliding along actin filaments, and causing contractility. Ca^{2+}/calmodulin dependent activation of MLCK, RhoA-ROCK dependent inactivation of MLCP, as well as the small GTPases (Rac, and Cdc42) are implicated in phosphorylation of MLC and acto-myosin based endothelial contractility.
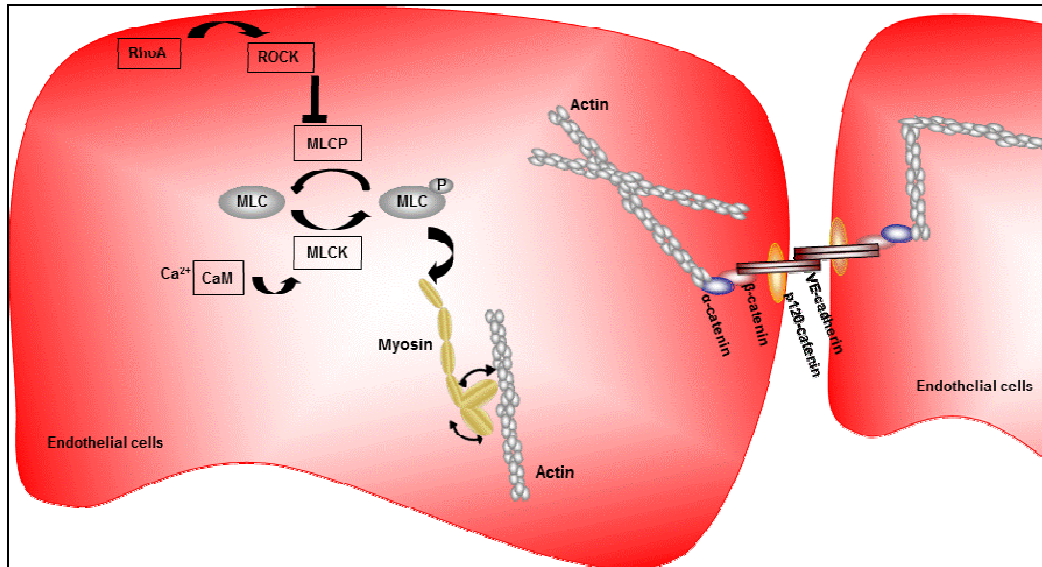
3.2.2.2.   Static functions of cytoskeleton in vascular permeability

Besides the role of actin in the active contractile apparatus, disruption and rearrangement of actin cytoskeleton are of equal importance in the development of endothelial gaps (Baldwin & Thurston, 2001; Schnittler et al., 1990). Upon stimulation by inflammatory mediators and neutrophils, as well as during ischemia–reperfusion injury, actin directly undergoes polymerization and redistribution to form stress fibers followed by the formation of intercellular gaps (Korthuis et al., 1991; Schnittler et al., 1990; Shasby et al., 1982). However, those effects can totally be abolished by actin stabilization agents *in vitro* and *ex vivo*, such as phalloidin, antamanide, cytochalasin B, or cytochalasin D (Korthuis et al., 1991; Shasby et al., 1982). In a study using confocal microscopic analysis in rat mesenteric venules, the time course of development and recovery of histamine-induced venular leaks is coincident with the rearrangement of endothelial actin fibers (Baldwinand & Thurston, 1995). Local breaks in the peripheral actin rim of endothelial cells are accompanying

histamine-induced focal leaks and hyperpermeability, whereas the central actin fibers are involved in the structural and functional recovery phase rather than the hyperpermeability-inducing phase. (For review see Yuan, 2002; Schnittler et al., 1990).

In addition to actin and myosin, microtubules, another important cytoskeletal component in endothelial cells, are also implicated in response to inflammatory stimuli (Mehta & Malik, 2006). Microtubule assembly is necessary for maintenance of actin-dependent barrier integrity (Vadenbroucke et al., 2008). In human pulmonary artery endothelial cells, TNFα- induced barrier disruption was shown to be independent of MLC phosphorylation and involved the destabilization of the microtubule network (Petrache et al., 2003). TNFα can induce a decrease in stable tubulin content and partial dissolution of peripheral microtubule network as detected by immunofluorescent analysis of acetylated tubulin and beta-tubulin (Petrache et al., 2003). Inhibitors of microtubule polymerization (e.g. nocodazole or vinblastine), disrupt endothelial barrier function associated with increased stress fiber content and MLC phosphorylation, whereas a microtubule stabilizer (paclitaxel) attenuates this effect (Verin et al., 2001). The increase of MLC phosphorylation and endothelial cell contractility are attributed to a RhoA/ROCK-dependent and MLCK-independent mechanism (Verin et al., 2001). More in-depth, the downstream effector of ROCK, LimK domain containing kinase 1 (LIMK1), is considered be of importance in regulating actin and microtubule assembly in a MLCK-independent manner (Gorovoy et al., 2005; Verin et al., 2001). Taken together, microtubule destabilization may serve to amplify endothelial cell contractility (beyond that induced by myosin-actin cross-bridging), thereby inducing a profound endothelial hyperpermeability (reviewed by Vadenbroucke et al., 2008).

3.2.3. Role of cAMP in regulating vascular permeability

The intracellular second messenger cAMP is involved in a multitude of biological functions, ranging from metabolism, gene expression, cell division and growth, cell differentiation and apoptosis, as well as secretion and

neurotransmission. So diverse essential physiological processes, such as learning and memory, contractility and relaxation of the heart, and fluid homeostasis in the gut and kidney are regulated by cAMP. Cyclic AMP mediated signaling is also involved in pathological conditions, such as diabetes mellitus, heart failure, and cancer (reviewed by Cheng et al., 2008).

Binding of a ligand to a GPCR at the cell surface transduces the extracellular signal across the cell membrane via stimulatory or inhibitory heterotrimeric G-proteins, interacting with the membrane-bound adenylate cyclase (AC), and regulates intracellular cAMP production. In eukaryotic cells, cAMP mediates its biological function via two ubiquitously expressed intracellular cAMP receptors, the classic protein kinase A (PKA) as well as the recently discovered exchange protein directly activated by cAMP (Epac). However, it is believed that cAMP mediates its biological function in mammalian cells predominantly via PKA. In addition cyclic nucleotide-gated ion channels (CNGs) are directly regulated by cAMP in photoreceptor cells, olfactory sensory neurons, and cardiac sinoatrial node cells (Zufall et al., 1997; Cheng et al., 2008).

A large number of studies extensively document that stimulation of cAMP signaling stabilizes endothelial barrier function (Stelzner et al., 1989). By using tool compounds, such as forskolin (FSK), an activator of membrane associated adenylat cyclases, or 8-Br-cAMP, a cAMP analogous, the effects of cAMP on vascular contact integrity are demonstrated (reviewed by Mehta & Malik, 2006; Aslam et al., 2010; Yuan, 2002). Other cAMP increasing receptor agonists, such as prostacyclins or prostaglandins, also attenuate inflammatory stimuli-induced endothelial hyperpermeability (Farmer et al., 2001). Interestingly, also the glycocalyx of endothelial cells contributes to cAMP-mediated stabilization of endothelial barrier function in intact microvessels (Huxley et al., 1997; Huxley & Williams, 2000).

The signaling of cAMP/PKA is assumed to stabilize endothelial barriers due to an inactivation of the contractile machinery and a decrease of phosphorylation of MLC. Besides the initial identified action to directly inactivate MLCK, cAMP/PKA is also shown to induce site-specific MLC phosphatase activation

(Bindewald et al., 2004). Moreover, PKA is shown to inhibit RhoA activation via phosphorylation of Rho-GDP dissociation inhibitor, a negative regulator of Rho, and thus protects the endothelial barrier against Rho-dependent hyperpermeability (Qiao et al., 2003). In addition, PKA can also directly inhibit RhoA activity through direct phosphorylation of RhoA (Dong et al., 1998; Lang et al., 1996). Beside its effect on the contractile apparatus, cAMP dependent PKA activity is also involved in cytoskeleton rearrangement and microtubule assembly in endothelial cells (Liu et al., 2001; Birukova et al., 2004a).

Upon binding to cAMP, Epac, activates the small GTPases Rap1 and Rap2, which are involved in diverse cAMP-mediated biological functions and pathologies, ranging from integrin-mediated cell adhesion, cadherin-mediated cell junction formation, exocytosis and secretion, cell differentiation and proliferation, phagocytosis, gene expression, apoptosis, as well as cardiac hypertrophy (reviewed by Cheng et al., 2008). Studies using human umbilical vein endothelial cells (HUVECs) show that Epac can induce redistribution of junctional molecules to cell-cell contacts and increase cortical actin, contributing to stabilization of endothelial barrier function. This effect of Epac is mediated by activation of Rap1, which is enriched at endothelial cell-cell contacts (Cullere et al., 2005; Kooistra et al., 2005; Fukuhara et al., 2005). Activation of Epac can suppress Rho GTPase activation and thus antagonize thrombin-induced hyperpermeability (Cullere et al., 2005). Cyclic AMP strengthens VE-cadherin mediated cell-cell junction in an Epac-Rap1 dependent manner thus supporting endothelial barrier function (Kooistra et al., 2005; Fukuhara et al., 2005). In rat mesentery, Epac/Rap1 pathway attenuates the platelet-activating factor (PAF)-induced microvascular hyperpermeability as measured by hydraulic conductivity, and prevents the PAF-induced rearrangement of VE-cadherin (Adamson et al., 2008). These results suggest an important role of Epac/Rap1 signaling in maintaining endothelial barrier function. Moreover, Mei et al. showed that Epac promotes microtubule growth in a Rap1-independent manner (Mei & Cheng, 2005). Epac activation is observed to reverse microtubule-dependent vascular leakage induced by tumor necrosis factor-α (TNFα) and transforming growth factor-β (TGFβ) (Mei & Cheng, 2005). These studies suggest a two-leg strategy of Epac1 to regulate endothelial barrier function: a

Rap1-depedent regulation of cortical actin and VE-cadherin mediated cell-cell contacts, as well as a Rap-independent regulation of microtubules (Sehrawat et al., 2008).

3.3. Transendothelial migration of leukocytes

An important aspect of the inflammatory process is the translocation of leukocytes from blood stream to tissue. Transendothelial migration (TEM) of leukocytes is elemental in both adaptive and innate immune reaction and is of importance in routine immune surveillance and homing (Ley et al., 2007; Vestweber et al., 2008). Following stimulation in response to inflammation, immune cells, such as neutrophils, monocytes, and antigen-experienced lymphocytes, migrate across the vascular wall into lymphoid organs and infected tissues. However, excessive translocation of leukocytes can aggravate or even initiate a pathological process, such as atherosclerosis, multiple sclerosis, rheumatoid arthritis and acute lung injury (Hansson et al., 2006; Mattay & Zemans, 2011; Frohman et al., 2006).

Transmigration of leukocytes occurs in a sequential set of four phases which are illustrated below in **Figure 5**. Each single step is required to initiate signaling that facilitates progression to the next stage. The key element of this process is the interaction between leukocytes and endothelium which is facilitated by adhesion proteins from both endothelial cells and leukocytes as well as by direct signal exchange via adhesion proteins and cytokines (Panés & Granger, 1998).

Figure 5 Schematic diagram of leukocyte adhesion and transendothelial migration (Yuan et al., 2012)

In response to inflammatory stimuli, leukocytes initially weekly adhere on the endothelial cells, rolling along the vascular endothelial wall through transient selectin-mediated interactions. The activation stage allows the up-regulation of adhesion receptors expressed on the cell surfaces of both endothelial cells and leukocytes. This is required to initiate the firm adhesion of leukocytes to endothelium through binding intergrins on leukocytes to ICAM-1 and VCAM-1 on endothelial cells. Subsequently, leukocytes cross the endothelium and exit the bloodstream (transmigration or diapedesis).
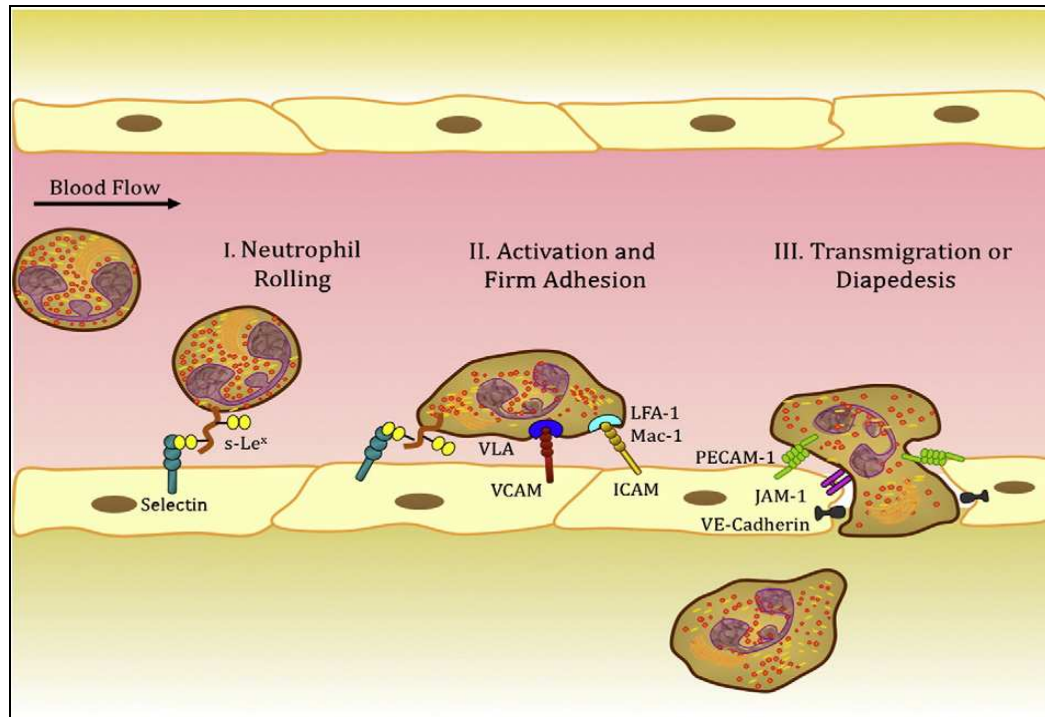
Rolling adhesion step

Rolling adhesion occurs when leukocytes are first captured from the bloodstream, and loosely tethered to the endothelial cells lining blood vessel wall. This first transient adhesion of rolling leukocytes is mediated by E-, L-, and P-selectins, which bind to sialyzed glykoligand of glykoproteins (Barreiro et al., 2004). While L-selectin is expressed on leukocytes, E- and P-selectin are expressed on the apical sites of activated endothelial cells (Vestweber & Blanks, 1999). Upon binding to selectins, leukocytes slow down and roll on the surface of the endothelium, allowing exposure to a local environment and initiating the activation step.

Activation step

In this stage, β1- and β2-integrins take over the function from selectins. While leukocytes initiate to up-regulate the expression of integrins upon activation of G-protein coupled chemokine receptors, endothelial cells increase expression of immunoglobulin family proteins, such as intercellular adhesion molecule (ICAM-1, ICAM-2, ICAM-3), vascular adhesion molecule (VCAM)-1 and MAdCAM-1 (Ebnet & Vestweber, 1999). All these processes result in deformation of leukocytes morphology and facilitating transmigration.

Firm adhesion step

In the next step, strong adhesion of leukocytes to the surface of endothelial cells is mediated through the interaction of Ig-family adhesion molecules on endothelial cells and integrins on leukocytes, including ICAM-1 binding to LFA-1 (CD11a/CD18; $\alpha_L\beta_2$), MAC-1 (CD11b/CD18; $\alpha_M\beta_2$), and p150,95 ($\alpha_X\beta_2$), as well as VCAM-1 binding to $\alpha_D\beta_2$ (reviewed by Yuan et al., 2012). *In vitro*-studies using HUVECs show that the firm adhesion of leukocytes on endothelial cells forms transmigratory cups or docking structures, containing microvilli around the attached leukocytes which are composed of high levels of ICAM-1, VCAM-1 and LFA-1 (Carman & Springer, 2004). ICAM-1 is considered to be predominant in this interaction. Furthermore, cross-linking of ICAM-1 causes the activation of Rho, PLCγ, PKC and Src, as well as the phosphorylation of cortactin (Vestweber, 2007).

Diapedesis step

The final step is the diapedesis, in which leukocytes transmigrate through endothelial barrier, basal membrane, and the pericyte layer, and thus enter into inflammatory sides of infected tissue along a cytokine gradient (Springer, 1994). The mechanisms in this process are largely unknown, and have been intensely investigated in the recent years (Vestweber, 2007). The route by which leukocytes transmigrate through the endothelium can be broken down into two distinct modes: transcellular and paracellular. The transcellular route occurs when a leukocyte transmigrates directly through the body of a single endothelial cell, probably via the transient formation of a pore. The factors for the preference of paracellular or transcellular route are still largely unknown. For

leukocytes, both paracellular and transcellular routes are observed, although the paracellular route is considered as the most prevalent mechanism *in vitro* (Carman & Springer, 2004). Moreover, in regions where specific matrix proteins are less expressed, neutrophils prefer the transcellular route to penetrate the vascular basement membrane *in vivo* (Wang et al., 2006).

Linking transmembrane junctional proteins to the actin cytoskeleton dynamically regulates endothelial junctions during transendothelial migration of leukocytes. The actin-myosin based generation of contractile force promotes the cell shape changes and junctional breakdown necessary for transendothelial migration of leukocytes. While pre-treating endothelial cells with specific MLCK inhibitors significantly reduces neutrophil transmigration, the adhesion of neutrophils to endothelial monolayer directly increases MLC phosphorylation (Garcia et al., 1998; Saito et al., 1998; Hixenbaugh et al., 1997). It is believed that acto-myosin based endothelial contractility facilitates the actual migration of leukocytes across the endothelium (Wittchen, 2009).

3.4. Aims of the study

In summary the extensive body of evidence from literature supports the concept that ADM has a strong protective potency during inflammatory processes which might be mediated by modulation of the endothelial barrier function with respect to transition of fluid and cells of the immune defense. Notably, the potential translation of this concept into clinical trials is supported by the recent positive opinion of the Committee for Orphan Medicinal Products of the European Medicines Agency. On the 9th June 2010, the development of ADM as an orphan medicinal product (EU/3/10/744) was granted by the European Commission to Prof Dr. Stefan Hippenstiel (Charité, Berlin, Germany) for the treatment of acute lung injury (EMA/COMP/169921/2010).

In endothelial cells, binding of ADM to its receptor was shown to induce measurable accumulation of intracellular second messenger cAMP. The effects of cAMP on vascular contact integrity have been extensively demonstrated by

using tool compounds (reviewed by Mehta & Malik, 2006; Aslam et al., 2010; Yuan, 2002). However, as previous studies have shown, cAMP levels that were measurable at comparable efficacy were notably lower with ADM than with FSK (Hippenstiel et al., 2002). Therefore, it was hypothesized that beside cAMP-dependent pathways, also cAMP-independent pathways might be involved in ADM mediated regulation of vascular permeability (e.g. direct effects on cell-cell-junctions, on cytoskeleton, on ion channels, or on endothelial glycocalyx) (Hippenstiel et al., 2002; Szokodi et al., 1998).

The main goal of the present studies was to investigate and determine the signal transduction mechanisms which are responsible for ADM-mediated improvement of endothelial barrier function with respect to transition of fluid, macromolecules and polymorphonuclear garnulocytes. The following main topics have been worked out:

- Analysis of ADM-mediated effects on endothelial barrier function in response to inflammatory stimuli.
- Search for evidence of cAMP-independent effects of ADM in modulation of endothelial barrier function - including ADM-mediated effects on endothelial gene expression.
- Dissection of the cAMP signaling pathways: impacts of PKA and Epac/Rap1 in ADM signaling on endothelial cell-cell junctions and cytoskeleton

4. MATERIAL AND METHODS

4.1. Material

4.1.1. Chemical reagents and assay kits

Table 1 List of chemical reagents, assay kits and their providers

Chemical/Reagent/Kit	Provider
Adrenomedullin human	Bachem (Weil am Rhein)
Alexa Fluor® 555 phalloidin	Invitrogen (Darmstadt)
Aprotinin from bovine lung	Merck (Darmstadt)
Gibco® Cell Culture β-mercaptoethanol	Invitrogen (Darmstadt)
BAPTA/AM	Merck (Darmstadt)
BCECF/AM	Invitrogen (Darmstadt)
Benz-cAMP	Biolog (Bremen)
B-Mercaptoethanol	Sigma Aldrich (Steinheim)
Bond-Breaker TCEP Solution, Neutral pH	Thermo Scientific (Bonn)
Bovine serum albumin (BSA)	Sigma Aldrich (Steinheim)
Rp- isomer (Rp-8-Br-cAMP)	Biolog (Bremen)
Casy™ blue	Roche (Basel)
Casy™ clean	Roche (Basel)
Casyton isoton solution	Roche (Basel)
Cell Freezing Medium-DMSO Serum free 1x	Sigma Aldrich (Steinheim)
C5a	R&D (Wiesbaden)
8-pCPT-2'-O-Me-cAMP or "007")	Biolog (Bremen)
Complete EDTA-free protease inhibitor cocktail	Roche (Basel)
Cytochalasin B	Sigma Aldrich (Steinheim)
Cytochalasin D	Sigma Aldrich (Steinheim)
DAKO fluorescent mounting medium	Dako Inc. (Glostrup)
Deoxyribonuclease I, Amplification Grade	Invitrogen (Darmstadt)
Dextran fluorescein 40,000MW	Invitrogen (Darmstadt)
Dimethyl sulfoxide (DMSO)	Sigma Aldrich (Steinheim)
Dulbecco's Phosphate Buffered Saline	Sigma Aldrich (Steinheim)
Dulbecco`s PBS with Ca/Mg	PAA laboratories (Cölbe)
ECL™ Western Blotting Detection Reagents	GE healthcare (Munich)
EBM-2 Basal Medium 500 ml	Lonza (Cologne)
EGM-2 MV SingleQuot Kit Suppl. & Growth Factors	Lonza (Cologne)

EGM-2 SingleQuots	Lonza (Cologne)
Ethanol	Merck (Darmstadt)
Ethylendiamintetra essig acid (EDTA)	Serva (Heidelberg)
Evans Blue E2129 - Dye content ≥75 %	Sigma Aldrich (Steinheim)
Fetal bovine serum (FBS) mycoplex	PAA laboratories (Cölbe)
Fibronctin from bovine plasma	Sigma Aldrich (Steinheim)
fMLP	Sigma Aldrich (Steinheim)
Formamid zur Analyse EMSURE®	Merck (Darmstadt)
Forskolin	Sigma Aldrich (Steinheim)
Gelatin solution 2%	Sigma Aldrich (Steinheim)
Glycerin	Merck (Darmstadt)
HBSS without Ca/Mg with Phenolred	PAA laboratories (Cölbe)
HBSS without Phenolred	PAA laboratories (Cölbe)
Hanks'-based cell dissociation buffer Gibco®	Invitrogen (Darmstadt)
HEPES solution (1M, pH 6,5-7,5)	Sigma Aldrich (Steinheim)
Histamine	Sigma Aldrich (Steinheim)
Histopaque 1077	Sigma Aldrich (Steinheim)
Histopaque 1119	Sigma Aldrich (Steinheim)
Hoechst dye 33342 (10mg/ml)	Invitrogen (Darmstadt)
Hydrogen peroxide	Serva (Heidelberg)
IBMX	Sigma Aldrich (Steinheim)
IL-1ß/IL-1F2 (recombinant Human)	R&D (Wiesbaden)
IL-8 (recombinant Human)	Peprotech (Hamburg)
Isofluran (Foren)	Baxter (Unterschleißheim)
Isopropanol	Merck (Darmstadt)
Leupeptin, Hemisulfate, Microbial	Merck (Darmstadt)
L-Glutamin Gibco® Cell Culture (100x)	Invitrogen (Darmstadt)
Lipopolysaccharides from Escherichia coli	Sigma Aldrich (Steinheim)
Magnesium chlorid	Sigma Aldrich (Steinheim)
MCDB 131 medium	Invitrogen (Darmstadt)
Medium 199 (10x)	Invitrogen (Darmstadt)
Methanol EMPLURA®	Merck (Darmstadt)
ML-9	Merck (Darmstadt)
N6-Benzoyl-cAMP	Biolog life science (Bremen)
Nonessential amino acids (NEAA) (100x)	Invitrogen (Darmstadt)
Novex® Sharp Pre-stained Protein Standard	Invitrogen (Darmstadt)
NuPAGE® LDS Sample Buffer (4X)	Invitrogen (Darmstadt)
NuPAGE® MES SDS Running Buffer	Invitrogen (Darmstadt)
NuPAGE® MOPS SDS Running Buffer	Invitrogen (Darmstadt)

Paraformaldehyde (PFA)	Sigma Aldrich (Steinheim)
8-pCPT-2´-O-Me-cAMP / ``007``	Biolog life science (Bremen)
Penicillin / Streptomycin Gibco® Cell Culture	Invitrogen (Darmstadt)
2-Propanol	Merck (Darmstadt)
Protein A Sepharose	Sigma Aldrich (Steinheim)
Sodium Bicarbonate Gibco® Cell Culture 7.5%,	Invitrogen (Darmstadt)
Sodium fluoride for analysis EMSURE®	Merck (Darmstadt)
Sodium Orthovanadate	Merck (Darmstadt)
Sodium pyruvat Gibco® Cell Culture (100x)	Invitrogen (Darmstadt)
Stop Reagent for TMB Substrate	Sigma Aldrich (Steinheim)
Thrombin from human plasma	Sigma Aldrich (Steinheim)
TMB Liquid Substrate System	Sigma Aldrich (Steinheim)
TNFα (recombinant human)	Peprotech (Hamburg)
Triza base	Sigma Aldrich (Steinheim)
Trypsin-EDTA- solution	Lonza (Cologne)
Trypanblue solotion	Sigma Aldrich (Steinheim)
Tyrode puffer (calcium free, pH7.4) (CAFTY)	PAA laboratories (Cölbe)
Tween-20	Merck (Darmstadt)
VEGF 165 (recombinant human)	R&D (Wiesbaden)
Triton buffer	PAA laboratories (Cölbe)
TRIzol® RNA extraction reagent	Invitrogen (Darmstadt)
Water, sterile-filtered (cell culture)	Sigma Aldrich (Steinheim)
W54011	Sigma Aldrich (Steinheim)
Assay/Kits	**Provider**
cAMP Biotrak Enzymeimmunoassay System	GE healthcare (Munich)
BCA Protein Assay (bicinchoninic acid)	Thermo Scientific (Bonn)
ImProm-IITM Reverse Transcription System	Promega (Mannheim)
Nucleofector® kit-OLD	Lonza (Cologne)
qPCR MasterMix Plus 7.5 ml	Eurogentec (Belgium)
Rap1 activation assay kit	Upstate technology (Billercia)
RNase mini kit	Qiagen (Hilden)

4.1.2. Antibodies

Table 2 List of primary antibodies and their providers

Antigen (reactivity)	Clone	Source	Company
β-actin	(monoclonal)	Mouse	Sigma Aldrich (Steinheim)
β-tubulin	SAP.4G5 (monoclonal)	Mouse	Sigma Aldrich (Steinheim)
CD11b/Mac-1	ICRF44	Mouse	BD Bioscience (Heidelberg)
Cortactin (p80/85)	4F11 (monoclonal)	Mouse	Upstate technology (Billercia)
E-selectin (CD62E)	1.2B6 (monoclonal)	Mouse	Abcam (Cambridge, UK)
ICAM-1 (CD54)	MEM-111 (monoclonal)	Mouse	Abcam (Cambridge, UK)
ICAM-1 (CD54)	BBIG-I1 (11C81) (monoclonal)	Mouse	R&D systems (Wiesbaden)
Phospho-MLC 2 (Thr18/Ser19)	Polyclonal	Rabbit	Cell Signaling (Frankfurt)
VCAM-1	6G9 (monoclonal)	Mouse	Abcam (Cambridge, UK)
VASP (phospho Ser157)	(polyclonal)	Rabbit	Abcam (Cambridge, UK)
VASP	(monoclonal)	Mouse	Abcam (Cambridge, UK)
VE-cadherin (C-19)	(polyclonal)	Goat	Santa Cruz (Santa Cruz)
VE-cadherin (11D4.1)	11D4.1 (monoclonal)	Rat	BD Bioscience (Heidelberg)
Vinculin	hVIN-1 (monoclonal)	Mouse	Sigma Aldrich (Steinheim)

Table 3 List of secondary antibodies and their providers

Antibody	Company
ECL rabbit IgG, HRP Linked Secondary Ab	GE healthcare (Munich)
Peroxidase AffiniPure Donkey Anti- Rat IgG (H+L)	Jackson (West Grove, PA)
ECL Mouse IgG, HRP-Linked Whole Ab (from sheep)	GE healthcare (Munich)
Alexa Fluor® 488 donkey anti-goat IgG (H+L) 2 mg/mL	Invitrogen (Darmstadt)
Alexa Fluor® 488 donkey anti-mouse IgG (H+L) 2 mg/mL	Invitrogen (Darmstadt)

4.1.3. Buffers

Table 4 Composition of buffers

Buffer	Composition
ACK lysis buffer	4.145 g NH_4Cl
	0.5 g $NaHCO_3$
	18.6 mg EDTA
	Add H_2O 500 ml
	pH 7.3
Lysis buffer for Co-immunoprecipitation (CoIP)	20 mM Imidazol (pH=6.8)
	100 mM NaCl
	2 mM $CaCl_2$
	1% (v/v) Triton-X-100
	0.04% (w/v) NaN_3
Lysis buffer to detect phosphorylation of MLC	20 mM Imidazol (pH=7.4)
	150 mM NaCl
	2 mM $CaCl_2$
	1 mM Na_3VO_4
	1% (v/v) Triton-X-100
	0.04% (w/v) NaN_3
Migration assay medium (MAM)	M199
	20% (v/v) FBS
	25 mM HEPES
PBST	PBS
	0.1% (v/v) Tween®-20
PMN wash buffer	HBSS
	10% (v/v) FBS
	25 mM HEPES
Phosphate Buffer (pH 6.8)	46.3 ml Na_2HPO4 (1M)
	53.7 ml NaH_2PO4 (1M)
	Add H_2O 1,000 ml
Rap1 lysis buffer	100 mM Tris-HCl, pH 7.4
	10% (v/v) glycerol
	5 mM $MgCl_2$
	1 M NaCl
	2% (v/v) NP40
	10 ug/ml aprotinin
	10 ug/ml leupeptin
	25 mM NaF
	1 mM sodium orthovanadate

TBST (10x)	80 g NaCl
	2 g KCl
	30 g Tris
	5 ml Tween 20
	Add H_2O 1,000 ml
	PH 7.5
Transfer buffer	2.42 g Tris
	11.25 g glycin
	5 ml 10% (m/v) SDS
	100 ml MeOH
	Add H_2O 1,000 ml
	PH 8.3-8.5

4.1.4. Materials

Table 5 List of materials and their providers

Mterials	Company
Amersham Hybond-P (30 cm × 3 m)	GE healthcare (Munich)
Falcon Conical Tubes (polystyrene) (15 ml, 50 ml, 200 ml)	BD (Heidelberg)
Falcon Cell Culture Flasks (75 cm², 175 cm²)	BD (Heidelberg)
Biohit proline (25-250 µl, 5-100 µl, 50-1200 µl)	Biohit (Rosbach)
CASY cups	Roche (Basel)
Falcon Multiwell(6-well, 12-well, 24-well)	BD (Heidelberg)
Cannula (27G.3/4") (26G.1/2") (23G.1 1/4")	BD (Heidelberg)
Cell cultrue dishes CELLBIND 100 mm	Corning (Kaiserslautern)
Costar Stripette Serological Pipets, (polystyrene)(5 - 50 ml)	Corning (Kaiserslautern)
Corning Cell Lifter	Corning (Kaiserslautern)
Corning Vacuum Filter/Storage Bottle System, 0.22 µm Pore	Corning (Kaiserslautern)
Corning Tubes (polypropylene)(15 ml, 50 ml)	Corning (Kaiserslautern)
Cryo 1°C freezing container Nalgene	Nalgene (Tuntenhausen)
CryoTube Vials 1.8 ml NUNC	Thermo Scientific (Bonn)
ECIS arrays-10 electrode array (96 well)	Ibidi (Munich)
Eppendorf- reaction tubes (0.5 ml, 1.5 ml, 2.0 ml)	Eppendorf (Hamburg)
EpT.I.P.S. Pipettenspitzen (10 µl - 1000 µl)	Eppendorf (Hamburg)
Eppendorf Pipetten (2.5 µl - 1000 µl)	Eppendorf (Hamburg)
Glas coverslides (12 mm, round)	Menzel (Braunschweig)
Kodak BioMax XAR Film	Sigma (Steinheim)
Membrane Nitrocellulose	GE healthcare (Munich)
Membrane PVDF	GE healthcare (Munich)

Microscope slides 76-26 mm	Menzel (Braunschweig)
Microplates 96-well (UB, VB, FB)	Greiner (Frickenhausen)
Microtiter plates Cellstar 384-well	Greiner (Frickenhausen)
Millex GP 0.22 µm Filter	Millipore (Bedford, MA)
Neolus 20G x2 ¾''0.9x70 mm steril	Terumo (Eschborn)
NuPAGE Novex 4-12% Bis-Tris Gel 1.0 mm, 10 well	Invitrogen (Darmstadt)
NuPAGE Novex 12% Bis-Tris Gel 1.0 mm, 10 well	Invitrogen (Darmstadt)
NuPAGE Novex 10% Bis-Tris Gel 1.0 mm, 10 well	Invitrogen (Darmstadt)
NuPAGE Novex 8% Bis-Tris Gel 1.0 mm, 10 well	Invitrogen (Darmstadt)
NuPAGE Novex 6% Bis-Tris Gel 1.0 mm, 10 well	Invitrogen (Darmstadt)
PC transwell inserts 6.5-mm-diameter, 5.0-µm pore size	Corning (Kaiserslautern)
PC transwell inserts 6.5-mm-diameter, 0.4-µm pore size	Corning (Kaiserslautern)
QIAshredder (250)	Qiagen (Hilden)
STIEFEL Biopsy punch 8 mm	GSK (Bühl)
Thick Blot paper	BioRad (Munich)

4.1.5. Equipments

Table 6 List of equipments and their providers

Equipments	Company
PRISM 7900HT sequence detection system	Applied Biosystems (Darmstadt)
BBD 6220 Incubator	Heraeus (Hanau)
GFL water quench	GFL (Burgwedel)
CASY cell counter	Roche (Basel)
Cell QuestTM Pro (Version 5.2.1)	Becton Dickinson (Heidelberg)
Centrifuge Varifuge 3.0R	Heraeus (Hanau)
Centrifuge 5415R	Eppendorf (Hamburg)
ECIS Model 9600	Applied Biosystems (Darmstadt)
Developer Curix 60	Agfa (Mortel-Belgien)
FACS Calibur	Becton Dickinson (Heidelberg)
Fluorescence microscope Axioskop	Carl Zeiss AG (Jena)
GeneChip® Human Gene 1.0 ST	Affymetrix (Santa Clara, CA, USA)
Genedata Expressionist®	Genedata (Martinsried, Germany)
iBlot Gel Transfer Device	Invitrogen (Darmstadt)
KS250 basic	IKA (Staufen)
LSM 510 meta	Carl Zeiss AG (Jena)
LSM 710	Carl Zeiss AG (Jena)
Lumino box	Hamamatsu (Japan)
Microscope Axiovert 135	Carl Zeiss AG (Jena)
Amaxa Nucleofector® I Device	Lonza (Cologne)

pH meter	WTW (Weilheim)
Steril bank HeraSafe	Heraeus (Hanau)
Tecan Safire miccroplate reader	Tecan (Crailsheim)
Thermomixer comfort (1.5 ml and 2.0 ml)	Eppendorf (Hamburg)
Trans-Blot SD Semi-Dry Transfer Cell	BioRad (Munich)
XCell SureLock™ Mini-Cell Electrophoresis System	Invitrogen (Darmstadt)

4.2. Methods

4.2.1. Molecular biological methods

4.2.1.1. Microarray analysis

After 12 h of serum starvation in basal medium, HUVECs were further cultured in EBM-2 supplemented with 100 nM ADM, 10 µM FSK or without compounds for 4 h and 16 h. The entire process was performed according to the Affymetrix instructions. Total RNA was isolated from the cells using TRIzol® RNA extraction reagent. Double-stranded cDNA was synthesized from total RNA, and *in vitro*-transcription was performed to produce biotinlabeled cRNA. After fragmentation, the cRNA was hybridized onto a GeneChip® Human Gene 1.0 ST Array at 45 ℃ with 60 rpm for 17 hours in a Hyb ridization oven. Normalization, filtering, and gene ontology analyses of the data were performed with Genedata Expressionist® software. GeneChip® Human Gene 1.0 ST Array consists of approximately 764,885 probe sets with a resolution number of 26 probes per gene, covering over 28,869 genes, whereas only genes with at least two fold changes were considered as significant. (Microarray and computational analysis were performed by Dr. Stefan Golz, Bayer HealthCareAG)

4.2.1.2. Quantitative Real-Time RT-PCR analysis

Endothelial cells cultured in 6 well plates or fresh isolated human PMNs were lysed with RLT buffer. Total RNA was isolated from the cell lysate using RNeasy mini kit, and converted to cDNA by reverse transcription using ImProm-II^{TM} Reverse Transcription System. The PCR was carried out under the following conditions: an initial denaturation step at 95 ℃ for 10 min, followed by 40 cycles at 95 ℃ for 15 s and 60 ℃ for 60 s. Qua ntitative Taq-Man analysis was performed using the PRISM 7900 sequence detection system. Normalization was performed using β-actin as internal control, and relative expression was calculated using the following formula: relative expression=$2^{(15 - (CT_{probe} - CT_{actin}))}$. The parameter CT is defined as the threshold cycle number at which the amplification plot passed a fixed threshold above baseline. The resulting expression is given in arbitrary units.

Table 7 List of primers and fluorescent probes

CRLR (mouse)	
Primer 1	5'- GGCTTTTCCCACTCTGATGCT -3'
Primer 2	5'- GGCTGTACCCTTGCATGTCA -3'
Probe	5'- TCCGCAGTGCATCCTACACAGTG -3'

RAMP2 (mouse)	
Primer 1	5'- GCAGCCCACCTTCTCTGATC -3'
Primer 2	5'- GGAACGGGATGAGGCAGAT -3'
Probe	5'- AGAGGATGTGCTCCTGGCCATG -3'

RAMP3 (mouse)	
Primer 1	5'- ACCCCCCGGATGAAGTACTC -3'
Primer 2	5'- ACCACCAGGCCAGCCATAG -3'
Probe	5'- ATCGCGGTTCCTGTCGTGCTGACT -3'

β-actin (mouse)	
Primer 1	5'- ACGGCCAGGTCATCACTATTG -3'
Primer 2	5'- AGGAAGGCTGGAAAAGAGCC -3'
Probe	5'- CAACGAGCGGTTCCGATGCCC -3'

CRLR (human)	
Primer 1	5'- CTGATTCCATGGCGACCTG -3'
Primer 2	5'- CCCTGGAAGTGCATAAGGATG -3'
Probe	5'- AGGAAAGATTGCAGAGGAGGTATATGACTACATCATG -3'

RAMP2 (human)	
Primer 1	5'- GATCCACTTTGCCAACTGCTC -3'
Primer 2	5'- TGGCCAGGAGTACATCCTCTG -3'
Probe	5'- TGGTGCAGCCCACCTTCTCTGACC -3'

RAMP3 (human)	
Primer 1	5'- TTCTCATCCCGCTGATCGTT -3'
Primer 2	5'- ACACCACCAGGCCAGCC -3'
Probe	5'- ACCCGTCGTTCTGACTGTCGCCA -3'

ICAM-1 (human)	
Primer 1	5'- CCCCCCGGTATGAGATTGT -3'
Primer 2	5'- GCCTGCAGTGCCCATTATG -3'
Probe	5'- CATCACTGTGGTAGCAGCCGCA -3'

VCAM-1 (human)	
Primer 1	5'- AAGAGGCTGTAGCTCCCCG -3'
Primer 2	5'- TGACATGCTTGAGCCAGGG -3'
Probe	5'- ATCCTGTGGAGCAGGCAGCTCCCTA -3'

E-Selectin (human)

Primer 1	5'- TGCCTACTATGCCAGATGCCT -3'
Primer 2	5'- CGTCCTTGCCTGCTGGACT -3'
Probe	5'- ACCGCAACACCCATCACCACTTCAAT -3'

PECAM (human)

Primer 1	5'- TCTCCCAGCCCAGGATTTC -3'
Primer 2	5'- GATTCGCAACGGACTTCGAT -3'
Probe	5'- ATGCCCAGTTTGAGGTCATAAAAGGA -3'

β-actin (human)

Forward	5'- TCCACCTTCCAGCAGATGTG -3'
Reverse	5'- CTAGAAGCATTTGCGGTGGAC -3'
Probe	5'- ATCAGCAAGCAGGAGTATGACGAGTCCG -3'

4.2.1.3.   RNA interference

SiRNAs directed against the mRNAs of cortactin (QIAGEN) were transfected into HUVECs by Nucleofector® I device according to manufacturer's instructions. 1~1.5x10^6 HUVECs (Passage 2) were transfected with 3 μg siRNA using Nucleofector® Kit-OLD. Hs_CTTN_5 (target sequence: 5'-CACCAGGAGCATATCAACATA -3') and Hs_CTTN_6 (target sequence: 5'-ATGCAACTTATTGTATCTGAA -3') were used to down-regulate gene expression of human cortactin. The Lamin A/C siRNA (target sequence: 5'-AACTGGACTTCCAGAAGAACA-3') served as negative control. Efficiency of gene silencing was evaluated by Western blot of cortactin (1 μg/ml mouse-anti-cortactin antibody). All experiments to detect endothelial permeability and leukocyte extravasation were performed 48 h after transfection.

4.2.2.   Biochemical methods

4.2.2.1.   Measurement of cyclic AMP

Measurements of intracellular cAMP levels were performed using Amersham cAMP biotrack enzymeimmunoassay system according to the manufacturer`s instructions with minor modifications. Briefly, endothelial cells cultured in 24-well cell culture plate or freshly isolated PMNs were washed and stimulated at 37 ⁰C as indicated. After being stimulated, endothelial cells were washed with ice-cold

PBS containing Ca^{2+}/Mg^{2+} and extracted in 70% (v/v) ethanol overnight at -20 ⁰C. The extracts were collected in 1.5 ml Eppendorf tubes and ethanol was removed using vacuum centrifugation. Aliquots of the extracts and standards were processed for ELISA according to the manufactures instructions.

4.2.2.2.   Detection of VASP activation

After treatment, HUVECs grown in 6-well cell culture plate were rinsed with ice-cold PBS containing Ca^{2+}/Mg^{2+}, lysed with 300 µl of SDS sample buffer with freshly added Bond breaker TCEP solution, scraped into 1.5 ml Eppendorf tubes, and boiled immediately for 5 min. Extracts (20 µl) were separated on 4-12% gradient SDS-PAGE and transferred to polyvinylidenefluoride (PVDF) membrane using a Trans-Blot SD Semi-Dry Transfer Cell. PVDF blots were then incubated in TBST for 1 h and were blocked with 5% (w/v) nonfat milk in TBST for further 1 h. VASP phosphorylation was detected with 1 µg/ml of rabbit anti-phospho Ser157-VASP antibody and total VASP was detected with 1 µg/ml mouse monoclonal anti-VASP antibody. After incubation with primary antibodies diluted in TBST at 4 ⁰C overnight, PVDF blots were washed with TBST (3 x 5 min), incubated with peroxidase-conjugated secondary antibodies (goat anti-rabbit IgG, 1:10,000 dilution; or goat anti-mouse IgG, 1:10,000 dilution) diluted in TBST for 1 h, and completely washed with TBST (4 x 15 min). Finally, binding of antibodies was visualized on Hyperfilm x-ray films using ECL detection system. Tubulin blots were performed as loading control.

4.2.2.3.   Detection of MLC phosphorylation

After treatment, endothelial cells cultured in 6-well plate were washed with ice-cold PBS containing Ca^{2+}/Mg^{2+}, lysed with 200 µl of lysis buffer for detection of tyrosine-phosphorylation, and scraped into 1.5 ml Eppendorf tubes. Lysates were centrifuged at 4 ℃ for 10 min at 13,000 rpm. Supernatants were then adjusted with SDS sample buffer (4x) and bond-breaker solution (20x), and boiled immediately for 5 min. 20 µl of Extracts were separated on 12% SDS-PAGE and transferred to PVDF membrane. Blots were analyzed as previously described (**4.2.2.2**). However, blocking buffer was replaced by 2% (w/v) BSA and 200 µM Na_3VO_4 was added overall to TBST, to preserve tyrosine phosphorylation during Western blot process by inhibition of any phosphatase

activity. MLC phosphorylation was detected with 1 µg/ml of rabbit anti- phospho-MLC 2 (Thr18/Ser19) antibody and vinculins were detected with mouse monoclonal anti-VASP antibody (1:1,000) as loading control.

4.2.2.4.   Rap1 Pull-down assay

To test for the activation levels of the small GTPase Rap1 the Rap1 pull down assay (Millipore) was employed according to the manufacturer's recommendations. In brief: a GST-tagged fusion protein, corresponding to residues 788-884 of human Ral GDS-Rap Binding Domain (RBD), expressed in *E. Coli.* and bound to glutathione-agarose (Millipore) is provided with the detection kit as probe for coimmunoprecipitation of GTP bound (active) Rap1.. RBD is a specific interaction partner of GTP-RAP1.Endothelial cells grown in 90-mm dishes were cultured to 85-90% confluence and treated with either agonists or vehicle control in medium. The cells were lysed on ice in lysis buffer, scraped into 1.5 ml Eppendorf tubes and debris was removed by a 10 min centrifugation at 13,000 rpm (4 ºC). 50 µl of the supernatants were transferred into new 1.5 ml Eppendorf tubes and kept on ice during the assays as control of total Rap-1 expression in total lysates. The rest of supernatants were incubatede with 30 µg of Ral GDS-RBD glutathione-agarose for 1 h at 4 ºC with gentle agitation. Agarose beads with precipitated GTP-Rap-1 were washed three times with lysis buffer, lysed with 25 µl of 2x SDS sample buffer with Bond breaker TCEP solution and boiled immediately for 5 min.

20 µl Extracts were separated on 12% gradient SDS-PAGE and transferred electrophoretically to PVDF membranes. Blots were analyzed as previously described (**4.2.2.2**). PVDF blots were probed in primary anti-Rap1 antibodies (1:500 dilution in TBST) at 4 ºC overnight, and incubated with peroxidase-conjugated secondary antibodies (goat anti-rabbit IgG, 1:10,000 dilution in TBST) for 1 h at room temperature, followed by ECL detection system. Total Rap1 iwas determined in cell lysates without previous precipitation.

4.2.2.5.   Co-immunoprecipitation of VE-PTP/VE-cadherin

bEnd.5 cells were washed and starved with MCDB 131 medium containing 1% (w/v) BSA for 2 h, followed by incubation with ADM (100 nM, 15 min) and

subsequently stimulation with VEGF (100 ng/ml, 30 min) in MCDB 131 medium with 1% (w/v) BSA. After stimulation, bEnd.5 cells were washed twice with ice-cold PBS to remove the stimulation medium. For docking of lymphocytes, bEnd.5s cells were pre-stimulated with TNFα (5 nM) overnight. On the day of assay, $3x10^7$ ovalbumin-specific antigen-stimulated T cells were allowed to bind to the bEnd.5 cells in a 90 mm-falcon cell culture dish for 10 min. Then, T-cells were carefully and completely removed by washing the cells with warm PBS, to avoid the degradation of VE-cadherin by lymphocyte proteases.

After stimulation with VEGF or docking of T-lymphocytes, bEnd.5 cells were lysed on ice in 500 µl lysis buffer for co-immunoprecipitations (CoIP) and scraped into 1.5 ml Eppendorf tubes. Lysates were centrifuged at 4 °C for 30 min at 13,000 rpm. 50 µl Aliquots were set aside on ice for direct blot analysis.Supernatants for CoIP were incubated for 2 h at 4 °C with 30 µl protein A-sepharose loaded with the 3 µg VE-PTPc antibodies (provided by Prof. Dietmar Vestweber). Immunocomplexes were washed five times with lysis buffer, subsequently dissolved in 25 µl SDS sample buffer (2x), and boiled immediately for 5 min. Total cell lysates were separated by electrophoresis on 8% SDS-PAGE, whereas immunocomplexes were separated on 6% SDS-PAGE. After being transferred to nitrocellulose membranes, blots were analyzed as previously described (**4.2.2.2**). Nitrocellulose blots were probed in 1 µg/ml primary anti-VE-cadherin (11D4) antibody at 4 °C overnight and incubated with peroxidase-conjugated secondary [donkey anti-rat antibodies (1:10,000)] for 1 h at room temperature. After washing with TBST, chemiluminescence signals were detected by use of ECL-detection system. After detection of VE-cadherin, blots were further used to detect VE-PTP. The same blots were washed with TBST for 1 h, blocked with 5% (w/v) nonfat milk for additional 1 h, and probed with anti-VE-PTPc antibody (0.5 µg/ml) for 1 h at room temperature, followed by incubation in peroxidase conjugated anti-rabbit antibody (1:10,000) for further 1 h. Chemiluminescence signals for VE-PTP were recorded on Hyperfilm x-ray films using ECL detection system.

4.2.2.6.   Immnuofluorescence staining

HUVECs were cultured on fibronectin-coated, 12-mm-diameter glass cover slides bathed in full medium. After the HUVECs reached confluence, endothelial monolayers were treated with the agonist or vehicle, fixed and permeabilized with ice-cold 100% (v/v) ethanol for 10 minutes at -20 ºC and were then incubated for 60 min in PBS containing 5% (w/v) BSA. Thereafter, the cover slides were immunolabeled for 60 min at room temperature with 5 µg/ml goat anti-VE-cadherin (C19) antibody or 10 µg/ml monoclonal anti-cortactin antibody. After rinsing twice with PBST and three times with PBS, binding of primary antibodies was visualized by incubation with Alexa-488-conjugated donkey anti-goat antibody (for VE-cadherin; 1:1,000) or Alexa-488-conjugated donkey anti-mouse antibody (for cortactin; 1:1,000) for 60 min at room temperature. The F-actin cytoskeleton was visualized by incubating cover slides with Alexa-555-conjugated phalloidin. The cover slides were then washed again twice with PBST and three times with PBS and covered with DAKO mounting medium. Prepared cover slides were analyzed using a confocal laser-scanning microscope LSM 710.

4.2.3.   Cell culture methods

4.2.3.1.   Cell culture condition

bEnd.5

The mouse endothelioma cell lines bEnd.5 cells were kindly provided by Prof. Dietmar Vestweber (MPI Münster, Germany). The bEnd.5 cells were cultivated at 37 ℃ and 10% CO_2 in Dulbecco's modified Eagle's medium (DMEM) supplemented with 10% (v/v) inactivated fetal calf serum (FCS), 2 mM L-glutamine, 1% (v/v) sodium pyruvate, 1% (v/v) penicillin/streptomycin, 1% (v/v) NEAA and 0.1% (v/v) β-mercaptoethanol. Cells were passaged 1:4 every 14 days in 90 mm falcon cell culture dishes.

CHO-ADM1-reporter cells

CHO-ADM1-reporter cells were generated and kindly provided by Dr. Frank Wunder (Bayer Healthcare, Wuppertal, Germany). Cells were cultured as

previously descript (Wunder et al., 2008) at 37 °C and 5% CO_2 in DMEM/NUT mix F-12 with L-glutamine, supplemented with 10% (v/v) inactivated FCS, 1 mM sodium pyruvate, 0.9 mM sodium bicarbonate, 50 U/ml penicillin, 50 µg/ml streptomycin, 2.5 µg/ml amphotericin B, 0.6 mg/ml hygromycin B, and 0.25 mg/ml zeocin. In addition, 1 mg/ml G-418 was added to the cell culture medium used for the ADM1 receptor cell lines. Cells were passaged using enzyme-free/Hanks'-based cell dissociation buffer.

CREB-reporter cells

Cells were generated and kindly provided by Dr. Frank Wunder (Bayer Healthcare, Wuppertal, Germany). Transfected CHO cells were cultured at 37 °C and 5% CO_2 in DMEM/NUT mix F-12, supplemented with 10% (v/v) inactivated FCS, 2% (v/v) sodium pyruvate, 2% (v/v) sodium bicarbonate, 1% (v/v) penicillin/streptomycin, 1% (v/v) HEPES, and 2% (v/v) Glutamin. Cells were passaged using 0.05% trypsin-EDTA.

Human umbilical vein endothelial cells (HUVECs)

HUVES were purchased from Lonza Inc. and propagated in EBM-2 basal medium supplemented with EGM-2 Single Kit containing 2% fetal bovine serum (FBS), hFGF-B, VEGF, R3-IGF, ascorbic acid, hEGF, GA-1000, heparin, and hydrocortisone at 37 °C in a humidified atmosphere of 5% CO_2. Confluent cultures of primary endothelial cells were detached with 0.05% trypsin-EDTA and seeded on 90-mm cell-culture CELLBIND dishes at 1:4 to confluence. Experiments were performed using confluent endothelial cell monolayer at passage 1-4.

Human lung microvessel endothelial cells (HLMECs)

HLMECs were obtained from Lonza Inc., cultured according to the manufacturer`s recommendations and used for experiments at passage 1-4. Cells were cultured in EBM-2 basal medium supplemented with EGM-2 MV SingleQuot Kit containing 5% FBS, hFGF-B, VEGF, R3-IGF, ascorbic acid, hEGF, GA-1000, heparin, and hydrocortisone at 37 °C in a humidified atmosphere of 5% CO_2. Cells were passaged with 0.05% trypsin-EDTA 1:4 in

90 mm Cellbind corning cell culture dishes. Confluent endothelial cell monolayer at passage 1-4 was used for our experiments.

OTII-Ova1-T-cells

OTII-Ova 1 T-cells with ovalbumin specific T-cell receptors were isolated from 6-8 week old OTII mice and were kindly provided by Prof. Dietmar Vestweber (MPI Münster, Germany). T-cells were restimulated at 37 °C and 10% CO_2 in RPMI medium supplemented with 10% (v/v) T-cell FCS, 4 mM L-glutamine, 1% (v/v) sodium pyruvate, 1% (v/v) penicillin/streptomycin, 1% (v/v) NEAA, 0.1% (v/v) β-mercaptoethanol, and 1% (v/v) IL-2 supernatant. $1{\sim}1.5x10^6$ T-cells were cultured for 2 days in a 90 mm-falcon cell culture dishes.

4.2.3.2. Aequorin luminescence measurements

Luminescence measurements were performed on opaque 384-well microtiter plates as previously describt with minor modification (Wunder et al., 2008). For the assays, 2,500 cells/well cultured for 24 h and were then loaded for 3 h with 0.6 µg/ml coelenterazine in Ca^{2+}-free Tyrode solution (CAFTY) at 37 °C and 5% CO_2. To prevent cAMP degradation by endogenous phosphodiesterases (PDEs), cells were pre-incubated with 3-Isobutyl-1-methylxanthine (IBMX) (200 µM) for 30 min. Afterwards, compounds were added for 6 min in CAFTY containing 0.1% bovine serum albumin. Immediately before adding Ca^{2+} ions (final concentration 3 mM), measurement of the aequorin luminescence was started using a luminometer. Luminescence was monitored continuously for 60 s.

4.2.3.3. CREB phosphorylation in luciferase-transfected CHO cells

Detection of CREB phosphorylation was performed on opaque 384-well microtiter plates using Luceferase-transfected CHO cells. 10,000 CHO-cells were cultured for 24 h in 25 µl medium on 384-well microtiter plates at 37 °C and 5% CO_2. For the assays, cells were incubated with 10 µl compounds for 4 h at 37 °C and 5% CO_2, followed by the addition of 35 µl luciferase buffer containing triton. Measurement of the luminescence was immediately started by using a luminometer. Luminescence was monitored continuously for 60 s.

4.2.3.4. Cell surface expression of adhesion molecules

Cell surface expression of adhesion proteins (ICAM-1, VCAM-1, and E-selectin) by HUVECs was quantified by use of cell surface ELISA. HUVECs were grown to subconfluence (~80%) in 96-well plates coated with 0.01% (v/v) fibronectin. After overnight pre-incubation with TNFα (5 nM), indicated concentrations of compounds were added to HUVECs for 30 min. Subsequently, the cells were washed with PBS (Ca^{2+}/Mg^{2+}) and fixed with 4% paraformaldehyde (PFA) for 30 min at 4 ºC, followed by the addition of 3% (v/v) nonfat milk in PBS for 1 h at room temperature to reduce nonspecific binding. Following washes with PBS, HUVECs were incubated with primary monoclonal antibody overnight at 4 ºC [ICAM-1 antibody (clone: MEM 111) 1:500; VCAM-1 antibody (clone: 6G9) 1:1,000; and E-selectin antibody (clone: 1.2B6) 1:3,000]. On the next day, the cells were washed with PBS and incubated with peroxidase-conjugated goat anti-mouse secondary antibody (1:500) for 1 h. After being completely washed with PBS, the cells were exposed to the TMB substrate solution, followed by addition of TMB stop solution. The absorbance at 490 nm was measured by use of a Tecan microplate reader.

4.2.3.5. Measurement of transendothelial electrical resistance (TEER)

Measurement of transendothelial electrical resistance (TEER) across confluent endothelial cells was performed using the electrical cell-substrate impedance sensing system (ECIS). Confluent cultures of primary endothelial cells were detached with 0.05% trypsin-EDTA, resuspended in fresh medium and 3×10^4 cells in 300 µl medium were seeded per ECIS well coated with 0.25% (v/v) gelatine. Cells were cultured for 24 h or 48 h to reach the confluence before the assay. For each assay, one group of wells without seeded endothelial cells was used to control the function of electrical arrays during the experimentation, while one group with seeded endothelial cells without any treatment was considered as control for the monolayer. Relative TEER in % was presented as the ratio of TEER measured at a given time point set to the middle value of TEER in the same group at the beginning time point of the experiment. Area under the curve (AUC) was calculated to quantify this assay by using a baseline at 100%. AUC

above the baseline was considered as positive value, whereas AUC under the baseline was considered as negative value.

4.2.3.6. Detection of paracellular macromolecular permeability

To determine paracellular permeability, 4×10^4 HUVECs were seeded per Transwell® filter (6.5-mm-diameter, 0.4-µm pore size), coated with 0.01% (v/v) bovine fibronectin. After 48 h incubation HUVECs reached confluence and were used for permeability assay on the third day after plating. Macromolecular permeability was analyzed with 0.25 mg/ml FITC-dextran (40 kDa). 50 µl FITC-dextran was added to the upper compartment of Transwell® filter. 30 min later, 100 µl aliquot was taken from the lower compartment for fluorescence measurement as the baseline value of the assay and 100 µl fresh medium was added immediately. 50 µl Vehicle or compounds as indicated were dissolved in FITC-dextran and added to the upper compartment. Every 30 min, fluorescence of a 100 µl aliquot from the lower compartment was measured and 100 µl fresh medium was refilled immediately during the whole assay. For the quantitative analysis of ADM and FSK, AUC was calculated. Area above X-axis and under the curve with relative FITC-intensity, as referred to to the mean value of the same group at the beginning time point of the experiment, was calculated as AUC.

4.2.3.7. Isolation of human neutrophils

Human polymorphonuclear neutrophils (PMNs) were isolated by Histopaque density gradients using the manufacturer's protocols with slight modification. First, 4 ml Histopaque-1077 was added to a 15 ml polypropylene centrifuge tube, after which 4 ml Histopaque-1119 was carefully added under the Histopaque-1077. 5 ml venous EDTA-coated blood samples were then carefully added to the upper gradient and centrifuged at 700x g for 30 min without brake at room temperature. After centrifugation, the neutrophils were located at the interface of the Histopaque-1077 and Histopaque-1119. The neutrophils were then transferred to a tube containing 30 ml PMN wash buffer and were washed twice by centrifugation at 400 x g for 10 min. Contaminating red blood cells were lysed by adding 5 ml ACK buffer for 4 min. Finally, neutrophils were

resuspended in migration assay medium (MAM) at a concentration of 1×10^7 PMN/ml and were kept at room temperature until used in the experiments.

4.2.3.8.   *In vitro*-transendothelial migration assay (TEM)

Quantitative leukocyte transmigration assay was performed using HUVECs plated at confluent density (2×10^4 cell/well) on Transwell® filter inserts (6.5-mm-diameter, 5.0 μm pore size), coated with 0.01% (v/v) bovine fibronectin. After 2 days, HUVECs reached confluence and were activated with 5nM TNFα overnight. As indicated, HUVECs or human PMNs were pre-treated with vehicle, compounds or antibodies for 30 min, then medium was removed and cells were washed three times to ensure that test compounds were largely absent during the incubation with leukocytes. 500,000 Human PMNs were added to the top Transwell® filter and were bathed in 600 μl MAM. Transmigration of PMNs across HUVEC monolayers was allowed for 60 min in MAM or 30 min in IL-8 stimulated MAM in a humidified incubator (37 ºC, 5% CO_2). After the transmigration, 500 μl cell-suspension from the bottom well was collected and transmigrated PMNs were counted using a CASY cell counter system.

4.2.3.9.   Adhesion assay

HUVECs were cultured on 96-well plates to confluence and pre-stimulated with 5 nM TNFα overnight. On the day of assay, HUVECs were washed twice with warm medium and treated with compounds for 30 min. Human PMNs were freshly isolated as previously described (**4.2.3.7**) and incubated in BCECF solution for 10 min at room temperature. After being labeled with BCECF, neutrophils were added to HUVEC monolayers and coincubated for 30 min at 37 ℃. Fluoresce intensity of the total applied cel ls was read using a Tecan plate reader. After being washed with medium (once, twice, and three times), the fluorescence intensity was measured after each wash. Relative fluorescence intensity was set to the fluorescence of total applied cells.

4.2.3.10.   Myeloperoxidase (MPO) activation assay

Human PMNs were freshly isolated from healthy volunteers as previously in **4.2.3.7** described. 2.5×10^4 PMNs in HBSS without Phenolred and 0.1% (v/v)

gelatine were pre-incubated with cytochalsin B (10 µg/ml) for 10 min at 37 ºC. The cells were then incubated with 10 µl PBS or increasing doses of compounds (ADM or FSK) for 10 min at 37 ºC, followed by further incubation with 10 µl C5a (10 nM) or fMLP (3 nM) for 10 min at 37 ºC. For the experiments to detect dose-response curves of C5a or fMLP, the cells were incubated with increasing doses of C5a (30 pM-30 nM) or fMLP (10 pM-30 µM) for further 10 min at 37 ºC. Finally, 30 µl of phosphate buffer (0.1 M, pH 6.8) were added to each well, followed by 60 µl of TMB substrate reagent for 20 min at room temperature. The reaction was stopped using 60 µl TMB stop solution. Absorbance was measured at 450 nm in a Tecan plate reader. Absorbance is an indicator for the level of released MPO.

4.2.3.11. Fluorescence activated cell sorting (FACS) analysis

PMNs (2×10^6) were incubated with vehicle and increasing doses of ADM (1 nM-1 µM) for 30 min at 37 ℃ in MAM buffer, followed by stimulation with 100 nM fMLP for further 30 min. Cells were then washed and incubated with phycoerythrin (PE)-labeled anti-CD11b monoclonal antibody or isotype control for 45 min on ice. Subsequently the neutrophils were washed three times with PBS and fixed with 1% PFA at room temperature. The expression level of CD11b was detected using FACSCalibur and data were analyzed with the software CellQuest™ Pro 5.2.1.

4.2.4. *In vivo*-experiments

4.2.4.1. Animals

All of the experiments conformed to the German federal animal protection law and were approved by the legal district authority. We used 5-6 weeks old adult male BALB/c mice (Harlan Nederland) and adult male 200 g -250 g Wistar rats (Harlan Nederland) for our study. All of the animals were housed in a standard room with a 12/12-hour light/dark cycle: white lights were on from 06:00 to 18:00 hours and the night phase was from 18:00 to 06:00 hours. The laboratory temperature was 23 ˚C and humidity 51.5% controlled. Food and water were available ad libitum, except during testing. The animals were randomly assigned to their respective treatment groups.

4.2.4.2.   Miles assay to determine vascular permeability

Modified Miles assays were performed as described previously (Schnoor et al., 2011). For mice, 100 µl Evans blue dye [1% (w/v)] and 100 µl vehicle or compounds (ADM, Benz-cAMP, and "007") were intravenously administered through retro-orbital injection under deep anesthesia with isoflurane. 10 min later, 50 µl PBS and 4.5 µg/ml histamine in PBS were injected intradermally into the back skin that was shaved 24 h before the assay. For rats, intravenous injection of 1 mg/kg body weight (BW) Evans blue dye [2% (w/v)] through a catheter into the femoral vein was performed. Afterwards, 100 µl PBS and 2.5 µg/ml, 5 µg/ml, 10 µg/ml, 20 µg/ml, and 40 µg/ml histamine were intradermally injected into the abdominal skin. 30 min later, mice and rats were sacrificed by an overdose of isoflurane and subsequent neck dislocation, and skin areas surrounding the sites of injections were excised using biopsy punch. Evans blue dye was extracted from the skin by incubation in formamide for 5 days at room temperature. Subsequently, the optic density of extracted dye was measured at 620 nm using a spectrophotometer. The concentration of extracted dye was calculated via a standard curve using 0, 1.25 mg/ml, 2.5 mg/ml, 5 mg/ml, 10 mg/ml, 20 mg/ml, 40 mg/ml, and 80 mg/ml Evans blue dyes. The ratio of extracted Evans blue dyes to skin sample weight was taken as a measure of vascular permeability.

4.2.4.3.   LPS-induced acute lung injury model

Neutrophil recruitment into the lung was analyzed in a murine model of LPS-induced pulmonary inflammation as previously described (Kang et al., 2001; Arsalane et al., 2000). Briefly, 1 mg/kg body weight (BW) of LPS in 100 µl saline was injected intratracheally under deep anesthesia with isoflurane and lungs were analyzed 48 h later. Sham animals received saline instead of LPS in the same manner. ADM or saline was injected subcutaneously immediately before and 24 h after LPS application. Mice were sacrificed with an overdose of isoflurane and the trachea of each mouse was intubated with a tube (PE 90) and bronchoalveolar lavage (BAL) fluid was collected (3x0.5 ml saline). BAL fluid was homogenated and the number of white blood cells (WBC) was

determined using Celldyn. Protein concentration was measured in the BAL fluid after the experiment using BCA Protein Assay Reagent.

4.2.5. Statistical analysis

Data are expressed as the means ± standard error of mean (SEM) or standard deviation (SD). The significance of differences between groups was assessed by the unpaired Student's t-test if allowed or otherwise by Mann-Whitney Rank Sum Test. Analysis, curve-fitting and calculation of the half-maximal effective concentrations (EC50) were performed using GraphPad Prim software (version 5.0; GraphPad Software Inc., San Diego, CA). Values of probability (P) < 0.05 were considered statistically significant.

5. RESULTS

5.1. Analysis of ADM receptor expression and signalling

ADM exerts its biological actions through binding to a heterodimeric GPCR complex composed of the CRLR associated with RAMP-2 or RAMP-3, which are essential to the receptor specificity, ligand affinity, and receptor desensitization. The first aim of the present studies was to characterize receptor expression and evaluate functional cAMP signaling of ADM in different endothelial cells.

First of all, the expression patterns of CRLR, RAMP-2, and -3 were analyzed by quantitative RT-PCR in three types of endothelial cells from mouse and man which are widely used in endothelial cell biology research: the murine brain endothelial cell line (bEnd.5), human primary umbilical vein endothelial cells (HUVECs) and human lung microvascular endothelial cells (HLMECs). Normalization was performed using β-actin as internal control, and relative expression was calculated as $2^{(15 - (CTprobe - CTactin))}$. The parameter CT is defined as the threshold cycle number at which the amplification plot passed a fixed threshold above baseline. The resulting expression is given in arbitrary units.

As shown in **Figure 6A**, in bEnd.5, relative expression levels of CRLR, RAMP-2, and -3 mRNA normalized to β-actin were equally high with approximately 10.000 arbitrary units. The absolute CT values of CRLR, RAMP-2, and -3 in bEnd.5 cells were 22.3 ± 0.4, 19.8 ± 0.3, 22.0 ± 0.1, respectively (mean ± SD). In primary human endothelial cells, the relative expressions of CRLR and RAMP 2 were lower than those in bEnd.5 cells. The CT values of CRLR and RAMP 2 in HLMECs were 33.2 ± 1.3 and 23.8 ± 0.2; while in HUVECs 31.7 ± 0.3 and 22.4 ± 0.1 (mean ± SD). The normalized expression levels of CRLR and RAMP-2 were comparable in HLMECs and HUVECs with 10 and 1,000 arbitrary units, respectively. RAMP-3 mRNA was hardly detectable (CT=40.0). In HUVECs, stimulation with ADM lead to an increase of intracellular cAMP in a

dose-dependent manner (**Figure 6B**). The saturation dose was achieved at 3 nM ADM inducing a maximal three-fold increase of cAMP levels. Because of their easy accessibility and their representative expression pattern of ADM receptor constituents for human endothelial cells and functional cAMP signaling after ADM stimulation, primary human umbilical endothelial cells were chosen to evaluate effects and signaling events of ADM *in vitro*.

Figure 6 Analysis of ADM receptor expression and signaling in endothelial cells

(A): Expression of CRLR, RAMP-2 and -3 in different endothelial cells. Quantitative real-time RT-PCR analysis was performed on mouse bEnd.5 cells (white bar), human lung microvascular endothelial cells (HLMVECs) (black bars) and human umbilical vein endothelial cells (HUVECs) (striped bars) using specific oligonucleotide primers and probes. Expression levels were normalized to β-actin as a house–keeping gene. (n=2, mean ± SD) **(B):** Evaluation of cAMP signaling in human endothelial cells. Intracellular cAMP accumulation was measured by use of a commercial ELISA. HUVECs were stimulated with different doses of ADM for 15 min and subjected to extraction in 70% (v/v) Ethanol overnight at -20 ºC. (n=2, mean ± SEM)
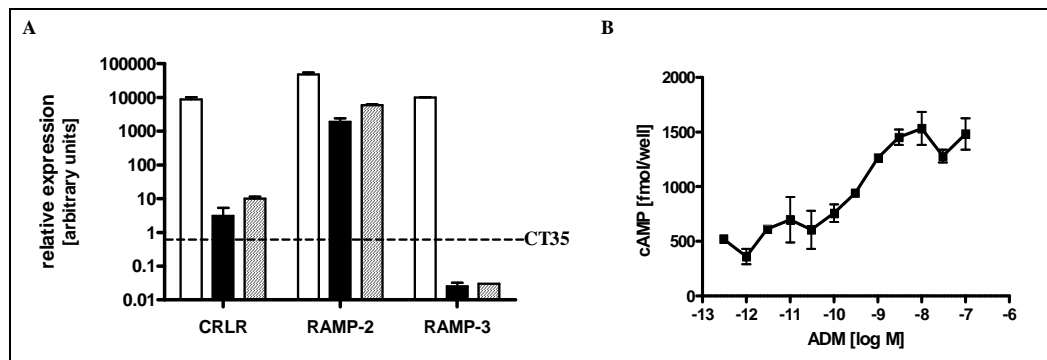
5.2. Effects of ADM on endothelial barrier integrity

Disruption of endothelial barrier contributes to tissue edema and facilitates leukocyte transmigration, which are hallmarks of inflammation. To evaluate the effects of ADM on endothelium under inflammatory conditions, two separate directions were explored: the regulation of endothelial permeability and the interference with granulocyte extravasation.

5.2.1. Anti-edematous effects of ADM *in vitro*

Cytokines such as TNFα, as well as components of the activated coagulation cascade such as thrombin are important mediators of acute inflammation. Thrombin impairs endothelial permeability via activation of protease activated receptors (PAR1-3) and in concert with TNFα, leads subsequently to vascular leakage thereby contributing to severe organ dysfunction (Seybold et al., 2005). Different stimuli, such as thrombin, TNFα, histamine, VEGF, IL-1β, and LPS, were used to mimic inflammation *in vitro*. Whether ADM could antagonize stimuli-induced hyperpermeability was first analyzed using different *in vitro*-models.

5.2.1.1. Effects of ADM on thrombin-induced endothelial hyperpermeability

Binding of thrombin to its PAR receptor activates heterotrimeric G-proteins, resulting in decrease of intracellular cAMP level, increase of calcium influx and activation of Rho-kinase, initially leading to phosphorylation of MLC and disrupted endothelial integrity (Garcia et al., 1995; Birukova et al., 2004b). On primary cultured HUVECs, two of the thrombin-responsive PARs, PAR-1 and -3, are expressed, of which only PAR-1 appears to be responsible for thrombin to affect cytoskeletal reorganization (Vouret-Craviari et al., 2002). Previous studies have demonstrated that pretreatment of ADM could reduce thrombin-induced hyperpermeability within 50 minutes using measurement of hydraulic conductivity (Hippenstiel et al. 2002). However, whether ADM could therapeutically attenuate thrombin-induced barrier dysfunction was still not investigated.

The ECIS model and the FITC-dextran model were applied to characterize permeability of endothelial monolayer *in vitro*. Using ECIS, the transendothelial electrical resistance (TEER) was determined as a surrogate for the permeability of the endothelial cell monolayer for water and ions. Untreated HUVECs displayed a stable monolayer over the entire experiment (**Figure 7A and B**). Thrombin induced a rapid decrease in TEER, which reached the peak of 36 ± 4.5% (mean ± SD) 45 min after stimulation. But this decrease was transient,

and TEER returned to its original level within 3 h after thrombin addition. The initial peak decrease is due to the release of calcium from intracellular stores, whereas the plateau phase accounts for extracellular calcium influx (Sandoval et al., 2001). The addition of ADM as a bolus rapidly enhanced the TEER of resting cells to 171 ± 5.7% (mean ± SD). TEER remained stable within the time frame tested. Addition of thrombin after ADM pre-incubation caused a similar netto decrease of TEER as without ADM pretreatment, however, the TEER was above the baseline value during the entire period and returned to 136 ± 15.9% (mean ± SD) similar to the ADM group without thrombin stimulation. Moreover, the decrease of TEER induced by thrombin was reverted immediately after ADM post-treatment and returned to 150 ± 7.4% (mean ± SD) which was in the same range as after ADM treatment without thrombin stimulation. Taken together, addition of ADM 30 min before or after thrombin administration antagonized and reversed thrombin-induced decrease of TEER, respectively.

In addition to TEER measurements, paracellular permeability for macromolecular 40 kDa FITC-dextran through an endothelial cell monolayer was analyzed (**Figure 7C-D**). Thrombin administration induced an increase of macromolecular permeability to 153 ± 27.2% (mean ± SD) after 60 min, which was consistent with the observations in the ECIS model. ADM pretreatment totally antagonized thrombin-induced hyperpermeability and even resulted in a less permeable monolayer as compared to the control cell monolayer during the entire experiment. Moreover, ADM post-treatment reversed thrombin-induced hyperpermeability to the levels of control monolayer.

Both methods consistently revealed that thrombin rapidly caused hyperpermeability of EC monolayers, whereas ADM attenuated this barrier disruption in both a prophylactic and therapeutic manner.

Figure 7 Effects of ADM on thrombin-induced hyperpermeability using different *in vitro*-models.

(A-B): HUVECs were seeded on 96-well ECIS microelectrode plates and TEER was continuously recorded. At the time points indicated by arrows, cells were treated with vehicle or 100 nM ADM or 0.5 U/ml thrombin and TEER was measured over 6 hours. Relative TEER was normalized to the TEER measured at the beginning of the experiment. **(C-D):** Endothelial cells were cultured on transwell filters and paracellular permeability for 40kDa FITC-dextran was determined at different time points. **(A and C):** Endothelial monolayer was pre-incubated with ADM 30 min prior to thrombin stimulation. **(B and D):** ADM administration was followed 30 min after thrombin incubation. (n=8 for ECIS and n=4 for FITC-dextran-permeability, mean ± SEM)
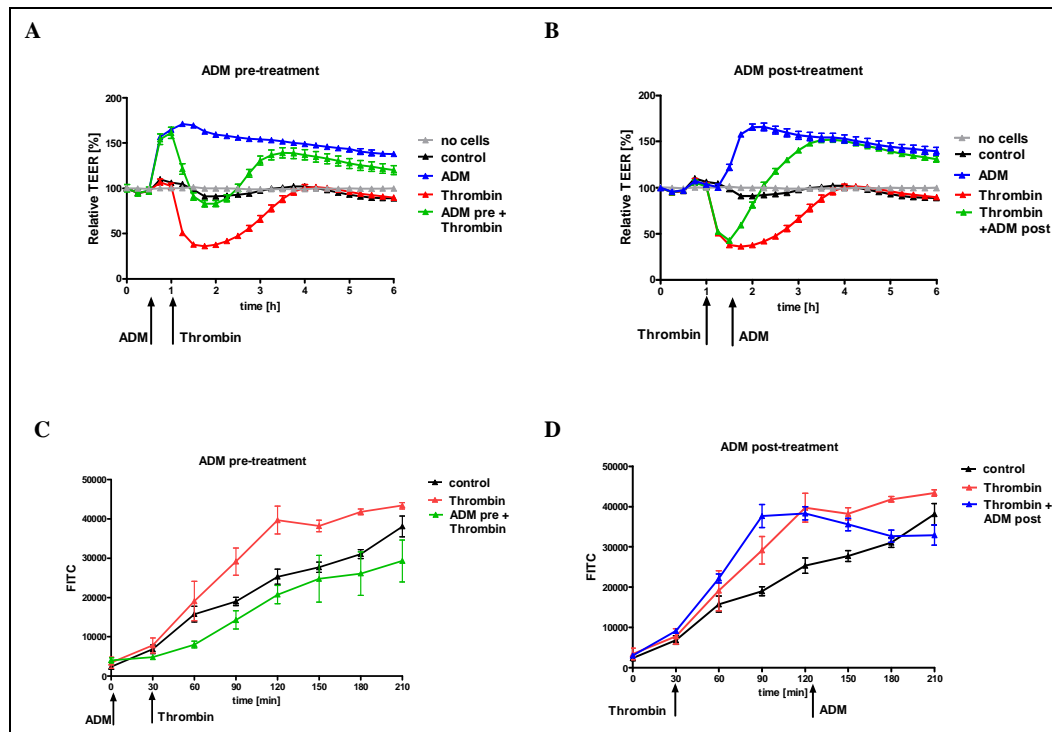
In the next step, fluorescence microscopy was applied to investigate whether the observed ADM effect on barrier integrity was paralleled by an effect on junctional proteins and the contractile apparatus. Cellular actin was visualized with Alexa-555 phalloidin and no changes in regular stress fiber and cortical actin architecture were observed after addition of ADM to quiescent cells (**Figure 8A and B**). Thrombin induced pronounced stress fiber formation followed by reduced cortical actin staining and retraction of cell mass toward the center (**Figure 8C**). In quiescent cells, the staining for VE-cadherin around cell border represents a continuous straight line (**Figure 8A**). This pattern was not changed by addition of ADM to normal cells (**Figure 8B**). Thrombin stimulation

led to visible cellular retraction and distorted VE-cadherin linear structure with visibly deficient VE-cadherin staining, forming a zigzagged line with gaps (**Figure 8C**). ADM incubation prevented the VE-cadherin distortion and gap formation, as well as stress fibers formation and retraction of the cell mass toward the center (**Figure 8D**). These findings suggested that ADM enhanced the association of VE-cadherin with membrane structures, particularly peripheral cortical actin, thus stabilizing barrier integrity.

Figure 8 Effect of ADM on thrombin-induced F-actin and VE-cadherin distribution.
HUVECs were grown to confluence on fibronectin-coated glass cover slides, stained for F-actin (red) and VE-cadherin (green), nucleus (blue), and visualized with 100-fold magnification. Cells treated with vehicle **(A)** or 100 nM ADM **(B)** displayed a well-arranged cortical actin with few stress fibers and continuous cell-cell junctions. Stimulation with 0.5 U/ml thrombin **(C)** caused a massive increase of stress fibers, distortion of VE-cadherin and formation of intercellular gaps. Pretreatment of ADM prior to thrombin stimulation **(D)** prevented VE-cadherin distortion and gap formation, and reduced stress fibers. Bars = 20 µm..
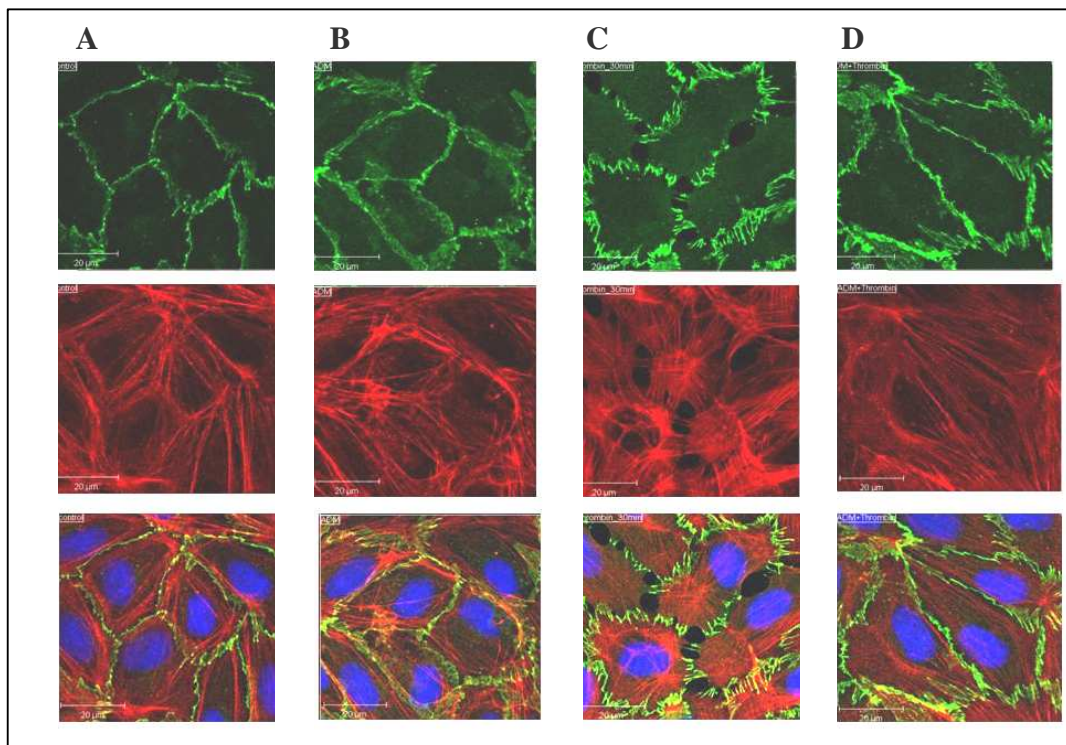
5.2.1.2. Effects of ADM on TNFα-induced endothelial hyperpermeability

TNFα is reported to induce vascular hyperpermeability *in vivo* and *in vitro* via direct activation of endothelial actomyosin-based cytoskeleton and formation of paracellular gaps via phosphorylation of MLCK. In addition, TNFα upregulates cyclic guanosine monophosphate (cGMP) -stimulated PDE2 thus decreasing intracellular cAMP levels thus facilitating barrier disruption (Seybold et al., 2005).

Unlike thrombin, TNFα provoked a slow and long lasting diminishing in TEER levels (**Figure 9A** and **B**). TEER gradually reached its trough at 63 ± 11.1% (mean ± SD) 5 h after stimulation with TNFα, and remained stable throughout the rest of the experiment. TEER did not recover as after thrombin stimulation. Addition of ADM as a bolus rapidly enhanced the TEER of resting cells to 159 ± 50.0% (mean ± SD) and stayed stable within the time frame tested. Similar to the group without ADM treatment, TNFα stimulation decreased TEER by ~50% after ADM pre-incubation, however, the TEER decreased only to its initial baseline level. Moreover, the TNFα induced decrease of TEER was reverted immediately after ADM posttreatment and returned to its initial baseline level with reaching the same level as the control group without stimulation. Addition of ADM 30 min prior to or 5 h following TNFα administration could both antagonize and reverse the decrease of TEER towards the baseline level of the control monolayer. This effect of ADM was also observed in the FITC-dextran model (**Figure 9C**). Addition of ADM reduced the endothelial permeability for FITC-dextran to 68 ± 7.2% (mean ± SD). 7 h TNFα stimulation induced a hyperpermeability of the endothelial monolayer to 164 ± 4.7%, whereas only to 143 ± 9.7% (mean ± SD) after ADM pretreatment. Like under thrombin stimulation, ADM attenuated TNFα induced endothelial hyperpermeability in both, a prophylactic and therapeutic manner.

Figure 9 Prophylactic and therapeutic potency of ADM on TNFα stimulation *in vitro.*
(A-B): HUVECs were grown on ECIS microelectrode plates to confluence. Monolayers were treated with vehicle or 100 nM ADM prior to or following 1 nM TNFα stimulation. **(C):** HUVECs were seeded onto transwell filters and paracellular permeability for 40 kDa FITC-dextran was determined. **(A and C):** Endothelial monolayer was pre-incubated with ADM 30 min prior to TNFα stimulation. **(B):** ADM was added 7 h after TNFα incubation. (n=8 for ECIS and n=4 for FITC-dextran-permeability, mean ± SEM) (*p<0.05; ***p<0.0005 vs. control group; ###p<0.0005 vs. TNFα group)
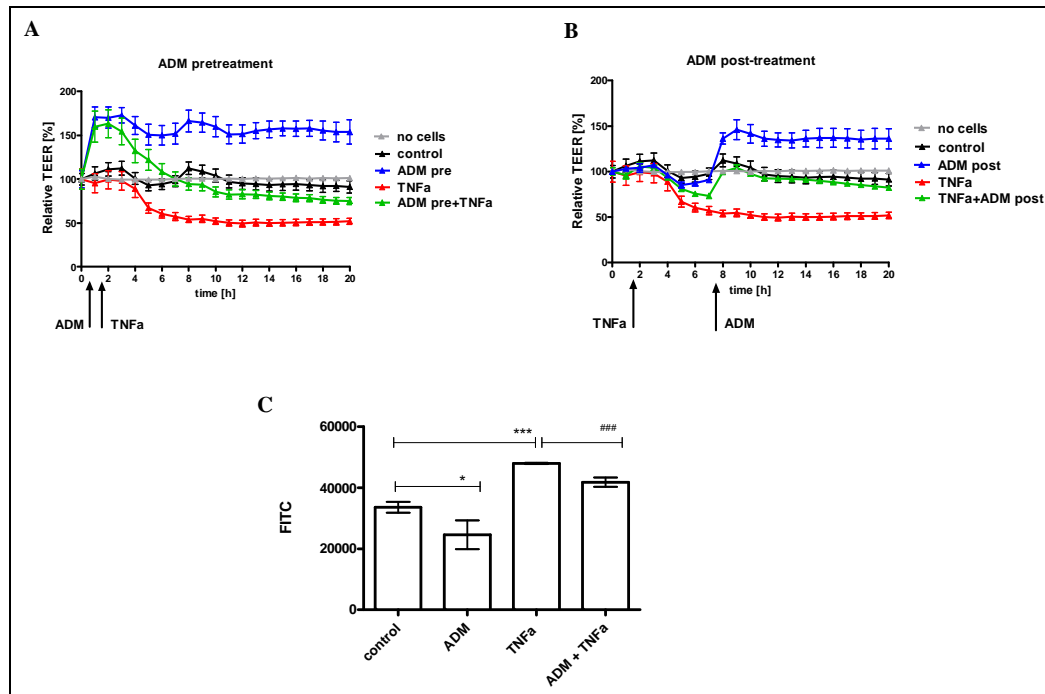
5.2.1.3.   Effects of ADM on endothelial hyperpermeability induced by different stimuli (LPS, Histamine, IL-1β, and VEGF)

Since ADM showed significant effects on stabilization of endothelial permeability against thrombin and TNFα stimulation, the question was raised whether these effects could also be transferred to other inflammatory stimuli, such as histamine, vascular endothelial growth factor (VEGF), lipopolysaccharide (LPS), and Interleukin 1β (IL-1β).

Histamine, an edematogenic factor mainly released by basophilic granulocytes, contributes to microvascular leakage in response to the acute inflammation associated with trauma, burns, and allergy. Upon binding of histamine to Gq-

coupled H1 receptor, intracellular calcium concentration is elevated, subsequently activating MLCK and triggering actin-myosin contraction. Histamine was also reported to activate MAP kinase downstream and to have direct effects on junctional proteins, phosphorylating and disrupting components of the adherence junction and tight junctions (reviewed by Kumar et al., 2009). In ECIS the barrier disrupting effects of histamine were less pronounced than after administration of thrombin. After application of saturating dose (data from pre-experiment not shown), the electrical resistance of a HUVEC monolayer rapidly dropped within 1 hour by $35 \pm 9.7\%$ (mean ± SD) and recovered completely to the level of control monolayer after 1 hour (**Figure 10A**). Pretreatment with 100 nM ADM (30 min) induced an increase of TEER to $134 \pm 11.7\%$ (mean ± SD) and attenuated the histamine evoked decrease of electrical resistance. However, the histamine induced drop-down by $16 \pm 10.0\%$ (mean ± SD) was not totally antagonized by treatment with ADM.

Beside its important role as angiogenesis factor, VEGF was originally identified as a vascular permeability factor, causing interstitial accumulation of intravenously injected dyes and ascites *in vivo*. There is evidence from ultra-structural studies that VEGF increases transcellular permeability, but also increase of paracellular permeability by promoting cellular contraction, influencing focal adhesion dynamics, as well as opening of cell-cell junctions (reviewed by Kumar et al., 2009). Similar to histamine, administration of saturating concentration of VEGF (100 ng/ml) induced a rapid decrease of electrical resistance by $23 \pm 11.1\%$ (mean ± SD) (as compared to control monolayer) within 1 hour (**Figure 10B**). However, the effect of VEGF was not reversible and remained at the same level during 20 h experiment. Pretreatment with ADM prevented the initial VEGF-induced drop in TEER by ~10%. This protective effect was gradually lost over the observation interval.

LPS has been identified as an important pathogenetic factor derived from the outer membrane of gram-negative bacteria which induces systemic inflammation and sepsis in mammals. Binding of LPS to Toll-like receptor 4 (TLR4) activates the MAP kinase cascade, contributing to gene expression of pro-inflammatory cytokines, remodeling of endothelial cytoskeleton, as well as

permeability changes (reviewed by Xing & Birukova, 2010). LPS in the saturating dose of 300 ng/ml provoked a slow and long lasting dwindling in TEER levels with the trough at 85 ± 4.0% (mean ± SD) after 5 h stimulation, which remained stable throughout the rest of the experiment (**Figure 10C**). Following treatment with ADM TEER was rapidly enhanced to 131 ± 8.7% and LPS stimulation decreased this TEER to 102 ± 5.5% (mean ± SD). Addition of ADM 30 min prior to LPS administration could antagonize the decrease of TEER towards the baseline level of the control monolayer. However, the amplitude of decrease in TEER was not influenced.

In the similar manner to LPS, the pro-inflammatory cytokine IL-1β in saturating dose of 10 pM slowly and irreversibly induced a decline of TEER levels with maximal drop-down to 59 ± 14.3% (mean ± SD) after approximately 5 h stimulation (**Figure 10D**). ADM pretreatment rapidly increased the TEER to 137 ± 5.6%, which was reduced to 87 ± 2.4% with the extent of 50 ± 6.9% (mean ± SD). Despite stimulation with IL-1β, ADM stabilized TEER. However, the absolute changes of TEER following IL-1β addition were not affected by ADM.

In summary the net gain in TEER which was inducible by treatment with ADM was not dependent on the cellular condition (i.e. resting or inflammatory stimulated). Therefore it might be speculated that ADM exerts its barrier stabilizing effects via a signaling pathway that is independent of the pathway(s) addressed by the stimuli tested.

Figure 10 Effects of ADM on endothelial barrier dysfunction induced by different stimuli
HUVECs were seeded on 96-well ECIS microelectrode plates and TEER was continuously recorded. At the time points indicated by the arrows, cells were pretreated with vehicle or 100 nM ADM for 30 min, followed by different stimuli, including 4.5 µg/ml histamine (**A**), 100 ng/ml VEGF (**B**), 300 ng/ml LPS (**C**), and 10 pM IL-1β (**D**). Relative TEER was normalized to the TEER measured at the beginning of the experiment. (n=8, mean ± SEM)
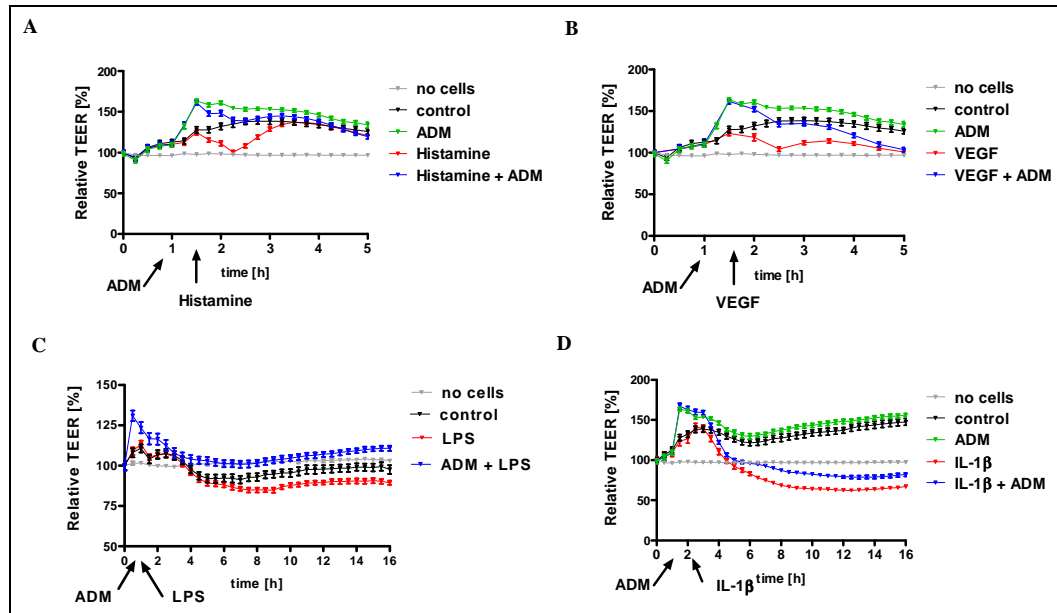
5.2.2. Effects of ADM on leukocyte transmigration *in vitro*

Transmigration of leukocytes from the bloodstream into the tissue is essential to the immune response that enables leukocytes to reach the site of infection and injury. This situation can be mimicked *in vitro* in a transmigration assay in which leukocytes are allowed to migrate through an endothelial monolayer grown on a filter membrane. While endothelial cells are stimulated by overnight pretreatment with TNFα, PMNs migrate towards the chemokine gradient of IL-8 (Downey et al., 1995). In pre-experiments, buffy coat which contained all kinds of leukocytes (~40% neutrophilic granulocytes, 40% lymphocytes, 10% monocytes, 4% eosinophilic-, and 1% basophilic-granulocytes; data from pre-experiment) was added to HUVEC monolayer. With >95% neutrophilic granulocytes (PMNs) were the predominant cell type having transmigrated the membraneBased on this observation, isolated PMNs were further used and discussed in the *in vitro*-leukocyte transmigration assays.

Because of the vital importance of leukocyte extravasation and an anti-inflammatory role of ADM described in the literature, it was questioned whether ADM could affect this process. ICAM-1 is the major endothelial adhesion receptor relevant to firm adhesion of neutrophils to endothelial cell surfaces; therefore ICAM-1 antibody was used as a positive control in the assays. After the incubation with ICAM-1 antibody, only ~10% of PMNs transmigrated through TNFα- stimulated HUVEC monolayers (**Figure 11A**). Also ADM significantly reduced PMN transmigration to $61 \pm 14.1\%$ (mean $\pm$ SD). In order to distinguish whether the effect of ADM was due to an effect on the endothelial cells or the leukocytes, in a parallel experiment PMNs were incubated with ADM and washed prior to transmigrating through the HUVEC monolayer. In contrast to its significant effect on endothelial cells, treatment of PMN with ADM or ICAM-1 antibody had no effect on the transmigration of leukocytes (**Figure 11B**).

Figure 11 Effects of ADM on TNFα-induced leukocyte transmigration

PMNs were allowed to transmigrate toward the chemokine IL-8 through a HUVEC monolayer on transwell filter which was stimulated overnight by TNFα (5 nM). Either the HUVECs **(A)** or the human neutrophils **(B)** were treated for 30 min with vehicle, ICAM-1 antibody (60 µg/ml), or ADM (100 nM). In each case, the number of neutrophils migrating under control condition was set to 100%. (n=3, mean $\pm$ SEM) (***p<0.0005 vs. control group)
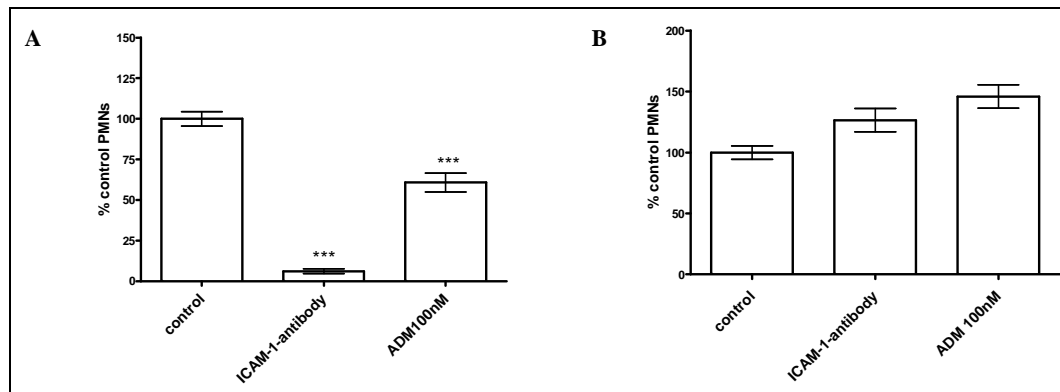
To more accurately comprehend any possible anti-inflammatory action of ADM on PMN, the expression of ADM receptors CRLR, RAMP-2, and -3 in PMNs were analyzed (**Figure 12A**). The absolute CT value of CRLR, RAMP-2 and -3 were 32.0 ± 0.1, 25.9 ± 0.7, 28.6 ± 0.3, respectively (mean $\pm$ SD). The relative

expression levels of CRLR and RAMP-2 normalized to β-actin were roughly at the same levels as in HUVECs, with 10 and 1000 arbitrary units, respectively. While RAMP-3 was hardly detectable in HUVECs, it was expressed in PMNs with relative expression of 100 arbitrary units. In PMNs, increasing concentrations of ADM (1 pM-1µM) had no effects on accumulation of intracellular cAMP (**Figure 12B**). In this assay, FSK, known as a strong cAMP elevator via direct activation of adenylate cyclase (AC), was used as positive control. Stimulation with FSK (100 µM) significantly increased intracellular cAMP in PMNs. Taken the data together, despite the expression of ADM receptor mRNA (CRLR, RAMP-2, and -3), no functional cAMP signaling of ADM was detectable in PMNs. Wheter ADM receptor protein is expressed by PMNs could not be decided due to the unavailability of a specific and sufficiently sensitive antibody.

Stimulated PMNs release a couple of hydrolytic and proteolytic enzymes as well as myeloperoxidase (MPO) from their cytoplasmic granules. MPO has a dual activity as peroxidase and chlorinating enzyme, generating other oxidant species and more particularly hypochlorous acid (HOCl), one of the most powerful oxidant molecules *in vivo*. Thus, MPO is an important component of the defense machinery (Franck et al., 2009). MPO release is a measure of MPO activation. A wide variety of stimuli (e.g. fMLP and the anaphylatoxin C5a) initiate the degranulation process of PMNs via specific receptor signaling (Patrick et al., 1996). In a modified MPO release assay (described by Paczkowski et al., 1999). it was examined whether ADM could affect MPO release from PMNs after stimulation with C5a or fMLP.

C5a is a component of the complement system that causes chemotaxis and degranulation of PMNsAs shown in **Figure 12C**, human C5a dose-dependently increased activation of human PMNs, with the minimal dose of 3 nM. In the next step PMNs, stimulated with 10 nM C5a, were pre-incubated with increasing doses of ADM (1 nM to 1 µM) and forskolin (FSK) (100 nM to 100 µM) (**Figure 12D**). W54011, a potent and highly selective C5a antagonist, was used in doses of 30 nM to 10 µM as positive control. While 1 µM W54011 totally antagonized

C5a-induced MPO release, neither ADM nor FSK showed any effects on PMN stimulation.

The synthetic tripeptide, N-Formyl-L-methionyl-L-leucyl-L-phenylalanine (fMLP), mimics the effect of various bacterial cell wall-derived peptides activating PMN via binding to a specific GPCR and thus is widely used as a GPCR-dependent stimulus of the PMNs and as a chemo attractant molecule (Brazil et al., 1998; Sheppard et al., 2005). As shown in **Figure 12E**, fMLP dose-dependently increased activation of human PMNs, with the minimal dose of 100 pM and the saturation dose of 1 μM. Increasing doses of ADM (1 nM to 1 μM) and FSK (100 nM to 100 μM) were applied to - PMNs stimulated with 3 nM fMLP (**Figure 12F**). Similarly to C5a-induced PMN activation, neither ADM nor FSK affected fMLP-induced activation of PMNs. A positive control was not available.

Figure 12 ADM Receptor expression and its effects on MPO release from human neutrophils

(A): Quantitative real-time RT-PCR analysis was performed on freshly isolated human neutrophils using specific oligonucleotide primers and probes. Expression levels of CRLR, RAMP-2, and -3 were normalized to β-actin. (n=2, mean ± SD) **(B):** Intracellular cAMP accumulation was measured by use of a commercial ELISA. 5×10^6 Human PMNs were stimulated with different doses of ADM (1 pM-1 μM) and FSK (10 μM) for 15 min. Then the cells were subjected to extraction in 70% (v/v) ethanol overnight at -20 ℃. (n=2, mean ± SD) **(C)** - **(F):** To investigate the activation of human neutrophils, levels of released MPO were determined. **(C)** and **(E):** 2.5×10^4 PMNs were incubated with increasing concentrations of C5a **(C)** or fMLP **(E)**. **(D)** and **(F):** PMNs were incubated with increasing concentrations of test compounds (W-54011, ADM or FSK) for 10 min at 37 ℃, following by incubating the cells for a further 10 min at 37 ℃ with 10 nM C5a **(D)** or 3 nM fMLP **(F).** The level of released MPO was determined by measuring absorbance at 450 nm. (n=2, mean ± SEM)
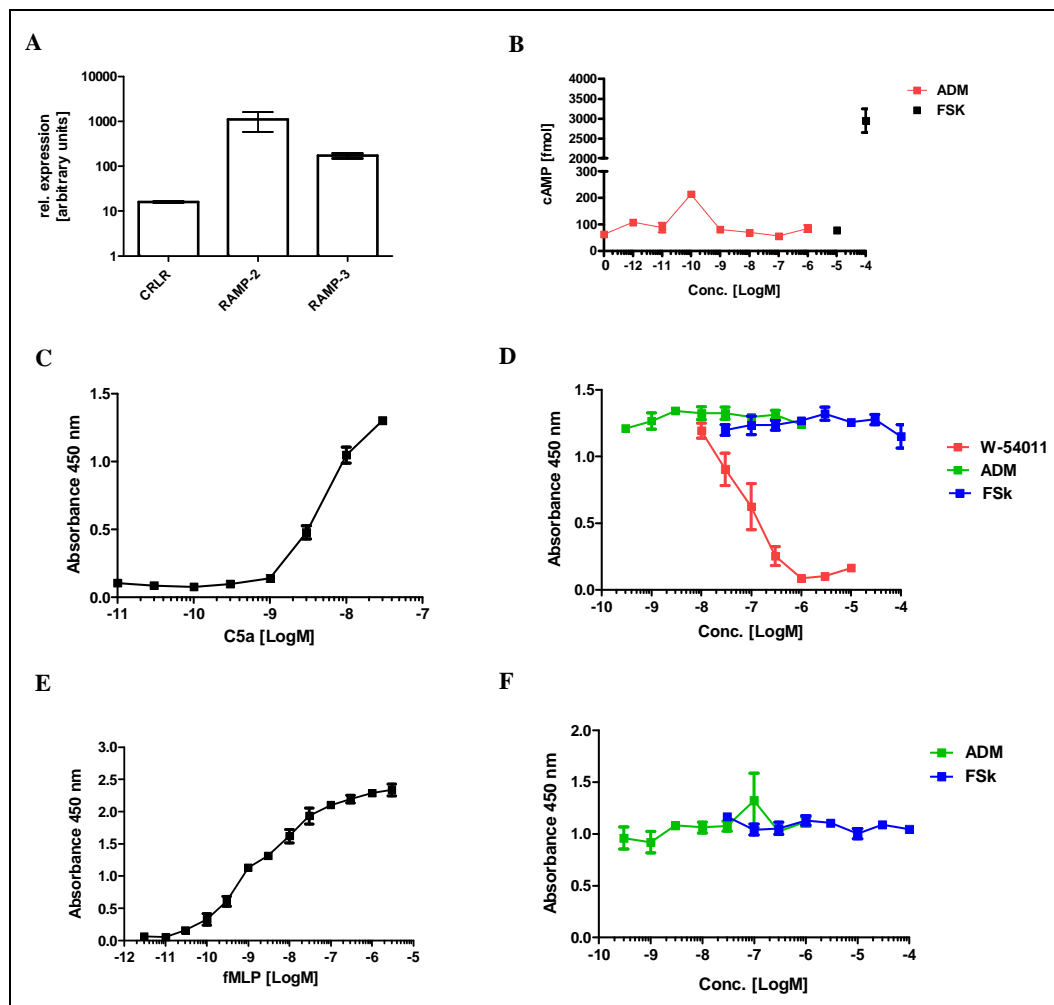
In response to inflammtion, cytokines up-regulate expression of CD11b/18 on neutrophils and ICAM-1 on endothelial cells, promotiong adhesion and interaction of neutrophils with endothelium (Smith, 1993; Saito et al., 2001). In a static adhesion assay, different doses of ADM were tested whether they wre able to affect the adhesion of PMNs to HUVECs (**Figure 13A-C**). None of the ADM doses were able to influence the adhesion of PMNs upon short term exposure for 30 min. In consistency with this observation, the cell surface expression level of CD11b on neutrophils was also not affected by ADM (**Figure 13D**).

Taken all these data together, prevention of TNFα-induced leukocytes transmigration was rather mediated by direct action of ADM on endothelial cells than on leukocytes. Despite the receptor mRNA expression, a significant effect of ADM on PMN activation and adhesion could not be established, which was consistent with lack of functional cAMP signaling.

Figure 13 Effect of ADM on cell adhesion of neutrophils to endothelial cells

(A): Static cell adhesion assay was performed for human neutrophils to HUVECs. HUVECs were pretreated with 5 nM TNFα and incubated with increasing doses of ADM (10 pM-100 nM) for 30 min. BCECF-labeled human neutrophils were added to HUVEC monolayer and allowed for 30 min co-incubation. Fluorescence intensity was measured for the total applied PMNs and for each wash. The relative fluorescence was set to the value of total applied PMNs. (n=4, mean ± SD) **(B):** The protein expression of CD11b was measured by use of FACS. Human PMNs were incubated with different doses of ADM (1 pM-1 µM) for 30 min, followed by stimulation with fMLP (100 nM). Then the cells were subjected to PE-labeled anti-CD11b antibody and isotype control, and then performed for FACS analysis. Only the data with 100 nM ADM was shown below.
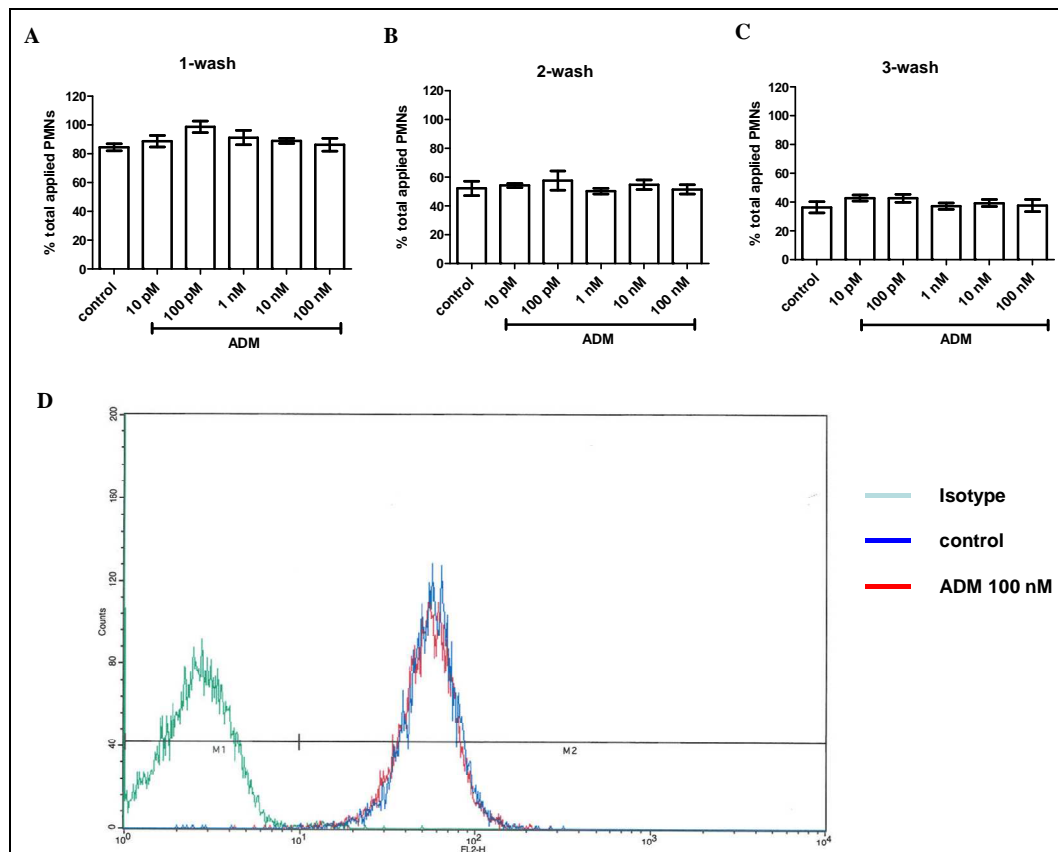
5.2.3. Anti-edematous effects of ADM *in vivo*

The *in vitro*-data provided evidence that ADM stabilized the endothelial barrier for water, ions and macromolecules and attenuated endothelial barrier disruption provoked by thrombin and TNFα. Next, it was addressed whether this *in vitro*-finding could be translated to *in vivo*-models. A modified Miles assay

was performed to detect vascular permeability in the skin of rats (**Figure 14A**) and mice (**Figure 14B**) using intravenously administered Evans blue dye as indicator for vascular hyperpermeability. Evans blue is a highly plasma protein bound dye and therefore used as an indicator for protein-rich fluid extravasation and vascular leakage.

In the rat vehicle group, intradermal administration of histamine dose-dependently increased permeability of Evans blue dye in the skin about two-fold (194 ± 37.0%; mean ± SD) at 40 µg/ml, as compared to basal permeability with intradermal PBS application. Intravenous application of 10 µg/kg BW ADM reduced basal permeability by ~33% and decreased histamine-induced hyperpermeability by ~35%. 30 µg/kg BW and 100 µg/kg BW ADM reduced basal permeability by ~80% to 19 ± 6.2% and 22 ± 11.1% (mean ± SD), respectively, and the histamine-induced hyperpermeability was both decreased by ~75%. 30 µg/kg BW ADM reached the maximal effect on regulation of permeability and thus represented the saturation dose. Albeit on a four-fold lower level, histamine still caused a two-fold increase of permeability in rats, which was not diminished by the saturating dose of ADM.

In the mouse vehicle group, intradermal administration of 4.5 µg/ml histamine induced a three-fold increase of permeability of Evans blue dye in the skin. Unlike Miles assay in rats, intravenous administration of 10 µg/kg BW ADM had no significant effect on vascular permeability in mice. Both 30 µg/kg BW and 100 µg/kg BW ADM decreased basal permeability by ~50% and histamine-induced hyperpermeablility by ~80%, which were consistent with the saturating doses in rats. These data were in support of the *in vitro*-finding that ADM stabilized endothelial barrier function and underscored its strong anti-edematous potency.

Figure 14 Effects of ADM on histamine-induced vascular hyperpermeability in the skin of rats and mice

Anesthetized rats **(A)** and mice **(B)** were i.v. injected with vehicle or ADM, then with Evans blue dye, and finally underwent intradermal injection of PBS or histamine and were sacrificed 30 min thereafter. The dye was extracted from skin samples and quantified. **(A):** Evans blue dye was normalized to the sample weight. Rats were divided into four groups: control (black), ADM 10 µg/kg BW (green), ADM 30 µg/kg BW (blue), and ADM 100 µg/kg BW (red). (Data are expressed as mean ± SEM, n=4~7.) **(B):** Mice were divided into five groups: vehicle, 3 µg/kg BW, 10 µg/kg BW, 30 µg/kg BW and 100 µg/kg BW ADM followed by intradermal injections of PBS (black bars) and histamine (white bars). (Data were expressed as mean ± SEM, n=5~8.) (#$p<0.05$ vs. control group with PBS injection; ***$p<0.0005$ vs. control group with histamine injection)
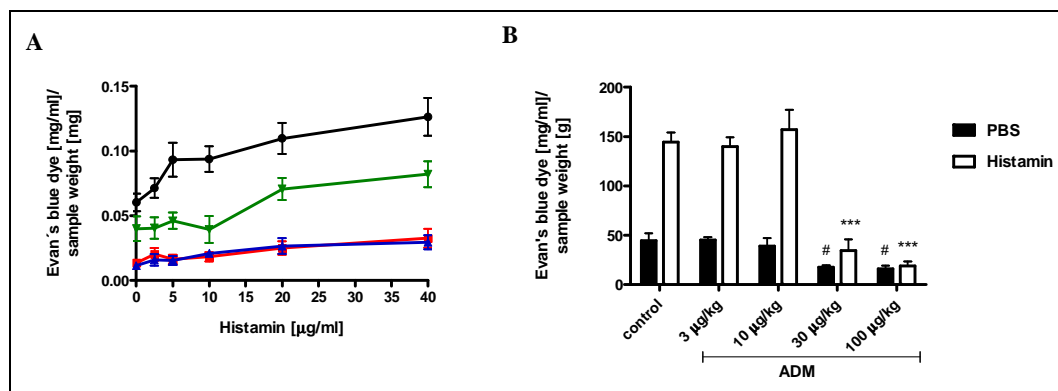
5.2.4. Anti-inflammatory effects of ADM *in vivo*

As the previous *in vitro*-data indicated the protective effects of ADM on endothelial permeability and granulocyte extravasation, anti-inflammatory effects of ADM *in vivo* were investigated. Intratracheal administration of LPS was performed in anesthetized mice as a model for acute lung injury which is characterized by increased permeability and granulocytes extravasation. As shown in **Figure 15**, after 48 h, challenge with LPS dose-dependently induced significant lung injury as indicated by increased lung weight (**A**), WBC-counts (**B**), and protein content (**C**) in bronchoalveolar lavage (BAL) fluid as compared to the sham group. 0.5 mg/kg BW LPS represented the saturating dose, which induced ~1.5 fold increase of lung weight, ~3.5 fold increase of protein content and ~20 fold increase of WBC in BAL fluid. Increased protein content in BAL fluid and increased lung weight are regarded as markers for increased endothelial permeability of macromolecules and water, while increased WBC

counts are resulting from the interaction of endothelium with leukocytes. The LPS induced acute lung injury model allowed the *in vivo*-detection of those two inflammatory parameters, permeability and leukocytes extravasation.

As shown in **Figure 16A**, 48 h after LPS challenge (1 mg/kg BW) a lung edema was present with increased lung weight to 170 ± 17.1% (mean ± SD), as compared to sham group. Treatment with ADM ameliorated the formation of lung edema, reducing the lung weight to 147 ± 17.8% (mean ± SD). Accompanied with lung edema formation, LPS challenge induced a 16 ± 5.4 (mean ± SD) -fold increase of WBC counts in BAL fluid, which was reduced to 12 ± 3.8 (mean ± SD) folds after ADM administration (**Figure 16B**). This *in vivo*-observation was consistent with the previous *in vitro*-finding, that ADM significantly prevented TNFα-induced PMN transmigration through HUVEC monolayers.

Figure 15 Challenge of LPS induced lung edema and accumulation of leukocytes and proteins in BAL fluid

Mice were intratracheally administrated with vehicle, 0.1 mg/kg BW, 0.5 mg/kg BW, 1 mg/kg BW and 3 mg/kg BW LPS. 48 hours later BAL was performed and lung injury was evaluated by measurement of wet lung weight **(A)**, WBC **(B)** and protein **(C)** counts in the BAL fluid. The values are shown as mean ± SEM, n=4. (*p<0.05, **p<0.005, and ***p<0.0005 vs. sham group)
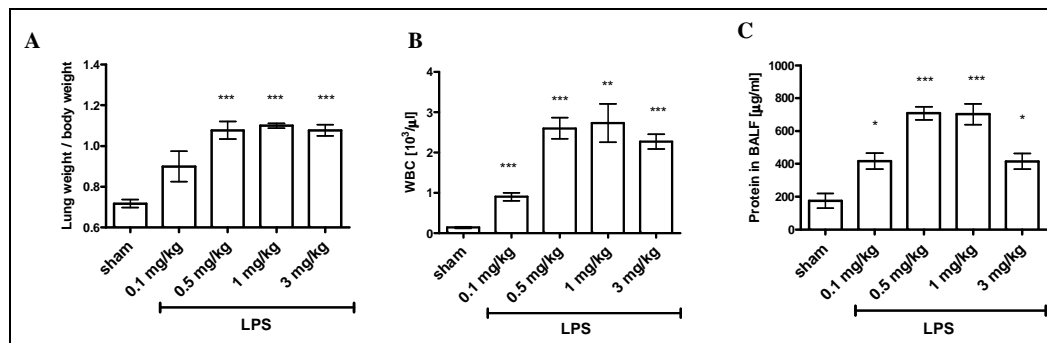
Figure 16 Anti-inflammatory effects of ADM in acute lung injury induced by LPS challenge

Mice were divided into three groups: 1) the sham group with intratracheal administration of saline (n=9); 2) the LPS group with intratracheal challenge of 1 mg/kg BW LPS (n=18); and 3) the LPS-ADM group pre-treated with ADM (100 µg/kg BW) and underwent intratracheal challenge with 1 mg/kg BW LPS (n=18). The severity of lung injury was evaluated regarding wet lung weight **(A)** and WBC **(B)** counts in the BAL fluid after 48 hours LPS administration. Data are shown as mean ± SEM. (***$p<0.0005$ vs. sham group; #$p<0.05$ and ###$p<0.0005$ vs. LPS group)
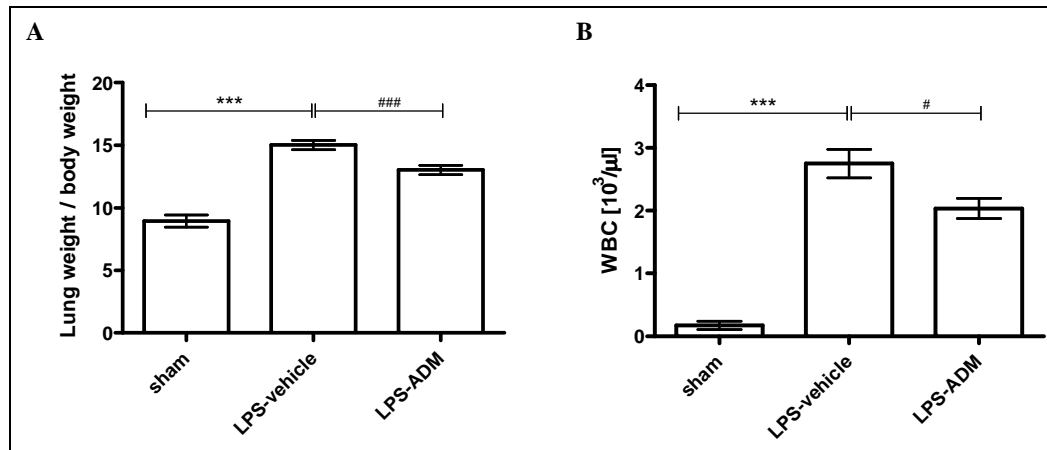
5.3. Analysis of cAMP-dependent pathway in ADM signalling

As shown in **Figure 6** ADM caused intracellular cAMP accumulation in primary endothelial cells. The intracellular second messenger cAMP is known to stabilize endothelial barrier function via two distinct downstream mechanisms (Bindewald et al., 2004), on one hand via PKA activation reducing phosphorylation of MLC and thereby relaxing the contractile machinery (Essler et al., 2000), and on the other hand increasing VE-cadherin mediated cell adhesion via Epac/Rap1 activation (Fukuhara et al., 2005). It seems reasonable to hypothesize that ADM exerts its regulatory function on the endothelial barrier mainly through cAMP signaling. However, ADM-cAMP-independent signaling has also been discussed with the consideration that ADM fully exerts its barrier protective function at much lower cAMP levels as compared to forskolin (FSK), a direct activator of adenylate cyclase (AC) (Hippenstiel et al., 2002). Therefore additional signaling pathways were postulated. However, the precise correlation of induced cAMP levels and their protective effects have not been elaborated by

these authors. It was the aim of the following studies to precisely determine the lowest effective doses and pEC50 values of ADM and FSK under exactly the same experimental conditions with respect to reduction of endothelial permeability and leukocyte transmigration. Accumulation of cAMP and further activation of cAMP signaling pathways (activation of PKA and Epac/Rap1) were analyzed and correlated with their effects.

5.3.1. Comparison of ADM and FSK effects on generation cAMP

For the initial characterization of ADM and FSK-induced cAMP response, a CHO cell line stably expressing cAMP-gated cation channel, the ADM receptor (CRLR and RAMP-2), and cytosolic apoaequorin was employed. In this CHO-ADM1-reporter system, ligand-mediated activation of Gs-coupled GPCRs increase cAMP levels by activation of adenylate cyclase and subsequent opening of the cAMP-gated cation channel, resulting in calcium influx from extracellular stores, which can be detected as aequorin luminescence signal. In addition, activation of Gq-coupled GPCR stimulates phospholipase C/IP3 pathway which can also be detected via aequorin luminescence stimulated by calcium release from intracellular stores, the endoplasmic reticulum (Wunder et al., 2008). As shown in **Figure 17A and B**, stimulation of CHO-ADM1-reporter cell line with ADM and FSK resulted in concentration-dependent luminescence signals with pEC50 value of -8.1 ± 0.1 [M] and -5.6 ± 0.1 [M] (mean ± SD), respectively. Furthermore, 1 nM ADM and 1 µM FSK were the lowest effective doses able to increase luminescence signals significantly. ADM was about 4-fold less efficacious than FSK.

Figure 17 Characterization of ADM and FSK in CHO-ADM1-reporter cells

Concentration-dependent luminescence signals generated after stimulation with ADM **(A)** and FSK **(B)** were detected in CHO-ADM1-reporter system. Agonists were added for 6 min in CAFTY solution and measurements were started immediately prior to adding the final concentration of Ca^{2+} at 3 mM. (n=4, mean ± SEM)
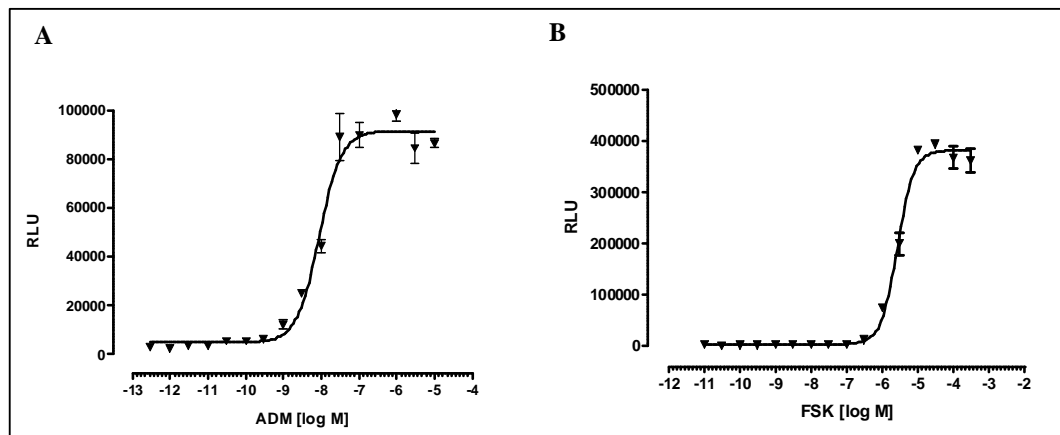
5.3.2. Comparision of ADM and FSK effects on cAMP accumulation

In the next step, the intracellular cAMP levels which were induced by ADM and FSK in primary human endothelial cells, were compared (**Figure 18A and B**). The lowest effective doses of ADM and FSK able to induce significant increase of cAMP were 100 pM and 100 nM, respectively. In addition, stimulation of ADM and FSK resulted in concentration-dependent increase of cAMP with pEC50 value of -9.9 ± 0.3 [M] and -5.5 ± 0.6 [M] (mean ± SD), respectively. Moreover, FSK could induce ~40-fold increase of cAMP levels, whereas ADM induced only ~4-fold increase at its saturation dose.

Figure 18 ADM and FSK increased accumulation of intracellular cAMP

Intracellular cAMP accumulation in HUVEC was measured using a commercial cAMP ELISA. The primary endothelial cells were stimulated with different doses of ADM **(A)** and FSK **(B)** for 30 min and were subjected to incubation in 70% (v/v) ethanol overnight at -20ºC to extract intracellular cAMP. ΔcAMP was set as the difference to the values measured in control wells in each group. (n=4, mean ± SEM) (* and # vs. control group; * parametric t-test, # non-parametric Mann-Whitney test)(*p<0.05, **p<0.005, ***p<0.0005, #p<0.05, and ##p<0.005)
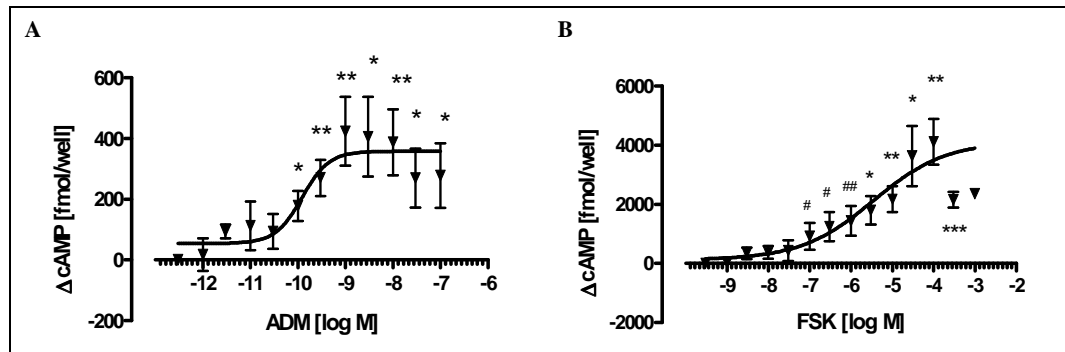
5.3.3. Comparision of ADM and FSK effects on permeability

The goal of the following studies was to correlate ADM and FSK-induced intracellular cAMP accumulation with their effects on permeability of HUVEC monolayer. In direct comparison using the ECIS methodel, ADM and FSK prevented thrombin induced hyperpermeability (as quantified by reduction of TEER) with pEC50 value of -9.6 ± 0.2 [M] and -5.6 ± 0.4 [M] (mean ± SD), respectively (**Figure 19**). 30 pM ADM and 30 nM FSK were the minimum doses to significantly reduce thrombin-induced hyperpermeability, respectively. In addition, FSK stimulation could induce much higher TEER after further dose escalation, as compared to ADM stimulation, which was consistent with the difference in accumulation of cAMP levels.

Figure 19 Comparison of ADM and FSK effects on electrical resistance by using ECIS

HUVECs were incubated with ADM **(A)** or FSK **(B)**, and were stimulated with 0.5 U/ml thrombin. Measurement of TEER was performed over 4 hours. Relative TEER values were normalized to the time point prior to adding thrombin and the TEER-AUC was calculated to quantify the effects of ADM and FSK. AUC was normalized to control group. (n=8, mean ± SEM) (*p<0.05, **p<0.005, ***p<0.0005 vs. thrombin group)
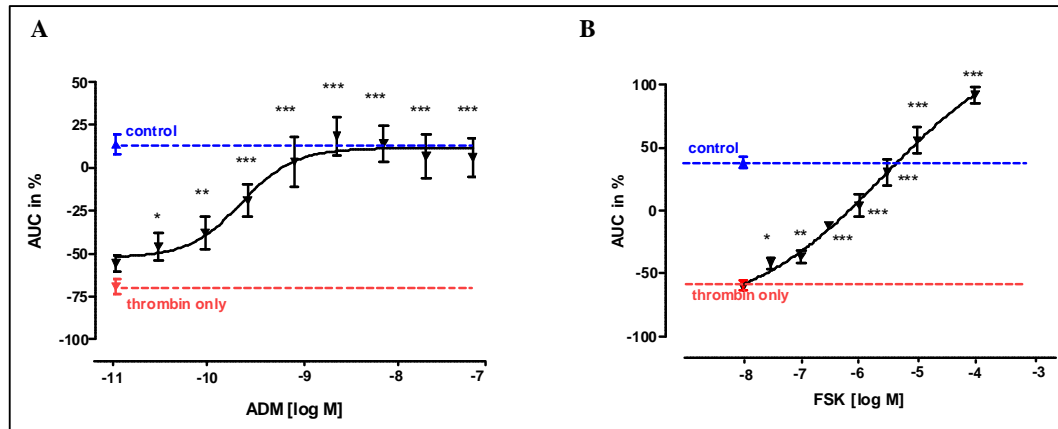
By using the FITC-dextran model for a further side by side comparison, both ADM and FSK dose-dependently reduced macromolecular permeability through a HUVEC monolayer with the lowest effective doses of 1 nM and 1 µM, respectively (**Figure 20A and B**). Similar to the observation in ECIS, FSK stimulation could induce stronger effects on macromolecular permeability after further dose escalation, as compared to ADM stimulation, which might be explained by the accumulation of much higher cAMP levels.

Figure 20 Comparison of ADM and FSK effects on macromolecular permeability

HUVECs were stimulated with ADM **(A)** and FSK **(B)** followed by stimulation with 0.5 U/ml thrombin. Macromolecular permeability was measured over 4 hours. The AUC was calculated to quantify the effects of ADM and FSK. (n=4, mean ± SEM) ($^{###}$p<0.0005 vs. control group; *p<0.05, **p<0.005, ***p<0.0005 vs. thrombin group)
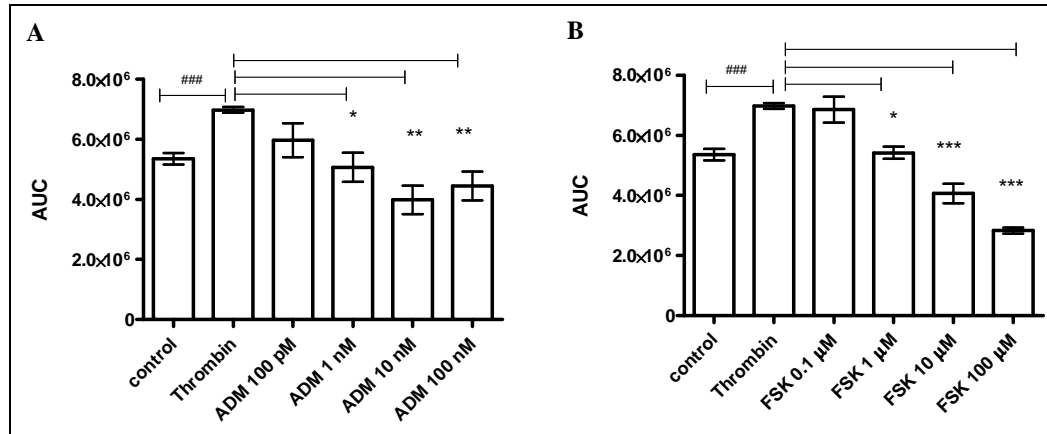
5.3.4. Comparision of ADM and FSK effects on PMN extravasation

As shown in **Figure 11**, ADM reduced granulocyte extravasation *in vitro* and protected the lungs against LPS-induced injury in terms of reduced lung edema and leukocytes in BAL fluid. The question is whether this anti-inflammatory effect results from cAMP signaling or whether additional signaling pathways are involved. Therefore, it was further investigated whether FSK could also affect granulocyte extravasation in a similar manner as ADM. Both ADM and FSK dose-dependently reduced transendothelial migration of leukocytes with effective doses of 1 nM and 1 µM, respectively (**Figure 21**). However, as compared to ADM, FSK caused stronger reduction of PMN transmigration after further dose escalation, which could be explained by a still increasing cAMP accumulation over this dose range, while cAMP accumulation was already saturated after exposure to 1 nM ADM (**Figure 18**). This data indicated the key role of cAMP signaling in ADM-mediated modulation of leukocyte transmigration. It can be speculated that the limited number of ADM receptors on endothelial cells is responsible for saturation of its effects at doses ≥10 nM.

Figure 21 Comparison of ADM and FSK effects on granulocyte extravasation

HUVEC monolayers on transwell filters were stimulated overnight with TNFα (5 nM) and treated with different doses of ADM **(A)** and FSK **(B)** prior to adding human PMNs. PMNs were allowed to transmigrate toward the chemokine IL-8 through EC monolayer for 30 min. The number of neutrophils migrating under control condition was set to 100%. (n=6, mean ± SEM) (**p<0.005, and ***p<0.0005 vs. control group)
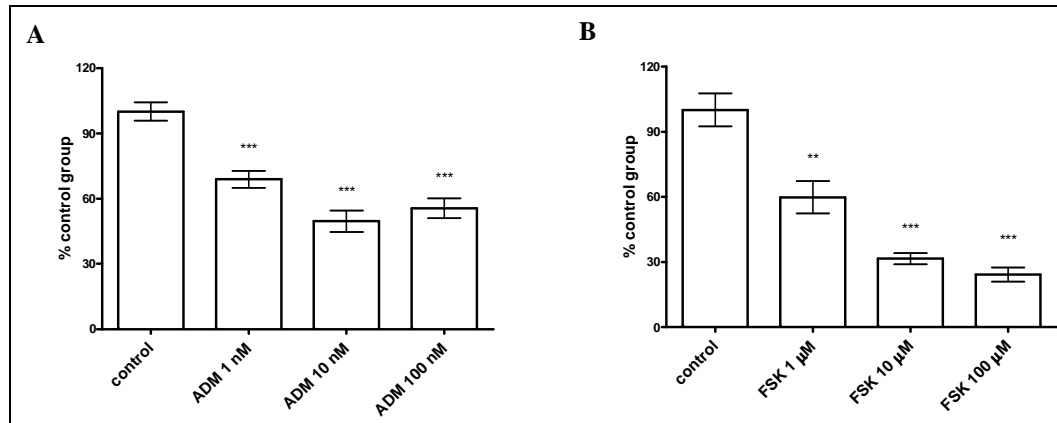
5.3.5. Comparision of ADM and FSK effects on PKA and Epac/Rap1 activation

The aforementioned data have shown that cAMP signaling is strongly involved in the regulation of endothelial permeability and granulocyte extravasation and a sufficient explanation for the effects of ADM on endothelial permeability. Because of the importance of cAMP pathway in ADM signaling, the downstream events of cAMP signaling were further investigated, namely the activation status of PKA and Epac/Rap1. Activation of PKA was assessed by the phosphorylation status of its direct substrate vasodilator-stimulated phosphoprotein (VASP), which is specifically phosphorylated by PKA at Ser157 (Butt et al., 1994). The specific PKA activator, N(6)-benzoyl-adenosine-3',5'-cyclic monophosphate (Benz-cAMP) and the Epac/Rap1 activator, 8- (4-Chlorophenylthio)- 2'- O- methyladenosine- 3', 5'- cyclic monophosphate (8-pCPT-2'-O-Me-cAMP or "007"), were employed as positive and negative controls in the experiment. As shown in **Figure 22**, Benz-cAMP increased the phosphorylation of VASP, indicating the activation of PKA; in contrast, "007" had no influence on the phosphorylation of VASP. Both ADM and FSK dose-

dependently increased the phosphorylation status of VASP with the lowest equally effective doses tested at 10 pM ADM and 10 nM FSK, respectively.

Figure 22 Effects of ADM and FSK on PKA activation
HUVECs were stimulated with ADM **(A)** and FSK **(B)** for 30 min. Upper panel: represented western blots of three separate experiments with independent cell preparation. Lower panel: densitometric analysis of western blots, in which VASP phosphorylation was normalized to total VASP. Relative VASP phosphorylation in control group was set to 100%. B-tubulin was used as loading control. (n=3, mean ± SEM) (*$p<0.05$ and **$p<0.005$ vs. control group)
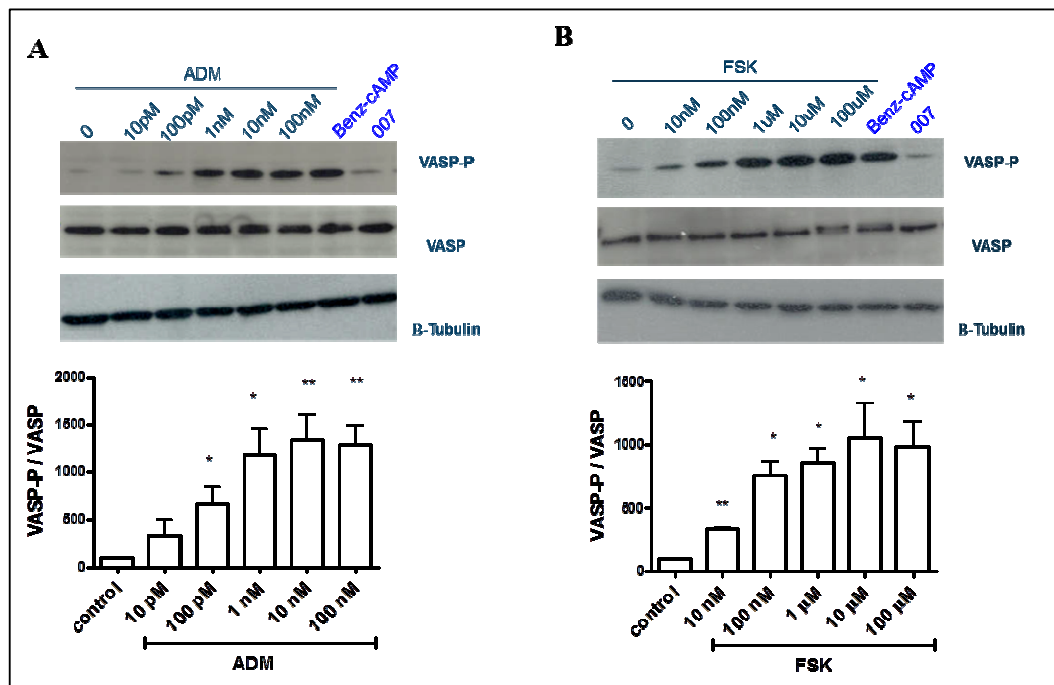
To analyze Epac/Rap1 signaling, the activation status of Rap1-GTPase, the direct target of Epac (de Rooij et al., 1998), was analyzed by using Rap1-pull-down assay. Both ADM and FSK increased the level of Rap1-GTP in a time-dependent manner, with the maximal activation at 15 min (**Figure 23**).

Figure 23 Effects of ADM and FSK on activation of Rap1 signaling

HUVECs were stimulated with 100 nM ADM **(A)** and 10 µM FSK **(B)** for 5 min, 15 min, and 30 min. Rap1-pull-down assay was performed to detect the activation status of Epac/Rap1 signaling.
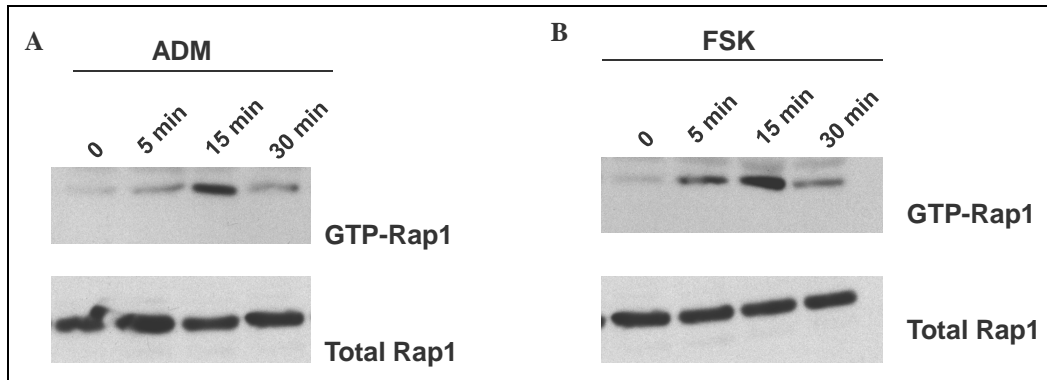
5.3.6. Comparision of ADM and FSK effects on gene expression

In the next study, the effects of ADM and FSK on gene expression in HUVECs were investigated through genome-wide microarray analysis. Gene expression after ADM and FSK stimulation with minimal two-fold changes was considered significant. Both stimulations were performed at two different time intervals: 3 hours and 16 hours. After 3 h ADM stimulation, 36 genes were found to be regulated (24 up- and 12 down-regulated), while 16 h ADM stimulation caused only 13 gene regulations (8 up- and 5 down-regulated). The ADM effect seemed to be weakened after 16 hours. Similarly, 3 h FSK incubation modified expression of 57 genes (43 up- and 14 down-regulated), while 16 h FSK incubation caused changes in expression of 43 genes (26 up- and 17 down-regulated).

After 3 h stimulation, there was an overlap in the exexpression of 20 genes which were stimulated by ADM and FSK, including PDE3A, RND1 (Rho family GTPase 1), MMP16 (Matrix metallopeptidase 16), CCRL1 (Chemokine C-C motified receptor like 1), as well as cell adherent receptors VCAM-1 and E-selectin. After 16 h stimulation only 5 genes were induced by both agents. Also ICAM-1 which was reported to be down-regulated in lymphatic endothelium by ADM (Jin et al., 2011), was also down-regulated by FSK with a factor of 1.9-fold, just below the limit of the exclusion criterion. Overall, both ADM and FSK

were shown to have similar effects and a tendency on gene regulation through the use of microarray analysis. An overview of regulated genes is given in **Table 8** for 3 h incubation and in **Table 9** for 16 h incubation.

Table 8 Microarray analysis in HUVECs after 3 h incubation with ADM and FSK

"Fold of changes" set to control group was listed. Only the gene expression after ADM and FSK stimulation with minimal two-fold changes was considered significant. (n.s.: not significant for <2.0 or >0.5 fold of changes)

Gene Symbol	Gene description	Fold of changes ADM	Fold of changes FSK
Gene regulated by ADM			
Septin14	septin 14	**0.4**	n.s.
CEP170	centrosomal protein 170kDa	**0.5**	n.s.
GRK5	G protein-coupled receptor kinase 5	**0.5**	n.s.
GNA14	guanine nucleotide binding protein alpha 14	**0.5**	n.s.
SFRS2IP	splicing factor. arginine/serine-rich 2. interacting protein	**0.5**	n.s.
ITPR1	inositol 1.4.5-triphosphate receptor. type 1	**0.5**	n.s.
TMF1	TATA element modulatory factor 1	**0.5**	n.s.
RELB	v-rel reticuloendotheliosis viral oncogene homolog B	**2.0**	n.s.
TNFAIP3	tumor necrosis factor. alpha-induced protein 3	**2.0**	n.s.
FLJ42220	FLJ42220 protein	**2.1**	n.s.
ICAM1	intercellular adhesion molecule 1	**2.1**	n.s.
CSF1	colony stimulating factor 1 (macrophage)	**2.1**	n.s.
CYP1A1	cytochrome P450. family 1. subfamily A. polypeptide 1	**2.2**	n.s.
TIFA	TRAF-interacting protein (forkhead-associated domain)	**2.2**	n.s.
CX3CL1	chemokine (C-X3-C motif) ligand 1	**2.3**	n.s.
SPRY4	sprouty homolog 4 (Drosophila)	**2.4**	n.s.
Gene regualted by FSK			
LOC388692	hypothetical LOC388692	n.s.	**0.3**
SIK1	salt-inducible kinase 1	n.s.	**0.4**
SOCS3	suppressor of cytokine signaling 3	n.s.	**0.4**
DUSP10	dual specificity phosphatase 10	n.s.	**0.4**
RNU4-2	RNA. U4 small nuclear 2	n.s.	**0.4**
PCMTD2	protein-L-isoaspartate O-methyltransferase domain cont.2	n.s.	**0.4**
RAPGEF5	Rap guanine nucleotide exchange factor (GEF) 5	n.s.	**0.4**
HLA-DPB1	major histocompatibility complex. class II. DP beta 1	n.s.	**0.4**
CREM	cAMP responsive element modulator	n.s.	**0.4**

DUSP1	dual specificity phosphatase 1	n.s.	**0.5**
ZNF518A	zinc finger protein 518A	n.s.	**0.5**
NIPBL	Nipped-B homolog (Drosophila)	n.s.	**0.5**
MGC24103	hypothetical MGC24103	n.s.	**0.5**
NBEAL1	neurobeachin-like 1	n.s.	**0.5**
PRKAA2	protein kinase. AMP-activated. alpha 2 catalytic subunit	n.s.	**0.5**
LOC100128868	testin-related protein TRG	n.s.	**0.5**
CP110	CP110 protein	n.s.	**0.5**
SAMD9L	sterile alpha motif domain containing 9-like	n.s.	**0.5**
PGAP1	post-GPI attachment to proteins 1	n.s.	**0.5**
ITPRIP	inositol 1.4.5-triphosphate receptor interacting protein	n.s.	**0.5**
PPAP2B	phosphatidic acid phosphatase type 2B	n.s.	**0.5**
PDE4D	phosphodiesterase 4D. cAMP-specific	n.s.	**0.5**
TTC30B	tetratricopeptide repeat domain 30B	n.s.	**0.5**
TAF4B	TAF4b RNA polymerase II.	n.s.	**0.5**
PSD3	pleckstrin and Sec7 domain containing 3	n.s.	**0.5**
ZNF81	zinc finger protein 81	n.s.	**0.5**
TBXA2R	thromboxane A2 receptor	n.s.	**2.0**
C10orf41	chromosome 10 open reading frame 41	n.s.	**2.0**
CELF5	CUGBP. Elav-like family member 5	n.s.	**2.0**
NCAN	neurocan	n.s.	**2.0**
CEACAM16	carcinoembryonic antigen-related cell adhesion molecule	n.s.	**2.0**
VSIG7	V-set and immunoglobulin domain containing 7	n.s.	**2.0**
KIR3DL1	killer cell immunoglobulin-like receptor.	n.s.	**2.1**
MYCN	v-myc myelocytomatosis viral related oncogene.	n.s.	**2.3**
FLJ31958	hypothetical LOC143153	n.s.	**2.4**
FLJ14100	hypothetical protein FLJ14100	n.s.	**2.4**
RUNDC2C	RUN domain containing 2C	n.s.	**3.5**
Gene regulated by both ADM and FSK			
CCRL1	chemokine (C-C motif) receptor-like 1	**0.3**	**0.4**
SESN3	sestrin 3	**0.3**	**0.3**
RIMKLB	ribosomal modification protein rimK-like family member B	**0.3**	**0.4**
PITPNC1	phosphatidylinositol transfer protein. cytoplasmic 1	**0.4**	**0.4**
PDE3A	phosphodiesterase 3A. cGMP-inhibited	**0.4**	**0.4**
SEMA3A	sema domain, secreted. (semaphorin) 3A	**0.4**	**0.4**
RNF152	ring finger protein 152	**0.4**	**0.4**
MMP16	matrix metallopeptidase 16 (membrane-inserted)	**0.4**	**0.4**
NOX4	NADPH oxidase 4	**0.4**	**0.5**
MOBKL1A	MOB1. Mps One Binder kinase activator-like 1A (yeast)	**0.4**	**0.4**

C12orf63	chromosome 12 open reading frame 63	**0.4**	**0.5**
N4BP2	NEDD4 binding protein 2	**0.5**	**0.4**
C10orf118	chromosome 10 open reading frame 118	**0.5**	**0.5**
ADAMTS18	ADAM metallopeptidase type 1, modif. 18	**0.5**	**0.4**
ADAMTS1	ADAM metallopeptidase with type 1, modif.1	**0.5**	**0.4**
CYorf15B	chromosome Y open reading frame 15B	**0.5**	**0.5**
ZNF654	zinc finger protein 654	**0.5**	**0.4**
RND1	Rho family GTPase 1	**2.2**	**2.2**
VCAM1	vascular cell adhesion molecule 1	**6.6**	**3.3**
SELE	selectin E	**12.4**	**5.5**

Table 9: Microarray analysis in HUVECs after 16 h incubation with ADM and FSK

"Fold of changes" set to control group was listed. Only the gene expression after ADM and FSK stimulation with minimal two-fold changes was considered significant. (n.s.: not significant for <2.0 or >0.5 fold of changes)

Gene Symbol	Gene description	*Fold of changes* ADM	*Fold of changes* FSK
Gene regulated by ADM			
CDRT1	CMT1A duplicated region transcript 1	**0.3**	n.s.
ZNF737	zinc finger protein 737	**0.4**	n.s.
LOC646508	hypothetical LOC646508	**0.4**	n.s.
RFC1	replication factor C (activator 1) 1. 145kDa	**0.5**	n.s.
ZNF680	zinc finger protein 680	**0.5**	n.s.
ZNF814	zinc finger protein 814	**0.5**	n.s.
EFCAB4B	EF-hand calcium binding domain 4B	**2.1**	n.s.
CSRP2	cysteine and glycine-rich protein 2	**2.3**	n.s.
Gene regulated by FSK			
PDE3A	phosphodiesterase 3A. cGMP-inhibited	n.s.	**0.4**
SELE	selectin E	n.s.	**0.4**
ANKRD11	ankyrin repeat domain 11	n.s.	**0.4**
GNA14	guanine nucleotide binding protein (G protein). alpha 14	n.s.	**0.4**
LOC100131826	TSSP3028	n.s.	**0.4**
BDNF	brain-derived neurotrophic factor	n.s.	**0.4**
FILIP1	filamin A interacting protein 1	n.s.	**0.4**
MME	membrane metallo-endopeptidase	n.s.	**0.5**
FAT1	FAT tumor suppressor homolog 1 (Drosophila)	n.s.	**0.5**
C12orf63	chromosome 12 open reading frame 63	n.s.	**0.5**
C5orf53	chromosome 5 open reading frame 53	n.s.	**0.5**

MMP16	matrix metallopeptidase 16 (membrane-inserted)	n.s.	**0.5**
DGKH	diacylglycerol kinase. eta	n.s.	**0.5**
TMEM229A	transmembrane protein 229A	n.s.	**0.5**
VSIG6	V-set and immunoglobulin domain containing 6	n.s.	**0.5**
DNAJC8	DnaJ (Hsp40) homolog. subfamily C. member 8	n.s.	**2.0**
RFT1	RFT1 homolog (S. cerevisiae)	n.s.	**2.1**
DHODH	dihydroorotate dehydrogenase	n.s.	**2.1**
FLJ43860	FLJ43860 protein	n.s.	**2.2**
SNORD25	small nucleolar RNA. C/D box 25	n.s.	**2.5**
Gene regulated by both ADM and FSK			
ADAMTS18	ADAM metallopeptidase with type 1 motif. 18	**0.5**	**0.4**
ANGPT2	angiopoietin 2	**0.5**	**0.5**
NCRNA00116	non-protein coding RNA 116	**2.0**	**2.2**
PRAMEF15	PRAME family member 15	**2.3**	**2.4**
GJA5	gap junction protein. alpha 5. 40kDa	**2.6**	**2.9**

5.3.7. Qualitative and quantitative comparision of ADM- and FSK-induced effects in different models

From a qualitative perspective, ADM and FSK showed identical effects throughout all the different models, which are summarized in **Table 10**. In the CHO-ADM1-reporter system, ADM and FSK resulted in concentration-dependent luminescence signals in correspondence with increased cAMP levels. In primary human endothelial cells, ADM and FSK induced significant accumulation of cAMP and activated cAMP signaling pathways, demonstrated by the activation of PKA and Epac/Rap1. Activation of PKA was demonstrated by downstream VASP phosphorylation, while activation of Epac was demonstrated by the levels of directly activated Rap1-GTPase (de Rooij et al., 1998). In primary human endothelial cells, both ADM and FSK are capable of increasing electrical resistance, decreasing macromolecular permeability, and inhibiting transendothelial migration of leukocytes.

Table 10 Effects of ADM and FSK in different models

Models	Effects
CHO-ADM1 reporter cell	Increase of luminescence signals (cAMP increase)
cAMP ELISA	Increase of intracellular cAMP levels
ECIS	Increase of transendothelial electrical resistance (TEER)
FITC-dextran permeability assay	Decrease of macromolecular permeability
TEM assay	Inhibition of leukocytes transmigration
VASP phosphorylation	Increased phosphorylation of VASP (PKA activation)
Rap1 activation	Activation of Epac/Rap1 pathway
Microarray analysis	Down regulation of ICAM-1, VCAM-1, and E-selectin

For a quantitative comparison, the ratio between the lowest effective doses of FSK and ADM was calculated (**Table 11**). On a molar basis equally effective concentrations of FSK and ADM differ from each other in all models tested by a factor of about 1,000. A factor of 10^3 to 10^4 is obtained by using pEC50 as the parameter for ratio calculation, although it must be mentioned that pEC50 could be analyzed in only three assays due to a limited number of the tested doses in the other assays or due to assay formats not suited for calculation of EC50 values. The relevant question was which increase in cAMP was required to achieve equivalent effects by FSK and ADM, respectively. As shown in **Table 12**, the effects at the lowest effective doses of ADM and FSK were comparable in all assays. However, the increase in cAMP (ΔcAMP) needed to achieve this effect was by a factor ~ 3-5 higher for FSK as compared with ADM.

Table 11 Quantitative comparison of ADM and FSK in different assays

Models		pEC50	Lowest effective doses	Factors of lowest effective doses
CHO-ADM reporter cell	ADM	-8.1 ± 0.1	1 nM	1,000
	FSK	-5.6 ± 0.1	1 µM	
ΔcAMP	ADM	-9.9 ± 0.3	100 pM	1,000
	FSK	-5.5 ± 0.6	100 nM	
ECIS	ADM	-9.6 ± 0.2	30 pM	1,000
	FSK	-5.6 ± 0.4	30 nM	
FITC-dextran permeability assay	ADM	not determined	1 nM	
	FSK	not determined	1 µM	1,000
TEM assay	ADM	not determined	1 nM	
	FSK	not determined	1 µM	1,000
VASP phosphorylation	ADM	not determined	10 pM	1,000
	FSK	not determined	10 nM	

Table 12 Quantitative comparison of ΔcAMP induced by ADM and FSK in different assays

Models		Lowest effective doses	Effects	ΔcAMP (fmol/well) (n=8)	Factors of ΔcAMP
ECIS	ADM	30 pM	-56 ± 21.5%	94 ± 162.4	
	FSK	30 nM	-42 ± 17.8%	439 ± 990.8	4.7
FITC-dextran permeability assay	ADM	1 nM	94.7 ± 18.2%	270 ± 169.3	
	FSK	1 uM	101.2 ± 7.3%	1245 ± 1396.7	4.7
VASP-Phosphorylation	ADM	10 pM	332.2 ± 29.4%	112 ± 212.5	
	FSK	10 nM	335.0 ± 14.2%	375 ± 603.9	3.3
TEM assay	ADM	1 nM	68.9 ± 8.5%	270 ± 169.3	
	FSK	1 µM	59.7 ± 18.3%	1245 ± 1396.7	4.7

5.4. Effects of ADM on gene expression

Data from the genome-wide microarray-analysis suggested that ADM down-regulated the expression of cell adhesion molecules (CAMs), such as ICAM-1, VCAM-1, and E-selectin which all exert distinct functions in the recruitment, adhesion and transmigration of leukocytes. Cytokines and growth factors which down-regulate the expression of cell adhesion molecules, are thought to have an anti-inflammatory effect. As data from Microarray analysis are not quantitative, the effects of ADM on the expression of those genes were analyzed in more details by use of quantitative RT-PCR (TaqMan® technique).

5.4.1. Analysis of time-dependent effects of ADM on CAMs

First of all, actions of ADM on gene expression were analyzed in quiescent HUVEC cells without any stimulation. ADM was used at a concentration of 100 nM which was previously shown to have satuated effects on endothelial barrier function. ADM reduced the mRNA levels of ICAM-1 by maximal 30%, as compared to control group (**Figure 24A**) in a time frame of 2 to 8 h. Similarly, mRNA levels of E-selectin were reduced maximally by 30% after 2h stimulation with ADM (**Figure 24C**). 16 h ADM stimulation had no impacts on regulation of E-selectin anymore. Expression of VCAM-1 and PECAM-1 were not influenced by ADM (**Figure 24B and D**). Taken together, under basal conditions, ADM showed no effects on gene regulation of VCAM-1 and PECAM-1 and only slight effects on ICAM-1 and E-selectin mRNA expression.

Figure 24 Effects of ADM on gene expression of adhesionce molecules

HUVECs were incubated with 100 nM ADM as indicated and mRNA levels were measured by QRT-PCR. mRNA expression levels were normalized to that of β-actin. Relative gene expression levels of ICAM-1 **(A)**, VCAM-1 **(B)**, E-selectin **(C)**, and PECAM-1 **(D)** are shown. Data are plotted as mean ± SEM, n=4.
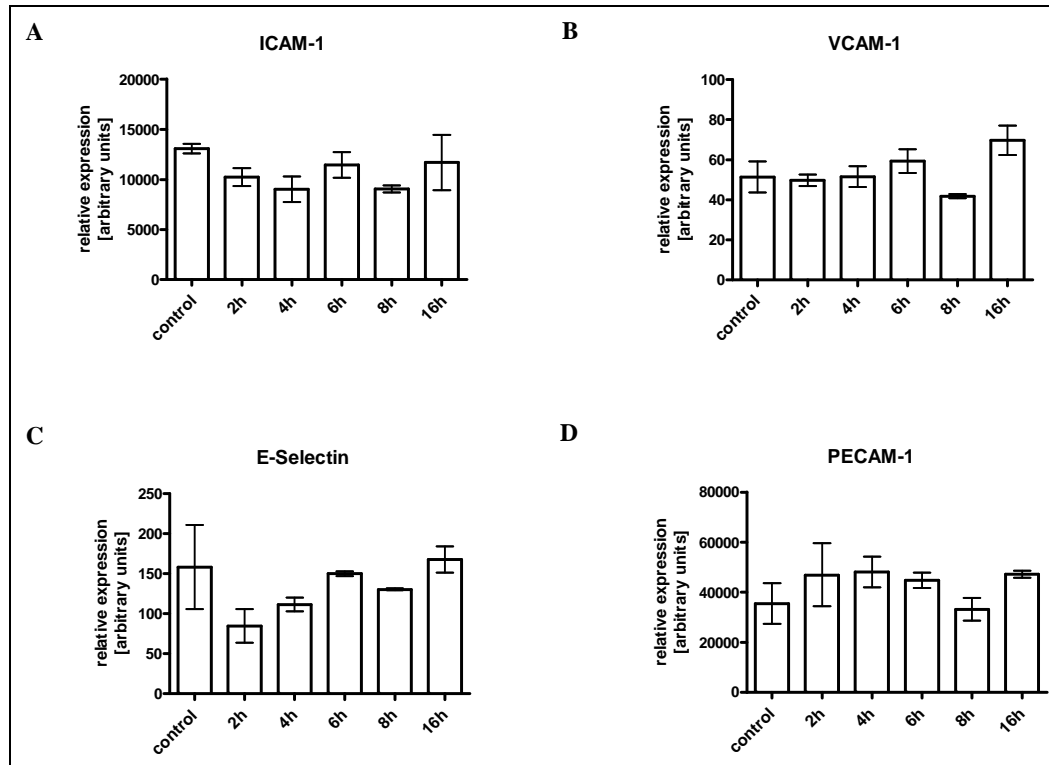
5.4.2. Effects of ADM on TNFα-induced expression of CAMs

Effects of ADM on gene expression were further analyzed in TNFα-stimulated HUVEC cells. As previously shown 5 nM TNFα induced endothelial barrier dysfunction, particularly endothelial hyperpermeability and granulocyte extravasation. Effects of increasing doses of TNFα (1 pM to 10 nM) were analyzed by using quantitative RT-PCR analysis. TNFα dose-dependently increased mRNA levels of ICAM-1, VCAM-1 and most prominently of E-selectin while mRNAs of PECAM-1 was slightly decreased. Induction factors as *fold of changes* refered to control group are given in **Table 13.** Interestingly, the mRNA levels of ADM receptors (CLRLR and RAMP-2) in HUVECs were down-regulated in a dose-dependent manner.

Table 13 Effects of TNFα on gene expression of adhesion molecules and ADM receptors
HUVECs were overnight incubated with increasing concentrations of TNFα (1 pM to 10 nM), and mRNA levels were measured by QRT-PCR. Relative gene expression levels were normalized to that of β-actin and *fold of changes* set to control group were listed. Cell adhesion molecules such as ICAM-1, VCAM-1, E-selectin, and PECAM-1, as well as ADM receptors CRLR and RAMP-2 were analyzed. Data are expressed as mean ± SD with n=4

Fold of changes (mRNA)	TNFα 1 pM	TNFα 10 pM	TNFα 100 pM	TNFα 1 nM	TNFα 10 nM
ICAM-1	1.0 ± 0.1	3.5 ± 0.6	21.7 ± 1.0	31.4 ± 2.2	37.6 ± 4.1
VCAM-1	0.9 ± 0.1	4.7 ± 0.6	50.8 ± 8.6	87.5 ± 12.5	87.6 ± 7.2
E-selectin	2.9 ± 0.7	6.3 ± 0.8	351.2 ± 44.9	721.2 ± 98.3	825.9 ± 77.0
PECAM	0.4 ± 0.3	0.7 ± 0.1	0.5 ± 0.0	0.3 ± 0.0	0.3 ± 0.0
CRLR	0.5 ± 0.1	0.8 ± 0.3	0.5 ± 0.2	0.4 ± 0.1	0.3 ± 0.1
RAMP2	1.1 ± 0.3	0.7 ± 0.3	0.3 ± 0.1	0.1 ± 0.0	0.2 ± 0.0

In the next step, HUVECs were treated with 100 nM ADM for 3 h and 16 h, and effects of ADM on basal as well as TNFα- induced mRNA levels of cell adhesion molecules were analyzed (**Figure 25**). None of the changes induced by 10 pM TNFα were affected by exposure to 100 nM ADM for 3 h or 16 h. Taken these data together, ADM showed no effects on mRNA expression of cell adhesion molecules, such as ICAM-1, VCAM-1, E-selectin and PECAM-1 in TNFα-stimulated endothelial cells.

Figure 25 Effects of ADM on TNFα-induced gene expression of cell adhesion molecules

HUVECs were overnight treated with 10 pM TNFα and 100 nM ADM for 16 h, or HUVECs were treated with ADM (100 nM) for 3 hours followed by overnight incubation with 10 pM TNFα. After stimulation, mRNA levels were measured by QRT-PCR. The mRNA expression levels were normalized to that of β-actin. Relative gene expression levels of cell adhesion molecules such as ICAM-1 **(A)**, VCAM-1 **(B)**, E-selectin **(C)**, and PECAM-1 **(D)** are shown. Data are plotted as mean ± SD, n=4.
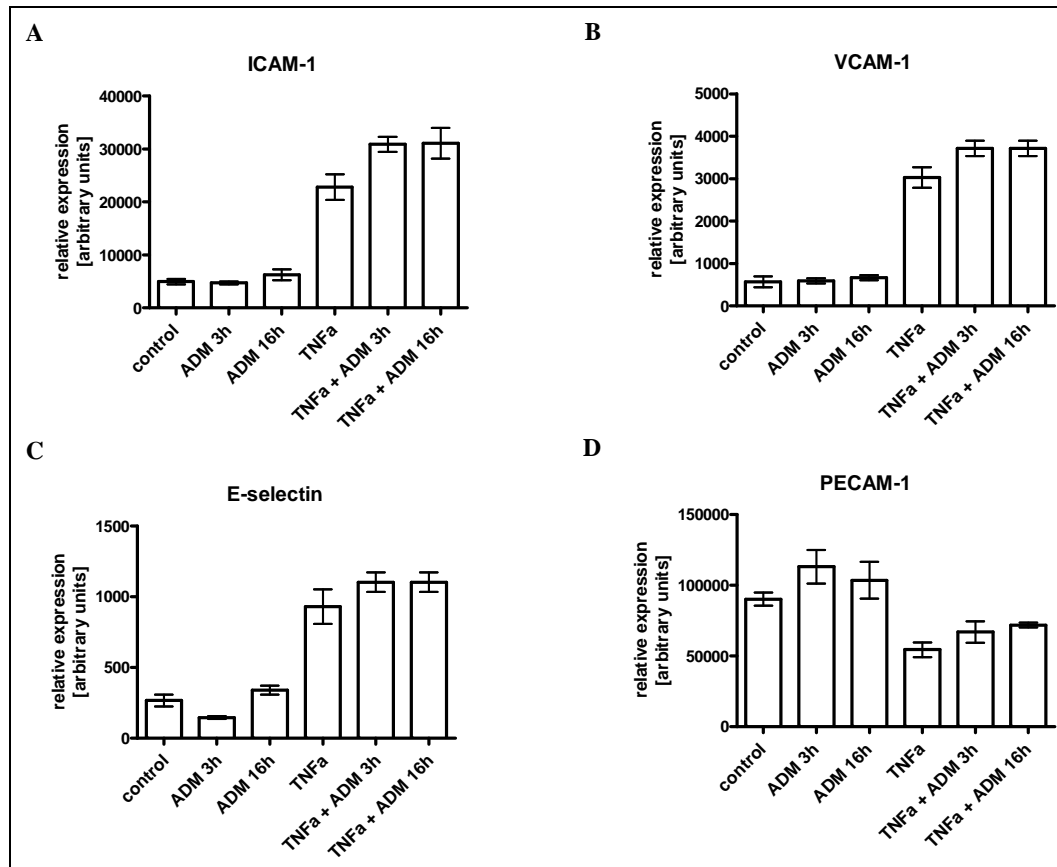
5.4.3. Effects of ADM on surface expression of CAMs

In addition to gene regulation of mRNAs, the protein expression of adhesion molecules on cell surface was further investigated by use of ELISA with specific antibodies against adhesion molecules. Similar to gene expression study, 100 pM TNFα caused a 7.3 ± 1.8 fold, 5.6 ± 0.8 fold, and 3.7 ± 0.4 fold increases in cell surface expressions of ICAM-1, VCAM-1, and E-selectin, respectively. However, pretreatment or post-treatment with ADM could not affect those increases of cell adhesion molecules on cell surface. Therefore, changes in

gene expression or surface expression of endothelial adhesion molecules cannot be used as explanation for the inhibition of PMN transmigration by ADM.

Figure 26 Effects of ADM on cell surface expressions of adhesions molecules after TNFα-stimulation

HUVECs were treated with 100 nM ADM 30 min prior to or following overnight incubation with 100 pM TNFα. After stimulation, primary antibodies against ICAM-1 **(A)**, VCAM-1 **(B)**, and E-selectin **(C)** were incubated for 60 min followed by incubation with peroxidase-conjugated secondary anti-mouse antibody for further 60 min. After adding TMB substrate solution, the absorbance signal on cell surface was measured. Cell surface expressions of adhesion proteins were quantified as the absorbance signals on cell surface. Data were expressed as mean ± SEM with n=4.
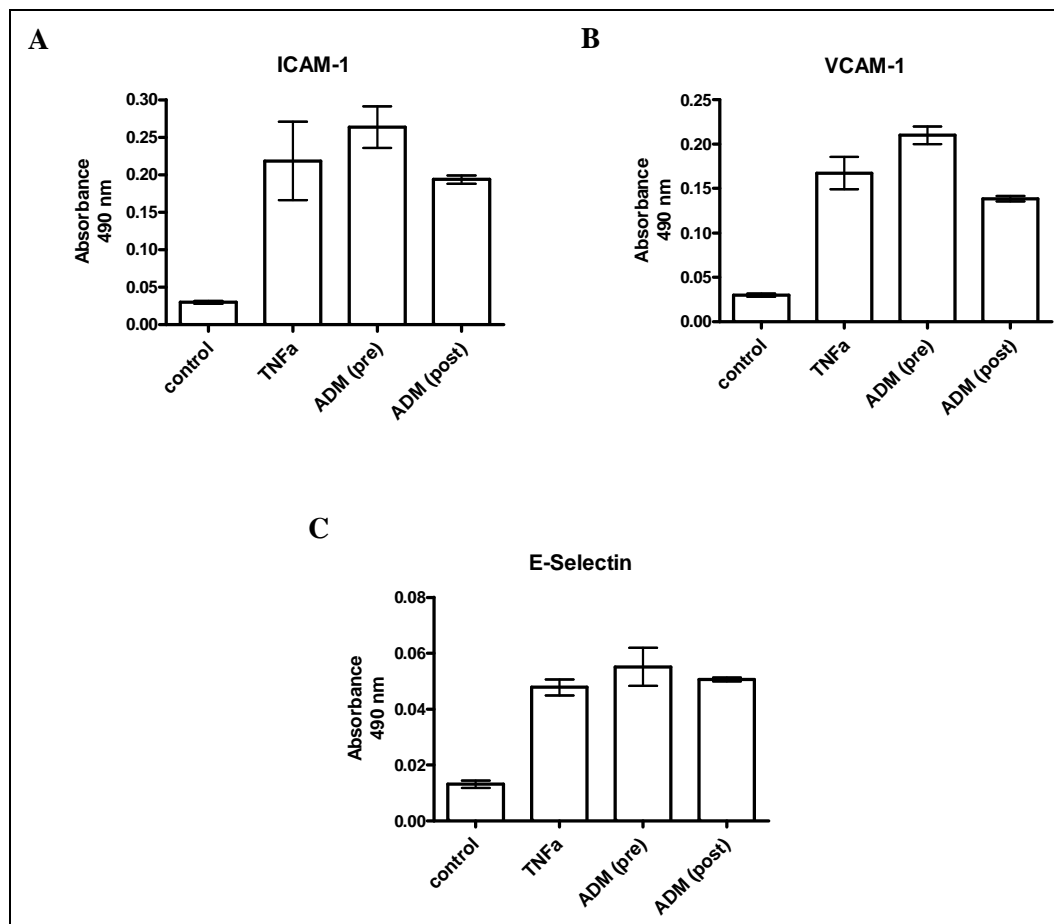
5.5. Role of PKA and Epac/Rap1 in ADM signalling

The previous data showed, that the effects of ADM on endothelial barrier function can entirely be explained as cAMP-mediated. Therefore the two

downstream branches of cAMP signaling relevant for endothelial barrier function, the PKA and Epac/Rap1 pathways, were further investigated for their relative contribution to effects of ADM signaling.

5.5.1. Dissection of PKA and Epac/Rap1 signaling

The specific PKA activator Benz-cAMP and the specific Epac/Rap1 activator "007" were chosen to further dissect cAMP downstream events. However, it was reported that the cAMP analogous "007", might have the potential to activate PKA at high concentrations (Holz et al., 2006). To verify or exclude the potential effect of "007" on PKA activation, the following experiments were performed: detection of CREB phosphorylation in Luceferase-transfected CHO cells as well as detection of VASP phosphorylation in primary human cells.

The cyclic AMP response element (CRE)-binding protein (CREB) is one of the best understood phosphorylation dependent transcription factors. Increased cAMP activates PKA by dissociating the regulatory from the catalytic subunits, which in turn is translocated into the nucleus and phosphorylates CREB, promoting CREB to recruit transcriptional co-activators that induce transcription of a variety of immediate early response genes. The CREB reporter cell line is derived from CHO cells with chromosomal integration of a luciferase reporter construct regulated by a cAMP response element (CHO-CRE-luciferase). As shown in **Figure 27C**, increasing doses of Benz-cAMP and "007" (10 µM-10 mM) were tested in the CREB reporter cell line. Beginning at 30 µM Benz-cAMP started to activate CREB-dependent luciferase transcription, serving as an indirect indicator of PKA activation. The maximum effect was at 3 mM. In contrast, "007" up to doses of 10 mM showed no effect on CREB dependent transcription.

PKA activation was indirectly monitored in HUVECs by detection of substrate phosphorylation by means of immnoblotting with an antibody against phospho-VASP. Different doses of Benz-cAMP and "007" (100 nM-1 mM) were analyzed (**Figure 27A and B**). At a concentration of 100 µM Benz-cAMP and higher

phosphorylation of VASP could be detected, whereas "007" had no effect on the VASP activation up to a concentration of 1mM.

In addition, to exclude potential effects of Benz-cAMP on Epac/Rap1 signaling, a Rap1 Pull-down assay was performed in which activated GTP-bound Rap1 is detected (**Figure 27D)**. While 100 µM "007" activated Epac/Rap1 signaling, 500 µM Benz-cAMP - a dose which significantly activated PKA signaling - had no effects. Based on this observation, 500 µM Benz-cAMP and 100 µM "007" were chosen for further experimental settings to dissect both pathways specifically.

Figure 27 Dissection of Benz-cAMP and "007" in different assays.
(A) and (B): HUVECs were treated with vehicle, Benz-cAMP (100 nM-1 mM) **(A)** or "007" (100 nM-1 mM) **(B)** or for 15 min followed by sample collection and western blot analysis of signaling pathway activation. Representative results from three independent experiments. **(C):** CHO-CREB-luciferase reporter cells were treated with Benz-cAMP (10 µM-10 mM) and "007" (10 µM-10 mM) for 15 min. The cAMP dependent increase of CREB phosphorylation is read out by luminescence signals. (n=4, mean ± SEM, *p<0.05, **p<0.005, ***p<0.0005 vs. vehicle group)
(D): HUVECs were treated with vehicle, "007" (100 µM) or Benz-cAMP (500 µM) for 15 min followed by sample collection and western blot analysis of signaling pathway activation. The small GTPase Rap1 activity was measured using Rap1-pull down assay. Representative results from a series of three independent experiments.
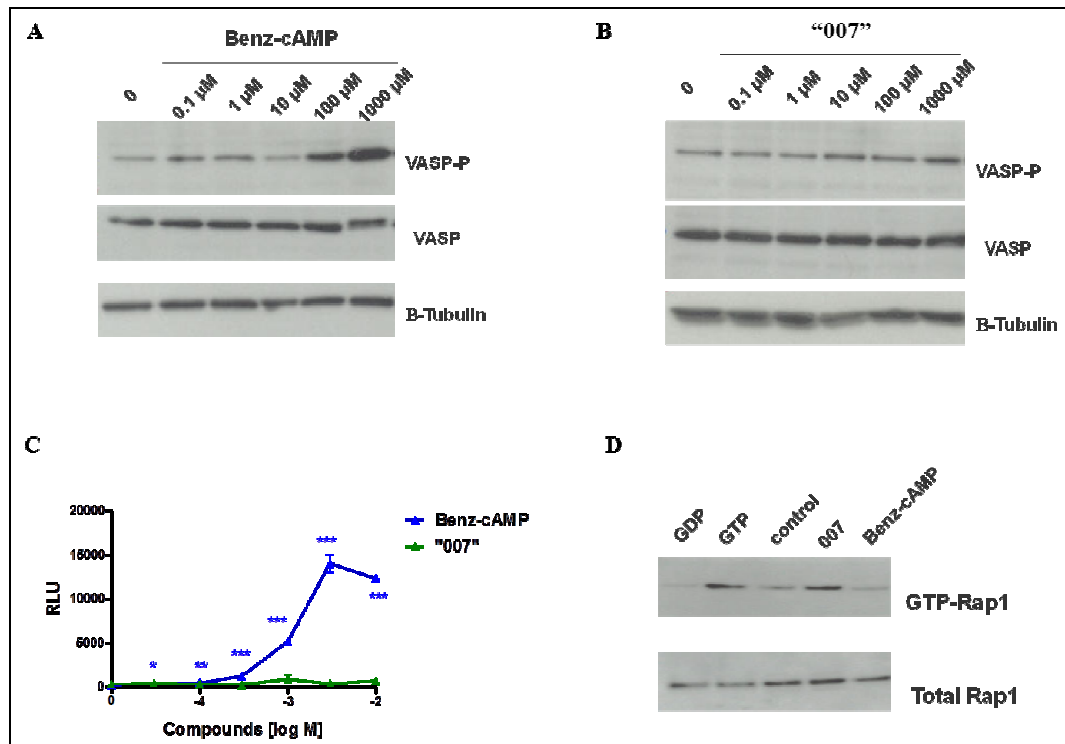
5.5.2. Impact of Epac/Rap1- and PKA-signaling on regulation of vascular permeability

Since the cAMP analogues Benz-cAMP and "007" were confirmed to specifically address the PKA and Epac/Rap1 pathways, the relative impact of the distinct cAMP-dependent signaling in the regulation of vascular permeability was further investigated by using these two tool compounds.

In ECIS, the addition of both cAMP analogues rapidly enhanced the transendothelial resistance of resting cell monolayer up to 175% within 30 min and remained constantly elevated over the entire experiment. This was the maximum achievable effect during dose escalation of the individual compounds (**Figure 28A**). However, combination of Benz-cAMP and "007" further enhanced TEER to 200% of control monolayer. The TEER reducing effect of thrombin was partially prevented by the individual compounds, more strongly by Benz-cAMP than by "007". Again the combination of both compounds showed enhanced effects also on thrombin induced hyperpermeability (**Figure 28B**). Like after ADM and FSK the level of TEER modulation by thrombin was shifted to more positive values rather than showing a true antagonism.

In parallel to TEER measurements, paracellular permeability for FITC-dextran was analyzed (**Figure 28C**). Both Benz-cAMP and "007" antagonized thrombin-induced hyperpermeability. However, both treatments reversed the permeability to that of resting cells, which was in contrast to ADM which reduced permeability below that of resting cell monolayers (**Figure 7C and D**).

In the next step, the effects of Benz-cAMP and "007" on vascular permeability in the skin of mice were examined by use of the modified Miles assay (**Figure 28D**). Intradermal application of histamine increased skin permeability to three-fold above base line. This effect was partially prevented by pretreatment with Benz-cAMP and "007". While Benz-cAMP reduced Histamine-induced hyperpermeability by about one third, "007" reduced permeability to almost normal values. In contrast to the *in vitro*-findings, combination of Benz-cAMP

and "007" showed no further enhancement of effects. In addition, Benz-cAMP and "007" also reduced basal vascular permeability significantly.

Throughout all these three models, both Benz-cAMP and "007" were equally effective with respect to resulting stabilization of endothelial barrier function *in vitro* and *in vivo*. However, combination of maximal active doses showed further enhancement of resulting effects. These observations suggest that both PKA- and Epac/Rap1-dependent cAMP signaling activate at least partially independent anti-edematous mechanisms.

Figure 28 Both PKA and Epac/Rap1 signaling are involved in regulating endothelial permeability *in vitro* and *in vivo*.

Transendothelial electrical resistance **(A and B)** and paracellular permeability for FITC-dextran **(C)** were measured over the time. HUVECs were pretreated with vehicle. "007" (100 µM) or Benz-cAMP (500 µM) followed by stimulation with thrombin (0.5 U/ml). Both cAMP analogues reduced thrombin-induced endothelial hyperpermeability *in vitro*. **(D) Miles Assay:** "007" (3 µM/mouse) as well as Benz-cAMP (3 µM/mouse) attenuated histamine-induced vascular hyperpermeability in the skin of mice. (N=6-10, mean ± SEM; [#]$p<0.05$ and [##]$p<0.005$ vs. vehicle group with PBS injection; *$p<0.05$ and ***$p<0.0005$ vs. vehicle group with histamine injection)
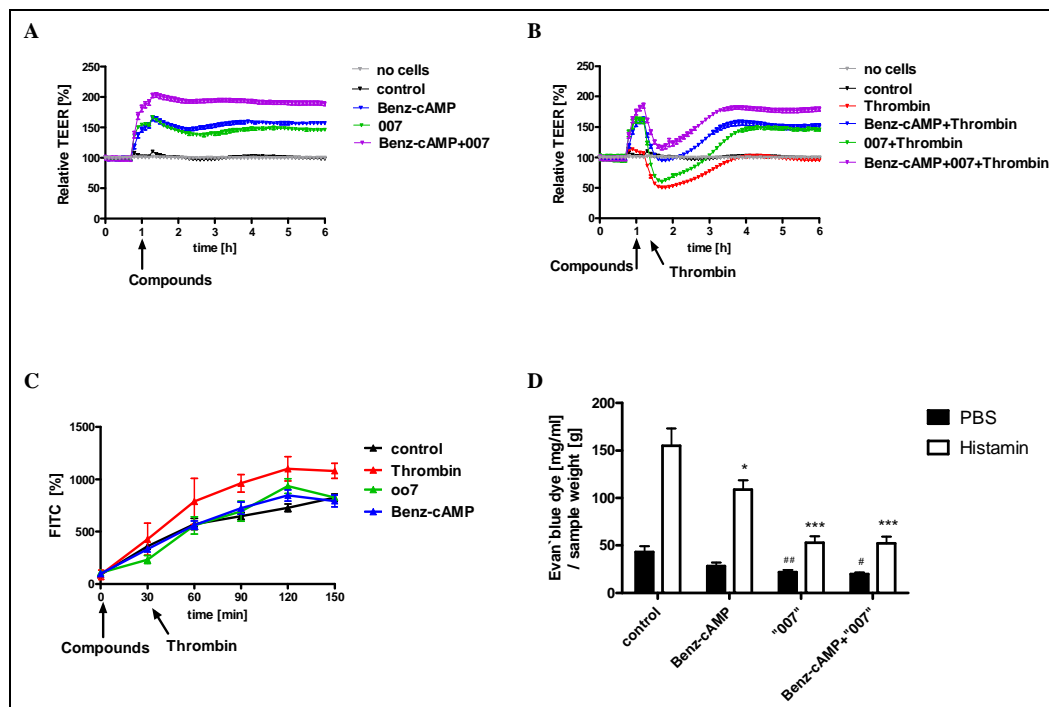
5.5.3. Role of PKA and Epac/Rap1 in regulation of granulocyte extravasation

5.5.3.1. Effects of PKA- and Epac/Rap1-signaling in PMN transmigration

As shown above ADM and FSK inhibited granulocyte extravasation in a dose-dependent manner, which was correlated with the induced intracellular cAMP levels. The question was raised whether both PKA and Epac/Rap1 signaling were involved in controlling granulocyte extravasation. As shown in **Figure 29A**, PKA activator, Benz-cAMP, inhibited granulocyte transmigration to 71.4 ± 5.0% (mean ± SD), which was comparable with the effect of ADM. In contrast, "007" showed no effect on granulocyte extravasation. Even the combination of Benz-cAMP and "007" had no additional inhibitory effects on granulocyte extravasation (56.3 ± 6.3%, mean ± SD), as compared to single treatment with Benz-cAMP. This result gave the first suggestion that only PKA-dependent cAMP-signaling might be involved in the regulation of granulocyte transmigration.

To further verify the effect of PKA on granulocyte transmigration, another cAMP analogous, 8- Bromoadenosine- 3', 5'- cyclic monophosphorothioate, Rp-isomer (Rp-8-Br-cAMP) was used to block the PKA dependent pathway (Aandahl et al., 1998). As shown in **Figure 29C**, 200 µM and 400 µM Rp-8-Br-cAMP, reduced ADM-induced phosphorylation of VASP in HUVECs, indicative of its inhibitory effect on PKA activation in endothelial cells. Thus, the dose of 400 µM was further used to fully block the PKA dependent pathway in ADM signaling in order to investigate its effect in the granulocyte transmigration assay (**Figure 29B**). While the PKA inhibitor alone had no effects on granulocyte transmigration, the initial inhibitory effect of ADM (56.7 ± 2.9%) was significantly weakened to 80.1 ± 2.6% of control group, further substantiating the PKA-dependency of the ADM effect (mean ± SD). Using both the activator and inhibitor of PKA signaling, evidence was provided for an involvement of PKA in the ADM-cAMP signaling in the regulation of granulocyte transmigration, while the Epac/Rap-1 pathway seems not to be involved.

Figure 29 PKA but not Epac/Rap1 is involved in leukocyte transmigration

(A): TNFα-stimulated HUVECs on Transwell filters were pretreated with vehicle, "007" (100 µM), Benz-cAMP (500 µM), or combination of "007" (100 µM) and Benz-cAMP (500 µM) for 30 min. (n=6; **$p<0.005$ vs. control group) **(B):** HUVEC on Transwell filters were stimulated overnight with TNFα (5 nM). On the day of experiment, HUVECs were pretreated with vehicle or Rp-8-Br-cAMP (400 µM) for 40 min, and subsequently treated with vehicle or ADM (100 nM) for 20 min. (n=6; *$p<0.05$ and **$p<0.005$ vs. control group; ###$p<0.0005$ vs. ADM group without Rp-8-Br-cAMP pretreatment) **(C):** Western blot was performed to detect phosphorylation status of VASP in HUVECs, indicative of PKA activation. HUVECs were pre-treated with vehicle or different doses of Rp-8-Br-cAMP (20 µM, 40 µM, 200 µM, and 400 µM) for 40 min and followed by subsequent stimulation with vehicle or ADM (100 nM) for 20 min. Anti-vinculin antibody was used as loading control. Representative data result from two independent experiments.
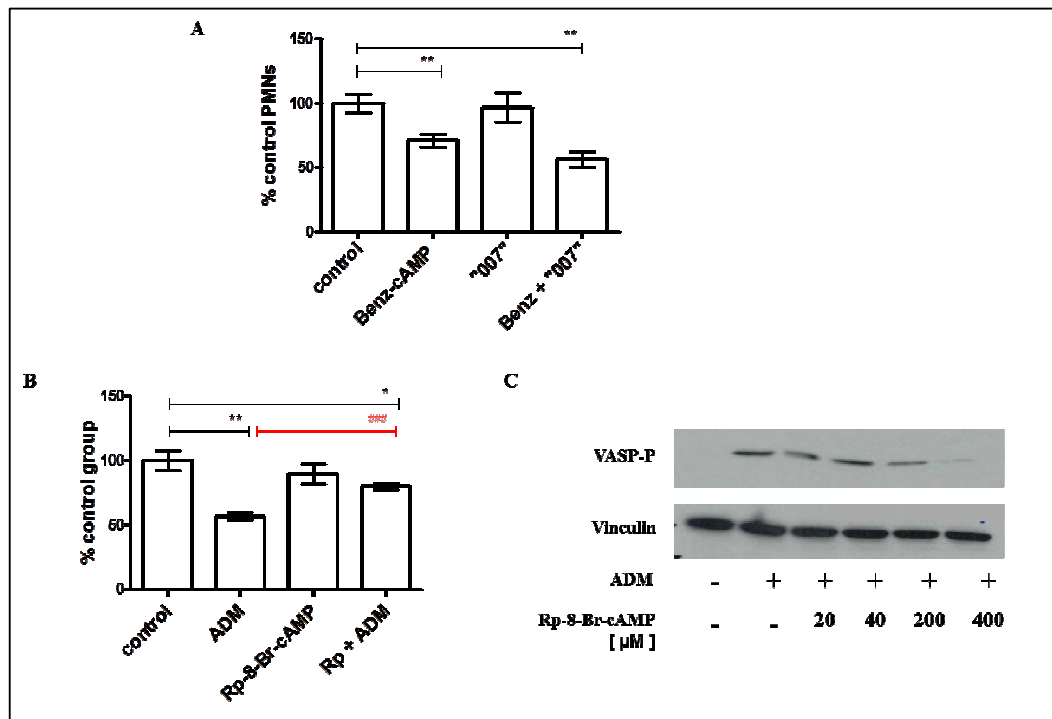
5.5.3.2. Role of PKA- and Epac/Rap1-signaling in regulation of PMN-induced hyperpermeability

There is emerging evidence that adhesion of activated leukocytes to endothelial cells not only actively prepares opening of endothelial contacts for transmigration but also contributes to endothelial hyperpermeability (reviewed by He, 2010; Yuan et al., 2012). It is further discussed that leukocyte induced hyperpermeability might be a prerequisite for transmigaration. Therefore the question was raised whether leukocyte-induced hyperpermeability could be

verified in the assay systems used, and if so, to which extent cAMP dependent signaling via PKA and Epac/Rap1 can modulate this process. Therefore similar conditions as used in the leukocyte transmigration assay were employed in the ECIS model. As shown in **Figure 30A**, in addition to TNFα-induced slow and prolonged decrease of electrical resistance to 74.3 ± 4.1% (mean ± SD), contact to PMN irreversibly reduced TEER and reached its trough within 2 hours. The extent of this effect of PMN was dependent on amounts of PMN added per well: the resistance was lowered to 70.2 ± 4.0% by 100,000 PMNs, to 54.0 ± 3.2% by 300,000 PMNs, to 47.4 ± 2.6% by 500,000 PMNs, and to 46.5 ± 1.3% by 1000,000 PMNs (mean ± SD). In the further assay (**Figure 30B**), the drop-down of electrical resistance evoked by 500,000 PMNs to 59.7 ± 4.0% was attenuated by addition of Benz-cAMP and "007" to 81.7 ± 3.1% and to 81.7 ± 4.8% (mean ± SD), respectively, when both compounds were added at maximal effective concentrations (as determined in pilot experiments, data not shown). The combined treatment of cells with both Benz-cAMP and "007" showed enhanced efficacy. These data were comparable to those obtained in TNFα stimulated cells without additional stimulation by PMNs: electrical resistance was decreased to 87.3 ± 6.4%, which was reversed to 127.1 ± 3.5% by Benz-cAMP, to 122.0 ± 7.8% by "007", and to 151.0 ± 6.4% (mean ± SD) by combination of Benz-cAMP and "007" (**Figure 30C**).

These data from ECIS assays confirm an additional and dose-dependent permeability inducing effect of PMN contact to TNFα stimulated HUVECs. Like in TNFα and Thrombin induced hyperpermeability both, PKA and Epac/Rap-1 pathway are involved in regulation of leukocyte induced hyperpermeability in endothelial cells. However, as hyperpermeability can effectively be prevted and reversed by "007" which has no impact on PMN transmigration, based on these data it can be excluded that PMN induced endothelial hyperpermeability is a prerequisite for their transmigration.

Figure 30 Effects of PKA- and Epac/Rap1 activator in regulating PMN-induced hyperpermeability

(A): HUVECs were grown on ECIS microelectrode plates to confluence and overnight incubated with TNFα (5 nM). On the day of experiment, cells were additionally stimulated with different amounts of PMNs (1×10^5, 3×10^5, 5×10^5 and 1×10^6 / well) and measurement of TEER was performed over 16 hours. **(B)-(C):** HUVECs were overnight stimulated with TNFα (5 nM). At the time indicated by the arrows, cells were treated with vehicle, "007" (100 µM), Benz-cAMP (500 µM), or combination of "007" (100 µM) and Benz-cAMP (500 µM) for 30 min, without any further treatment (**C**) or following by additional stimulation with 5×10^5 PMNs /well (**B**). TEER was normalized to the TEER measured at the beginning of the experiment. (n=8; mean ± SEM).
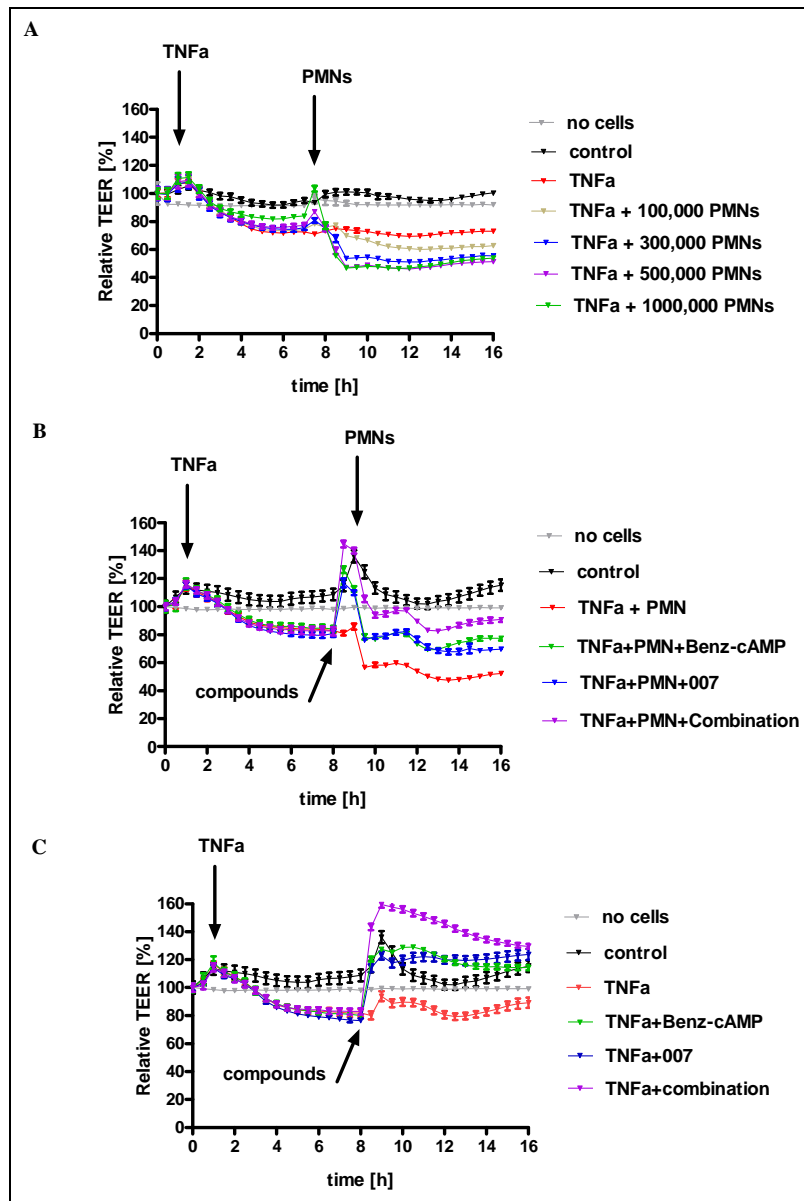
5.5.3.3. Impact of PKA- and Epac/Rap1-signaling on endothelial contractility

Adherence of neutrophils induces increase of intracellular calcium concentration and activation of MLC kinase in endothelial cells with subsequent activation of the contractile apparatus and paracellular gap formation, being a key determinant of leukocyte transendothelial migration in response to inflammation (Garcia et al., 1998). MLC kinase phosphorylates MLC at Ser-19 and Thr-18, which subsequently facilitates the interaction of myosin with actin, leading to the acto-myosin based contractile response.

ML-9 (1-[(5-chloro-1-naphthalenyl) sulfonyl] hexahydro-1H-1,4-diazepine) is a selective inhibitor of MLCK, which binds at or near the ATP-binding site of the active center and inhibits directly the catalytic activity of MLCK (Saitoh et al. 1987). BAPTA/AM, [1,2-Bis(2-aminophenoxy)ethane-*N,N,N',N'*-tetraacetic acid tetrakis(acetoxymethyl ester)], is a membrane-permeable intracellular calcium chelator, which inhibits calcium/calmodulin dependent activation of MLCK. In the established *in vitro*-leukocyte transmigration assay, both ML-9 and BAPTA/AM were shown to inhibit PMN transmigration dose dependently (**Figure 31A and B)**. Transmigration was reduced to 76.6 ± 3.2% and to 29.9 ± 11.2% (mean ± SD) by 100 and 300 μM ML-9, respectively, and to 70.3 ± 9.6% and to 51.1 ± 3.1% (mean ± SD) by 100 and 300 μM BAPTA/AM, respectively. The observations of those experiments were in line with previous reports (Saito et al., 1998), indicating that activity of calcium/calmodulin-dependent MLCK is necessary for transendothelial migration of granulocytes.

In addition to MLCK, also Rho kinase on one hand phosphorylates MLC on serine 19, and on the other hand phosphorylates the myosin–binding subunit (MBS) of MLCP thereby inactivating this enzyme, which is also crucial for regulating the phosphorylation status of MLC (Kawano et al., 1999; Amano et al., 1996). The azaindole derivative, 6-chloro-N4-{3,5-difluoro-4-[(3-methyl-1H-pyrrolo[2,3-b]pyridin-4-yl)oxy]-phenyl}pyrimidine-2,4-diamine (BAY77-7549), is a potent and selective Rho kinase inhibitor (Kast et al., 2007). BAY77-7549 inhibits granulocyte transmigration in a dose-dependent manner: to 47.7 ±

16.8% by 10 µM and to 18.6 ± 7.4% by 100 µM (mean ± SD) (**Figure 31C)**. Taken together, these results with all three inhibitors of independent pathways leading to MLC phosphorylation and activation, ML-9, BAPTA/AM, and BAY77-7549, provided evidence for the crucial role of the phosphorylation status of endothelial MLC in regulating transendothelial migration of granulocytes.

So, the question was raised whether Benz-cAMP and "007" which differently affect granulocyte transmigration show different effects on the phosphorylation of MLC. Phosphorylation status of MLC was analyzed using specific anti-phosphor-Ser19/Tyr18 antibody and thrombin was used to increase basal phosphorylation of MLC. As shown in **Figure 31D and E**, 100 nM ADM, 10 µM FSK, and 500 µM Benz-cAMP, which effectively inhibited leukocyte transmigration, also significantly reduced phosphorylation of MLC. In contrast, 100 µM "007" which protected endothelial permeability had no effect on the phosphorylation status of MLC. These data suggest that the fact that PMN transmigration is inhibited by activation of PKA but not of Epac/Rap1 is most probably due to PKA dependent inhibition of MLC phosphorylation thereby counteracting endothelial contractility.

Figure 31 Regulation of MLC is involved in cAMP-PKA pathway on granulocyte transmigration

(A) (B) and **(C):** Human neutrophils were allowed to transmigrate toward the IL-8 gradient through a HUVEC monolayer on transwell filter which was stimulated overnight with TNFα (5 nM). Endothelial monolayers were treated for 30 min with different doses of ML-9 (30 µM, 100 µM, and 300 µM) **(A)**, BAPTA (30 µM , 100 µM, and 300 µM) **(B)**, or RhoK-inhibitor BAY77-7549 (1 µM, 10 µM, and 100 µM) **(C)**. For each experiment, the number of neutrophils migrating under control condition (without compound treatment) was set to 100%. (n=3, mean ± SEM) (*p<0.05, **p<0.005, and ***p<0.0005 vs. control group) **(D-E)**: HUVECs were pretreated with vehicle, ADM (100 nM), FSK (10 µM), Benz-cAMP (500 µM), and "007" (100 µM) for 15 min followed by 15 min stimulation with thrombin (0.5 U/ml). Anti-vinculin was used as loading control. Representative results of three independent experiments.
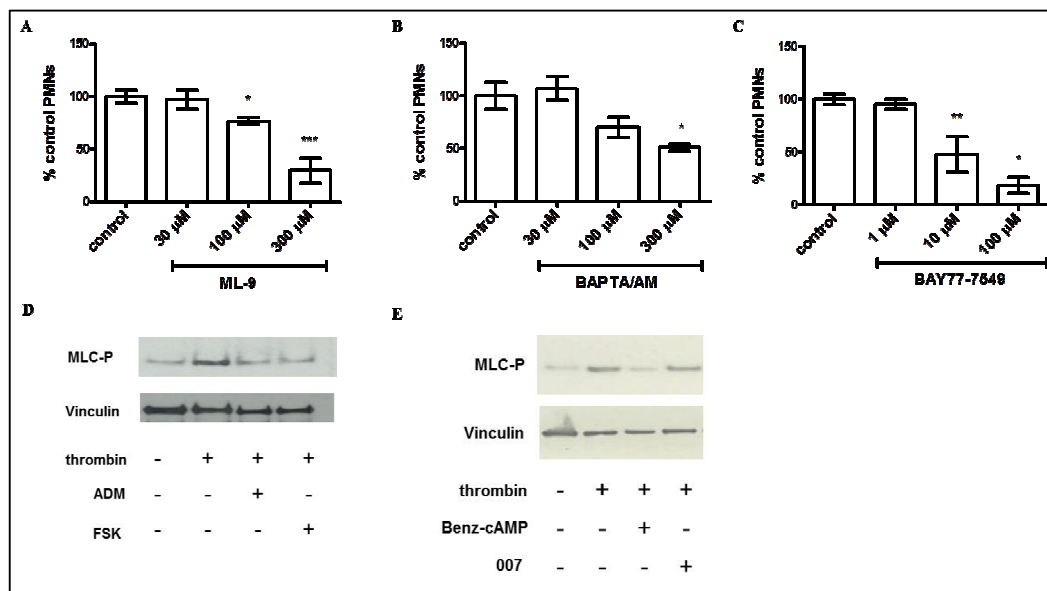
It was further investigated by means of immunohistochemistry whether both pathway activators had effects on junctional structures and contractile apparatus. Similarly to ADM (**Figure 8**), both cAMP analogous prevented thrombin-induced gap formation on cell-cell junctions, preserving a continuous straight line of VE-cadherin around the cell borders (**Figure 32**). Benz-cAMP seemed to reduce formation of stress fibers and retraction of the cell mass toward the center and to enhance peripheral cortical actin (**Figure 32C**). However, with "007" the formation of stress fibers seemed to be less affected (**Figure 32D**).

Taken together, the cAMP-PKA pathway most likely counteracts granulocyte transmigration by regulating the contractile apparatus via inhibition of MLC phosphorylation in contrast to the Epac/Rap1 pathway which does not inhibit MLC phosphorylation and fails to interfere with granulocyte transmigration.

Figure 32 Effects of PKA and Epac/rap1 on thrombin-induced F-actin and VE-cadherin distribution.

HUVECs were grown to confluence on fibronectin-coated glass cover slides and pretreated with vehicle, Benz-cAMP (500 µM) **(C)** or "007" (100 µM) **(D)** for 30 min, following thrombin (0.5 U/ml) stimulation for 30 min. Cells were fixed and permelized with 100% (v/v) ethanol (-20°C, 10 min) and stained for F-actin (red), VE-cadherin (green), and nucleus (blue). **(A)** quiescent cells and **(B)** thrombin-stimulated cells. Scale bars = 20 µm.
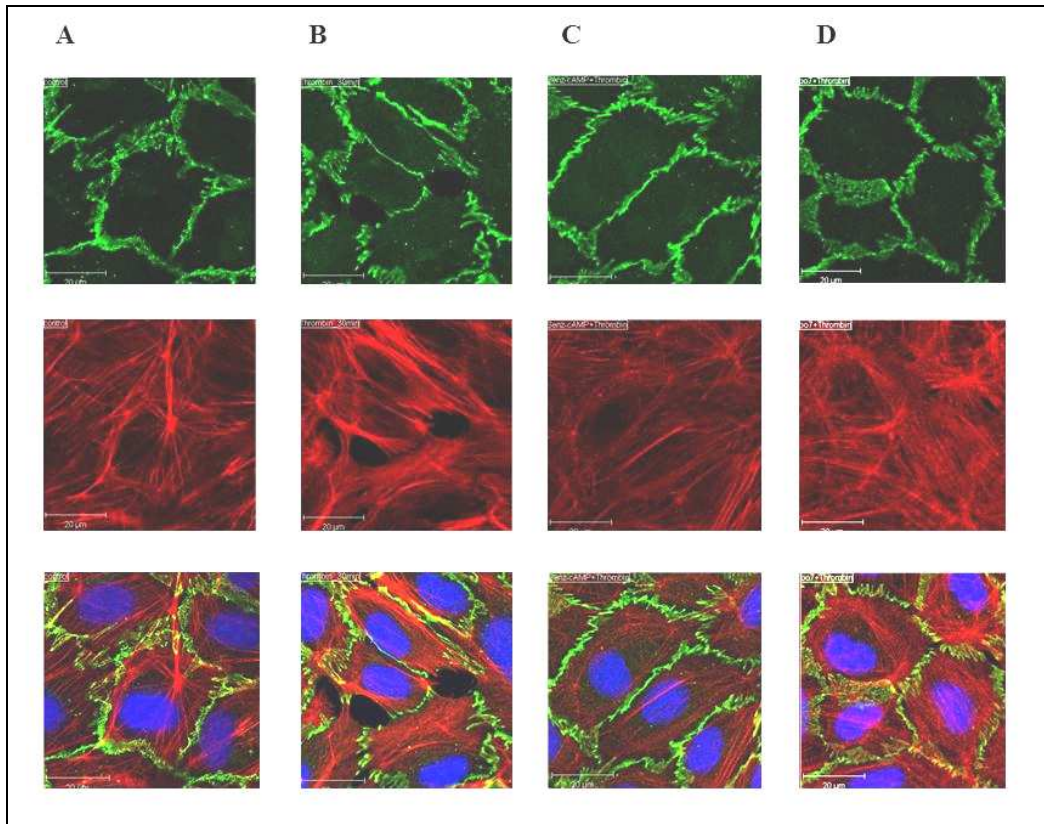
5.6. Direct effects of ADM on endothelial cytoskeleton and cell-cell junctions

5.6.1. Role of cortactin in ADM-mediated endothelial barrier modulation

Barrier protective effects of ADM could be related to a reduction of dynamic changes in myosin-actin based cellular contractility as refelected by the reduction of Myosin light chain phosphorylation and stress fiber formation. In the next step, it was addressed whether ADM could directly affect static cytoskeleton and cell-cell junctions. Beside a role of myosin-actin mediated cellular contraction, disruption and rearrangement of cytoskeleton are reported to be of equal importance in the development of endothelial gaps. One of the most important cytoskeletal components is the 80 to 85 kDa actin-binding protein, cortactin. Cortactin is involved in cortical actin assembly and dynamic actin rearrangement (Ammer & Weed, 2008). An important role of endothelial cortactin in leukocyte transmigration and barrier integrity is likely. Therefore the question was addressed whether this actin-binding protein is involved in ADM signaling with respect to the regulation of endothelial barrier function.

First of all, an immunocytochemical approach was performed to investigate whether ADM has influence on the distribution of cortactin in endothelial cells **(Figure 33).** In quiescent cells, cortical actin was well organized along the cell borders, while cortactin was diffusely distributed over the entire cytosol. The structure of cortical actin and the distribution pattern of cortactin seemed not to be affected after incubation of ADM and FSK.

Figure 33 Effect of ADM on cellular distribution of cortactin by using immunofluorescence microscopy

HUVECs were grown on fibronectin-coated glass cover slides and incubated with vehicle **(A)**, ADM (100 nM) **(B)**, or FSK (10 µM) **(C)** for 30 min. Cells were fixed and permelized with 100% (v/v) ethanol (-20°C, 10 min) and stained for F-actin (red), cortactin (green), and nucleus (blue). Scale bars = 10 µm.
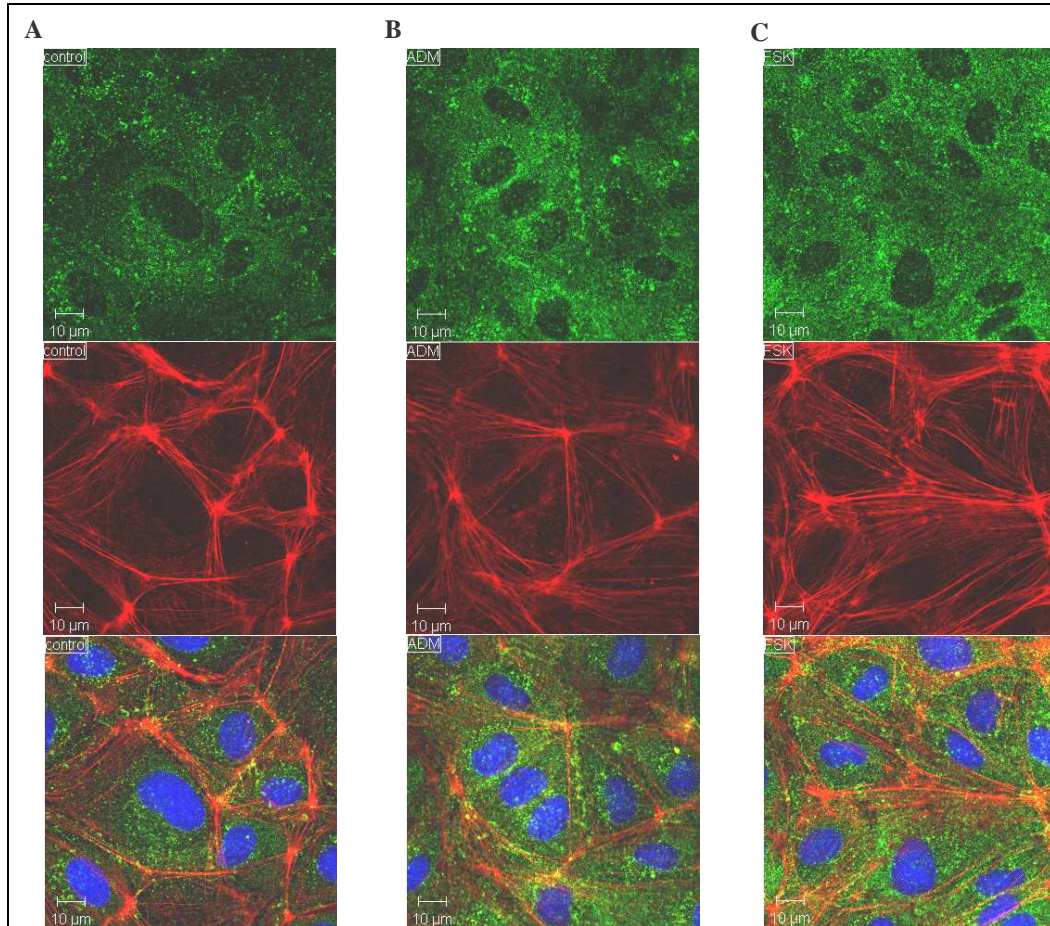
In the next step, RNA interference technique was applied to down-regulate the gene expression of cortactin. Silencing of cortactin by SiRNA transfection reached its maximal effect after 48 h in human endothelial cells (Schnoor et al., 2011) **(Figure 34 A).** Based on this result, assays for paracellular permeability for FITC-dextran **(Figure 34 B)** and transendothelial migration of human PMN **(Figure 34 C)** were performed 48 h after SiRNA transfection. Silencing of cortactin expression increased basal macromolecular permeability to 118.5 ± 5.7% (mean ± SD), which could be reversed to 83.7 ± 5.0% (mean ± SD) with ADM treatment. In the lamin-SiRNA transfected control group, treatment of ADM reduced basal permeability to 81.8 ± 3.2% (mean ± SD), which was

identical with the ADM-treated cortactin-SiRNA transfected group. This observation suggested that a cortactin-independent pathway was partly involved in ADM signaling regulating endothelial permeability.

Differently to endothelial permeability, down-regulation of cortactin expression decreased transendothelial migration of human neutrophils to $66.2 \pm 5.4\%$ (mean $\pm$ SD) of control SiRNA group. Similarly, in control-SiRNA group, ADM reduced transmigrated PMN to $66.2 \pm 5.7\%$ (mean $\pm$ SD) of vehicle group. However, in the group with down-regulated cortactin, ADM had no additional effect to $60.9 \pm 2.6\%$ (mean $\pm$ SD), meaning that the inhibitory effect of ADM on leukocyte transmigration disappeared in the absence of cortactin. In summary the consequences of cortactin knock down in HUVECs were inconsistent: with respect to leucocyte transmigration the data suggest a potential role of cortactin in ADM signaling but not with respect to endothelial permeability.

Figure 34 Role of cortactin in ADM signaling regulating endothelial permeability and granulocyte transmigration

(A): HUVEC were transfected with either lamin- or cortactin-specific SiRNAs and after 48 h were lysed for immunoblotting to detect expression levels of cortactin. Blotting for tubulin was used as loading control. Transfected HUVECs were seeded on transwell filter for 48 h and were used for paracellular permeability for FITC-Dextran **(B)** and leukocytes transmigration assay **(C).** For both assays, the cells were incubated with vehicle or ADM (100 nM) for 30 min. The relative FITC or relative transmigrated PMNs were set to the control group with lamin-SiRNA. (n=6, mean ± SEM) (*p<0.05 and **p<0.005 as compared to lamin SiRNA-transfected group treated with vehicle; ###p<0.0005 and n.s. not significant p>0.05 as compared to cortactin SiRNA-transfected group treated with vehicle)
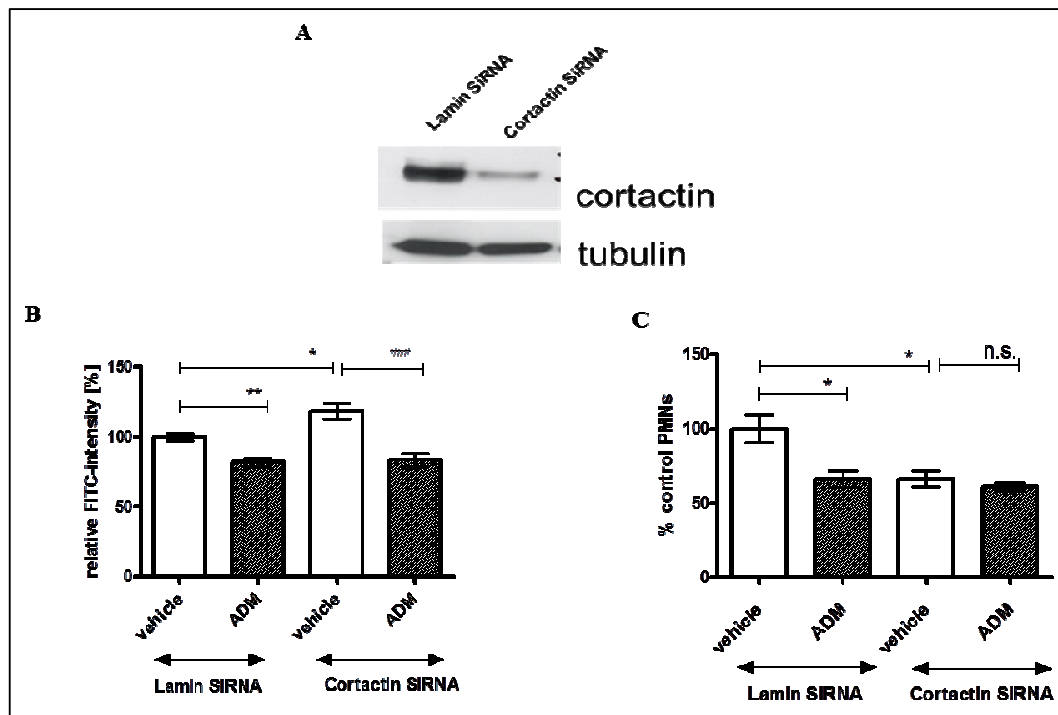
5.6.2. Analysis of ADM effects on the background of disrupted actin cytoskeleton

With the following experiments the question was addressed whether effects of ADM on endothelial barrier function are only based on its impact on actomyosin cytoskeleton. For this purpose, a mycotoxin which inhibited the actin polymerization, cytochalasin D (CytoD), was chosen to disrupt the endothelial actin cytoskeleton. The effects of ADM on junctional proteins and the cytoskeleton were investigated by laser scanning microscopy (**Figure 35**). In

quiescent cells, the staining for VE-cadherin around cell border represents a continuous straight line and staining of F-actin with Alex-555 phalloidin revealed a well-arranged structure of cortical actin fibers along the cell periphery **(Figure 35A)**. Cytochalasin D induced distortion of the linear structure of VE-cadherin with visibly defects of VE-cadherin staining, indicating intercellular clefts **(Figure 35B)**. In parallel, well-arranged distribution of cortical actin fibers along cell borders disappeared after treatment with cytochalasin D: the actin staining was intensely concentrated as a continuous straight line around the cell body and diffuse actin staining was also observed in the cytosol, indicating a severely disrupted endothelial cytoskeleton. Incubation of ADM prior to cytochalasin D seemed not to prevent the disruption of actin cytoskeleton, whereas the VE-cadherin linear structure was reestablished and gap formation was prevented **(Figure 35C).**

Figure 35 Effect of ADM on VE-cadherin and actin fibers in endothelial cells with intact cytoskeleton.

HUVECs were grown to confluence on fibronectin-coated glass cover slides, stained for F-actin (red) and VE-cadherin (green), nucleus (blue). Cells treated with vehicle **(A)** displayed well-arranged cortical actin fibers with few stress fibers and continuous cell-cell junctions. Treatment with 300 nM cytochalasin D **(B)** caused a massive decrease of actin fibers, distortion of VE-cadherin pattern and formation of intercellular gaps. Pretreatment of ADM prior to cytochalasin D **(C)** prevented VE-cadherin disruption and gap formation without affecting actin fibers. Scale bars = 20 μm..
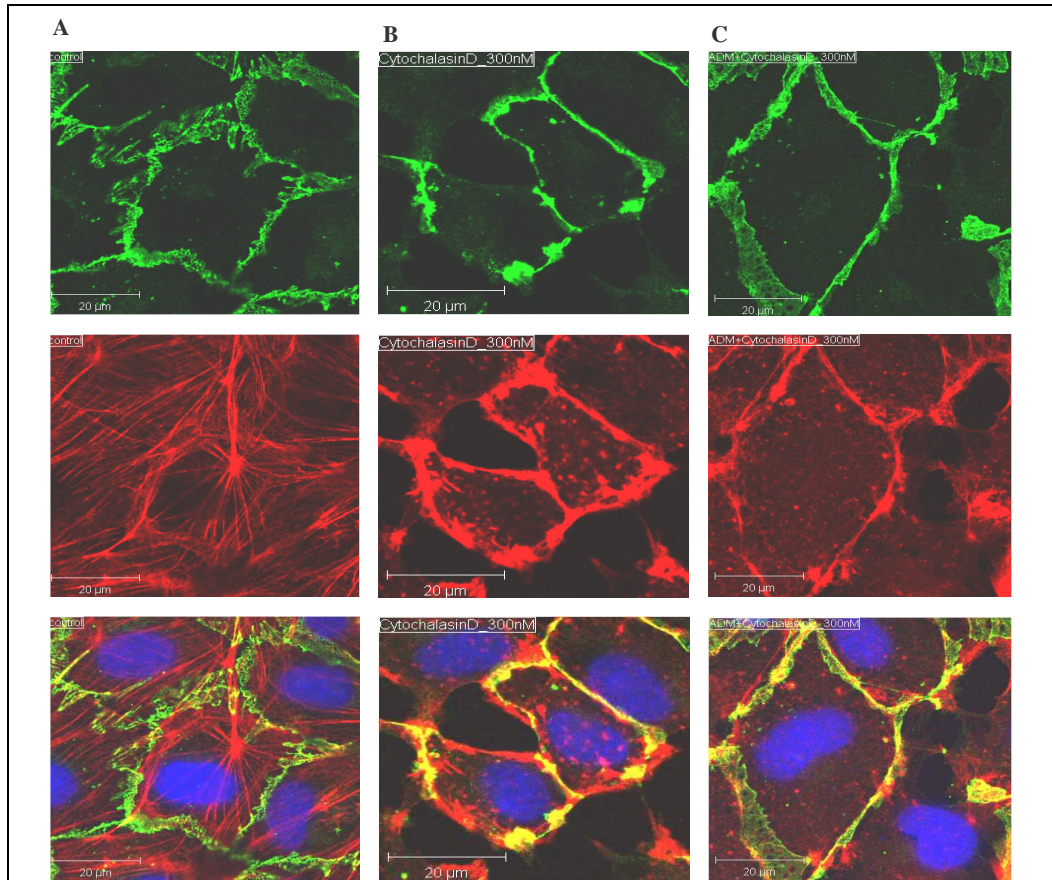
The effects of cytochalasin D on endothelial barrier integrity were further investigated by means of ECIS technique. As shown in **Figure 36A,** disruption of the actin cytoskeleton with cytochalasin D dose-dependently induced a rapid decline of TEER within minutes, which returned to baseline level after 13 hours. 30 nM Cytochalasin D was the lowest dose to slightly decrease TEER to 92.4%, whereas 300 nM reduced the TEER to 31.4% and was also the maximal dose from which the cells were still able to recover after 13 hours. If the cells were pretreated with ADM for 30 min prior to cytochalasin D treatment, the dropdown

of TEER to 31.4% was reduced to 66.0%, with the amplitude of 34.6% **(Figure 36C)**. This amplitude was identical with the increase of TEER induced by ADM on control cells, suggesting that the effect of ADM was not changed by the treatment with cytochalasin D. In parallel, ADM was also administered after cytochalasin D, **(Figure 36D)**. The decline of TEER to 31.4% induced by cytochalasin D was reversed by ADM to baseline within 2 hours and cells reached the same level of TEER followed by ADM on control cells after 12 hours.

In addition, the effects of cytochalasin D on macromolecular permeability were analyzed **(Figure 36B)**. Cytochalasin D induced hyperpermeability over the time and reached its maximal effect to 140.0% of control group after 2 hours, whereas ADM reduced macromolecular permeability to 48.8%. The Cytochalasin D induced hyperpermeability was antagonized to 81.3% by pre-treatment with ADM. The amplitude of ADM on cytochalasin D-induced hyperpermeability was 51.2%, identical with the direct ADM effect on basal permeability (51.2%). Taken all these findings together, in the endothelial cells with disrupted actin cytoskeleton, ADM could still stabilize barrier integrity with increased TEER and reduced macromolecular permeability, as well as VE-cadherin distribution on cell borders. These observations implicate that effects of ADM on endothelial barrier function are at least partly independent of the actin cytoskeleton and lead to direct stabilization of the VE-cadherin dependent barrier function.

Figure 36 Effect of ADM on barrier integrity in endothelial cells with disrupted actin cytoskeleton.

(A, C and D): HUVECs were grown on 96-well ECIS microelectrode plates and measurement of TEER was performed over 16 hour. Relative TEER was normalized to the TEER measured at the beginning of the experiment. **(A):** At the time indicated by the arrows, HUVECs were treated with vehicle or increasing doses of cytochalasin D (CytoD) (10 nM, 30 nM, 100 nM, and 300 nM). **(C):** Endothelial monolayer was pre-incubated with ADM (100 nM) 30min prior to cytochalasin D (300 nM) treatment. **(D):** ADM (100 nM) administration was performed after maximal effect of cytochalasin D reached in ECIS. **(B):** ECs were cultured on transwell filters and paracellular permeability for 40kDa FITC-dextran was determined at different time points. (For ECIS, n=8, mean ± SEM; for FITC-dextran assay: n=6, mean ± SEM)
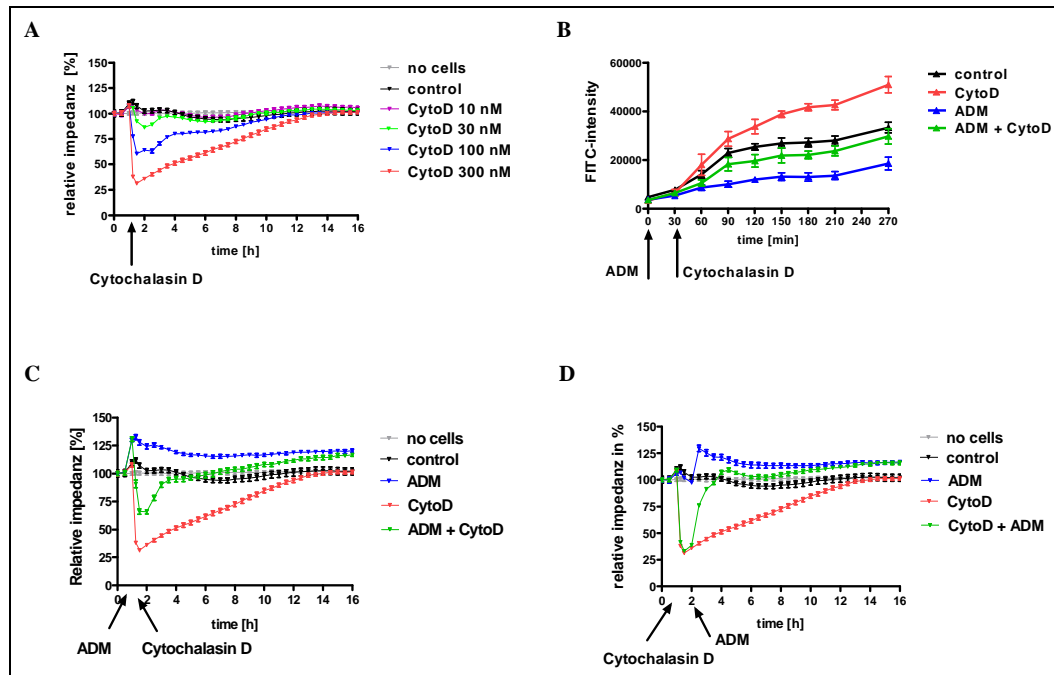
5.6.3. Effects of ADM on VE-PTP/VE-Cadherin complex

Stability of the VE-cadherin-catenin complex is important for endothelial permeability (Vestweber, 2008). Increased tyrosine phosphorylation of various components of the VE-cadherin-catenin complex is correlated with the decrease of VE-cadherin-mediated adhesion. Vasoactive stimuli, such as histamine, thrombin, VEGF and TNFα, have in common that they induce phosphorylation of the VE-cadherin-catenin components and thus lead to destabilization of the complex (Angelini et al., 2006; Vestweber, 2008). An important regulator of this phosphorylation is the vascular endothelial protein tyrosine phosphatase (VE-

PTP), which is associated with the Angiopoietin-1 receptor (Tie 2) and VE-cadherin. The work by Nottebaum et al. demonstrates the important role of VE-PTP in endothelial cell contact integrity. Down-regulation of VE-PTP expression inhibits VE-cadherin-mediated adhesion and thereby increases endothelial cell permeability and enhances leukocyte transmigration (Nottebaum et al., 2008). The importance of VE-PTP on regulation of cell-cell junctions raises the idea whether ADM mediates its regulatory effects in endothelial barrier function via action on VE-PTP.

As previously reported, docking of lymphocytes to TNFα-stimulated endothelial cells leads to dissociation of VE-PTP from VE-cadherin and is followed by destabilization of the endothelial barrier function (Nottebaum et al., 2008). A co-immunoprecipitation (CoIP) approach was performed to detect association and dissociation of VE-PTP from VE-cadherin in endothelial cells. Mouse brain endothelial cells bEnd.5 which expressed high level of ADM receptor (CRLR, RAMP2, and RAMP3) (see **Figure 6**) were chosen for this assay due to the availability of antibodies for mouse VE-PTP. Ovalbumin-specific antigen-stimulated T-lymphocytes were freshly prepared from mice and allowed to bind to the TNFα-stimulated endothelial cells for 10 min, and thereafter were completely removed before lysing endothelial cells for CoIP, in order to avoid degradation of VE-cadherin by neutrophil proteases during the experimentation (Moll et al., 1998). Endothelial cell lysates were immunoprecipited by VE-PTP antibody and the amount of coprecipitated VE-cadherin with VE-PTP was visualized in immunoblots by use of a specific anti VE-cadherin antibody. Aliquots of total cell lysates were subjected to immunoblots for VE-cadherin and were handled in the same way as the aliquots subjected to immunoprecipitations during the entire experiment, to exclude proteolysis as a potential reason for weakened VE-cadherin signaling. Immunoprecipitation of cell lysates with no antibody and isotype control antibody served as negative controls to exclude unspecific binding of antibodies. As shown in **Figure 37A**, the amount of immunoprecipitated VE-PTP (middle panel) and control VE-cadherin in total cell lysates (bottom panel) was at the same level in all samples, allowing a quantitative analysis of coprecipitated VE-cadherin (top panel). Upon docking of T-cells to the endothelial cells, the amount of

coprecipitated VE-cadherin was reduced to approximately 50%. Incubation of endothelial cells with ADM increased the amount of coprecipitated VE-cadherin to levels above control which was reduced to control level upon docking of T-cells to endothelial cells. In conclusion, treatment of endothelial cells with ADM prior to exposure to T-cells could strengthen the associated VE-cadherin to VE-PTP but could not abolish the T-cell induced dissociation of VE-PTP from VE-cadherin.

As another stimulus that leads to dissociation of the VE-PTP/VE-cadherin complex, VEGF was added to the starved endothelial cells for 30 min, and washed away before lysing endothelial cells for CoIP. As described above, endothelial cell lysates were immunoprecipited by VE-PTP antibody and the amount of coprecipitated VE-cadherin with VE-PTP was analyzed in immunoblots (**Figure 37B)**. The amount of immunoprecipitated VE-PTP (middle panel) and control VE-cadherin in total cell lysates (bottom panel) were at the same level in all samples, allowing a quantitative analysis of coprecipitated VE-cadherin (top panel). Stimulation of endothelial cells with VEGF reduced the amount of coprecipitated VE-cadherin to more than 50%. Incubation of endothelial cells with ADM increased the amount of coprecipitated VE-cadherin above control level, which was reduced to control level after VEGF stimulation. Also treatment with FSK increased the amount of coprecipitated VE-cadherin to above control level. VEGF stimulation after pre-treatment with FSK resulted in a reduction close to control levels. In conclusion pre-treatment of endothelial cells with FSK like ADM led to an increase of the VE-PTP/VE-cadherin complex in endothelial cells which was still sensitive to T-cell and VEGF induced dissociation. However the level of VE-PTP/VE-cadherin complex could be kept at normal levels. That the effect of ADM can be mimicked by FSK demonstrates its dependeny on cAMP mediated downstream signaling.

Figure 37 Effects of ADM on complex of VE-PTP and VE-Cadherin

(A): Mouse T-cells were added to overnight TNFα stimulated bEnd.5 cells. 10 min later, T-cells were removed by washing with PBS, and VE-PTP was immunoprecipitated (middle) and coprecipitated VE-cadherin (top) was analyzed in immunoblotting. Immunoprecipitation of cell lysates with no antibody (VE-PTP-/-) and isotype control antibody (IgG) served as negative controls to exclude unspecific binding of antibodies. The expression level of VE-cadherin in total cell lysates (bottom) was immunoblotted to exclude degradation of VE-cadherin during the experimentation. **(B):** 100 ng/ml VEGF was added to bEnd.5 cells for 30 min and cells were lysed for immunoprecipitation of VE-PTP (middle). Co-precipitated VE-cadherin (top) and expression levels of VE-cadherin in total cell lysates (bottom) were analyzed by immunoblotting. Molecular weight markers (kDa) are indicated on the left.
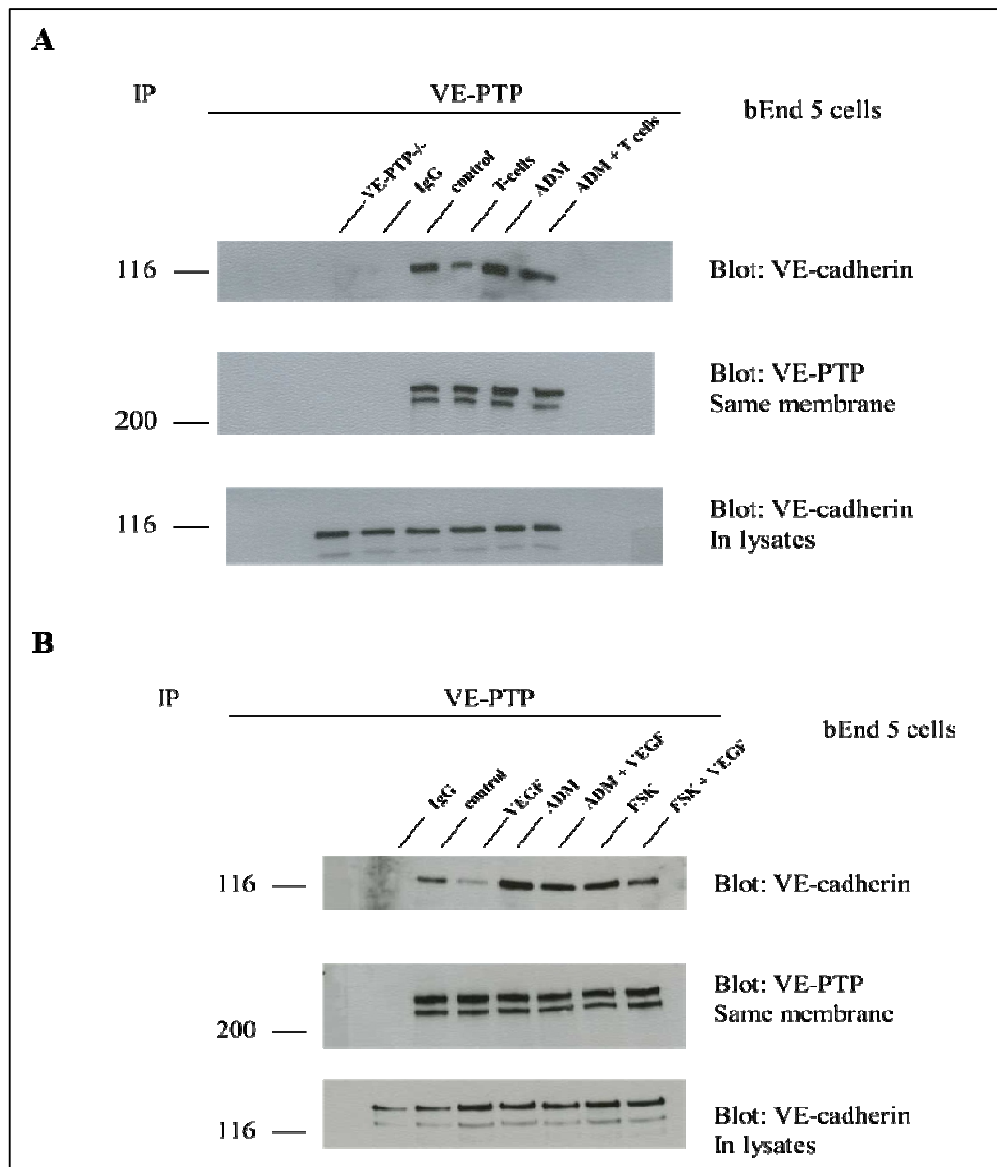
6. DISCUSSION

Vascular endothelium forms a semi-permeable barrier regulating the trafficking of macromolecules and blood cells across the blood vessel wall. Disruption of the endothelial barrier contributes to tissue edema and leukocyte extravasation, which are hallmarks of inflammation. The data from the present studies confirm the potent anti-edematous and anti-inflammatory effects of ADM *in vitro* and *in vivo*, and are in support of ADM as an attractive therapeutic target for inflammatory diseases. These effects of ADM are based on direct regulation of dynamic and static functions of the cytoskeleton (actomyosin-based contractility, cortical actin stability), and integrity of cell-cell junctions (VE-PTP/VE-cadherin interaction), rather than on interference with specific signaling mechanisms of different inflammatory stimuli. Increase of intracellular cAMP is the most important downstream signaling event of ADM receptor activation in endothelial cells. As all barrier-protective effects of ADM can be mimicked by FSK, no other pathway than the cAMP-dependent pathway is likely to contribute to these effects. Dissection of the downstream cascade by means of cAMP analogs, specific for PKA and Epac-Rap1 signaling, demonstrates that both pathways are equally effective with respect to permeability. In contrast, granulocyte transmigration is only reduced by PKA activation, which decreases myosin light chain phosphorylation linking effects of ADM on leukocyte extravasation to modulation of the contractile apparatus of the endothelial cell.

6.1. Effects of ADM in response to inflammation

6.1.1. Effects of ADM on endothelial permeability

The *in vitro*-ECIS methodology enables to show changes of electric resistance in endothelial cells in real time. As transendothelial electric resistance (TEER) is a surrogate for endothelial permeability, in addition, macromolecular permeability was directly determined in a second model in which labeled dextran was used as a tracer for permeability. Results from both systems are in line with the previous observations that ADM protects barrier permeability

seemingly in a way that is independent of stimuli (thrombin, VEGF, histamine, LI-1β, LPS, and TNFα) (Hippenstiel et al., 2002; Dunworth et al., 2008). Interestingly, ADM is therapeutically active even after effects of stimuli on permeability are fully established. As evident from ECIS data, the effects of ADM mainly consist in shifting endothelial resistance to higher levels rather than interfering with the stimulus induced reduction of TEER itself. It may be concluded that ADM exerts its effects via modulation of the factors determining endothelial permeability rather than counteracting specific signaling mechanisms induced by the different stimuli.

To investigate whether the *in vitro*-situation could be translated into the *in vivo*-models a modified Miles assay was applied. The Miles assay is a commonly used method to give information about the direct actions on vascular permeability in the skin using histamine as a short-acting agent causing microvascular leakage. Histamine contributes to vascular leakage in the course of acute inflammation associated with trauma, burns, and allergy. In line with *in vitro*-data, ADM reduces basal permeability, as well as antagonizes hyperpermeability induced by histamine in the skin of both rats and mice. It is of note that our present finding is in contradiction with previous reports (Grant et al., 2004; Tam et al., 2004), in which increased vascular permeability in the skin of mice after ADM administration was described. However, differing from our assay, ADM was directly injected into the skin of mice instead of intravenous administration, which might have caused increased vessel recruitment which potentially was misinterpreted as direct hyperpermeability (Grant et al., 2004; Tam et al., 2004).). The anti-edematous effect of ADM in the Miles assay is the first *in vivo*-finding that demonstrates its direct action on basal vascular permeability rather than that on inflammatory disturbed barrier function. Moreover, in the LPS-induced lung injury model, ADM treatment reduces lung weight and protein contents in BAL fluid, which displays the anti-edematous action of ADM under inflammatory conditions. These findings substantiate that ADM stabilizes endothelial barrier function also *in vivo* and represents a strongly anti-edematous principle.

6.1.2. Effects of ADM on granulocyte extravasation

Migration of leukocytes from the blood stream into the tissue at sites of inflammation is a key process of the immune system important for the clearance of infections and apoptotic cells. However, excessive or inappropriate translocation of leukocytes can contribute to pathological processes, such as atherosclerosis, multiple sclerosis, and rheumatoid arthritis. Overshooting leukocyte transmigration, predominantly of neutrophil granulocytes (PMN), is a hallmark of acute lung injury and accompanies disrupted endothelial barrier function. In the pre-experiment, the transmigrated leukocytes through TNFα stimulated HUVEC monolayer or in LPS-injured lung are mostly PMN (>95%). Thus, in the further experiments only this cell population was considered and discussed. ADM significantly prevents the TNFα-induced PMN transmigration. Notably, this is the first report about the direct effect of ADM on granulocyte extravasation in an *in vitro*-study, which may explain the beneficial effects of ADM observed in numerous *in vivo*-inflammatory models, in addition to its action on permeability. This finding is consistent with reduced white blood cells in BAL fluid in LPS-induced mouse models of acute lung injury.

6.1.2.1. Direct actions of ADM on human neutrophils

Neutrophils play an important role in the inflammatory reaction, such as acute lung injury. In animal studies of acute lung injury, both the lung tissues and bronchoalveolar lavage fluid exhibit dramatic neutrophil infiltration. Bacterially derived chemoattractants, such as LPS and fMLP, are shown to be able to up-regulate CD11b/18 expression on PMN and ICAM-1 expression on endothelial cells, thus facilitating adhesion of neutrophils to endothelium and migration into inflamed tissue (Smith 1993). By using cAMP analogous Bt2cAMP in mouse lymphoid cell line and human PMNs, elevation of cAMP inhibits chemoattractant stimulation of α4β1-integrin in lymphoid cells, as well as β2-integrin triggering in neutrophils (Laudanna et al., 1997). This anti-adhesive effect of cAMP is downstream of RhoA dependent integrin-mediated adhesion (Laudanna et al., 1997). However, in the transmigration assay used in the present study, ADM had no effects on adhesion of human PMNs to TNFα-stimulated HUVECs.

Notably, this adhesion assay was performed under static conditions. *In vitro*-assays under flow conditions may give rise to different results.

In the present study, the primary endothelial cells, HUVEC and HLMEC, expressed high levels of CRLR and RAMP2 (ADMR-1), which was in line with previously published reports (Wunder et al., 2008; Aslam et al., 2010). In mouse brain endothelioma cells (bEnd.5), CRLR, RAMP-2, and RAMP-3 (ADMR-1 and -2) are highly expressed. Similarly, CRLR, RAMP-2, and -3 (ADMR-1 and -2) are present in human PMN. While the expression level of CRLR and RAMP-2 in human PMN is comparable to that in human endothelial cells, RAMP-3 mRNA which is not detectable in endothelial cells is also abundantly expressed in human PMN. Despite the abundant expression of ADM receptor mRNAs, no functional cAMP signaling could be demonstrated in human PMN. FSK, however, induced cAMP albeit at higher concentrations than in endothelial cells and with lower efficacy. Increased intracellular cAMP in PMN is reported to antagonize fMLP-stimulated up-regulation of CD11b/18 as well as decreased bronchial epithelial cells (Derian et al., 1995; Friedman et al., 1998). ADM is also reported to suppress fMLP-induced up-regulation of CD11b/18 of human neutrophils, in a cAMP/PKA dependent manner (Saito et al., 2001). However, in the MPO activation assay neither ADM nor FSK had any influence on either fMLP or C5a activated PMNs. There was also no effect on CD11b expression on PMN after treatment with ADM by use of FACS analysis.

Consistently, while transmigration of PMN through the HUVEC monolayer was significantly inhibited by treatment of HUVECs with ADM, pretreatment of PMN with ADM had no effects on their transmigration. Altogether these observations provide evidence that prevention of TNFα-induced granulocyte transmigration was rather mediated by direct action of ADM on endothelial cells than on granulocytes.

6.1.2.2. Effects of ADM on gene expression of endothelial adhesion receptors

The primary element of leukocytes transmigration is the interaction between leukocytes and endothelium, which is facilitated by adhesion proteins from both

endothelial cells and leukocytes, as well as by direct signaling exchange via adhesion proteins and cytokines (Panes & Granger, 1998). Rolling adhesion occurs when leukocytes first capture from the bloodstream and loosely tether to the endothelial cells lining the blood vessel wall due to transient selectin mediated weak interactions between endothelial cells and leukocytes (Barreiro et al., 2004). Upon this rolling adhesion step, leukocytes slow down to pass through the blood vessel, which allows binding to endothelial cells and exposure to a local environment that initiates the activation step. This activation step is triggered by chemokine signals, such as TNFα. In the next step, firm adhesion of leukocytes to the surface of endothelial cells is mediated through the interaction of Ig-family adhesion molecules, such as ICAM and VCAM on endothelial cells, and activated integrins on leukocytes. Activation and gathering of endothelial cell adhesion molecules trigger a variety of signals within the endothelial cells and facilitate progression to the final diapedesis step, in which immune cells enter to inflammatory sites in infected tissue along a cytokine gradient.

In lymphatic endothelial cells, a genome-wide Microarray-analysis demonstrates that ADM profoundly suppresses gene expression of cell adhesion receptors and inflammatory factors, such as ICAM-1, VCAM-1, E-selectin, IL-8, and chemokines (Jin et al., 2011). Additionally, by using QRT-PCR and flow cytometry analysis, ADM dose-dependently suppresses the TNFα -induced mRNA and protein expression of ICAM-1 and VCAM-l in lymphatic endothelial cells (Jin et al., 2011). In HUVECs, ADM inhibits VEGF-stimulated ICAM-1, VCAM-1, and E-selectin mRNA expression through a phosphatidylinositol 3'-kinase/Akt pathway, and reduces VEGF-induced endothelial adhesiveness for leukocytes (Kim et al., 2003). However, controversial results are shown in the studies from Hagi-Pavli and colleagues: ADM up-regulates ICAM-1 expression in oral keratinocytes via a cAMP- and $NF_{\kappa B}$-involved pathway, explaining the immunostimulatory role of ADM in oral muocsa and skin (Hagi-Pavli et al., 2005). In addition, ADM is shown to induce cell surface expression of the adhesion molecules E-Selectin, VCAM-1, and ICAM-1 on HUVEC in a cAMP-dependent manner (Hagi-Pavli et al., 2004).

In the Microarray analysis on HUVECs of the present study, down-regulation of adhesion molecules, such as ICAM-1, VCAM-1 and E-selectin, is observed 3 hours after ADM administration. However, in the TaqMan®-QRT-PCR analysis, which provides more precise results than the microarray analysis, this observation on gene regulation of ADM under basal condition as well as after TNFα stimulation could not be confirmed. TNFα stimulation induces up-regulation of ICAM-1, VCAM-1 and E-Selectin, facilitating adhesion of neutrophils to endothelium and transmigration to inflamed tissue sides. Either long-term or short-term administration of ADM showed no effect on the TNFα-induced increase of ICAM-1, VCAM-1 and E-Selectin. The same was observed for the protein expressions of ICAM-1, VCAM-1, and E-selectin on cell surface: TNFα increases protein expression of adhesion receptors on cell surface, which is not influenced by ADM.

Moreover, in the leukocyte transmigration assay, short term administration of ADM was already sufficient to inhibit leukocyte transmigration, while long term administration of ADM had no additional effects (data not shown). Therefore, it can be assumed that the effects of ADM on leukocytes transmigration are mostly based on its direct action on the dynamic regulation of this process rather than regulation of gene expression of adhesion molecules.

6.1.3. Effects of ADM on endothelial cytoskeleton and junctions

6.1.3.1.   Effects of ADM on endothelial cytoskeleton

Endothelial cell contractility driven by the mechanochemical interaction between actin and myosin is of vital role in regulating vascular contact integrity. The contractility is characterized by the formation of stress fibers, bundles of actin filaments associated with nonmuscle myosin II (Wojciak-stothard & Ridley, 2002), and triggered by the phosphorylation of MLC, inducing myosin-actin cross-bridge cycling.In a simplified view contraction leads to dissociation of VE-cadherin (which is anchored to the actin cytoskeleton) from its adjacent partner thus forming inter-endothelial gaps (Garcia et al., 1995). In the present study, ADM was shown to prevent thrombin- induced stress fiber formation and retraction of cell mass toward the center and prevented endothelial barrier

disruption, visualized by preserved VE-Cadherin lining at the cell borders. Consistent with these immunofluorescence study observations, ADM abolished the thrombin-induced MLC phosphorylation, indicative of reduced actomyosin based cellular contractility. The observation that ADM significantly relaxed endothelial contractility is in line with previous reports (Hippenstiel et al., 2002). However, in the endothelial cells with disrupted actin cytoskeleton triggered by cytochalasin D, ADM still remained its barrier protective effects, correlated with the increased TEER, reduced macromolecular permeability, as well as linear VE-cadherin distribution at the cell borders. This data implicate that the effects of ADM regulating endothelial barrier function in endothelial cells are at least partly cytoskeleton-independent.

6.1.3.2. Effects of ADM on endothelial cell-cell junctions

Amounting data from the literature reveal a fundamental role of ADM in regulating the organization of junctional proteins in particular supporting the ability of VE-cadherin to associate with peripheral cortical actin even after stimulation with thrombin, hydrogen peroxide and S. aureus α–toxin (Hippenstiel et al., 2002; Brell et al., 2005; Hocke et al., 2006). Moreover, concerning the blood brain barrier function, in primary brain microvascular endothelial cells of rats, ADM is shown to up-regulate expression of claudin-5 (Honda et al., 2006). Additionally, in a recent study in lymphatic endothelial cells, ADM stimulation causes a reorganization of the tight junction protein ZO-1 and the adherens protein VE-cadherin at the plasma membrane, independently of changes in junctional protein gene expression (Dunworth et al., 2008).

The stability of VE-cadherin-catenin complex is dependent on its tyrosine phosphorylation status. Increased phosphorylation is correlated with the decreased adhesion. The vascular endothelial protein tyrosine phosphatase (VE-PTP), an endothelial membrane protein associated with VE-cadherin is known as an important regulator of this tyrosine phosphorylation thereby interfering with endothelial permeability and granulocyte extravasation *in vitro* and *in* vivo (Nottebaum et al., 2008; Broermann et al, 2011). Docking of neutrophil granulocytes or lymphocytes to TNFα-stimulated endothelial cells was shown to dissociate VE-PTP from VE-cadherin, thus leading to vascular

leakage (Nottebaum et al., 2008). Down-regulation of VE-PTP expression increased endothelial cell permeability, enhanced leukocyte transmigration, and inhibited VE-cadherin-mediated adhesion (Nottebaum et al., 2008). In the present CoIP study, ADM was demonstrated to strengthen the association of VE-cadherin to VE-PTP, which might explain the stabilization of ADM on basal barrier function. However, ADM could not completely abolish the VEGF or lymphocyteinduced dissociation of the VE-PTP/VE-cadherin complex. Notably, the present study highlights at the first time that ADM stabilizes the VE-cadherin junctional complex via its action on the VE-PTP/VE-cadherin association.

6.2. Cellular signalling of ADM: the cAMP-dependent pathway

ADM is a member of the CGRP super family and exerts its biological actions through binding to a CRLR/RAMP-2 and -3 receptor complex. RAMPs are essential for translocation of CRLR from the endoplasmic reticulum to the cell surface and regulate receptor specificity, ligand affinity, and receptor desensitization (McLatchie et al., 1998). The CRLRs and RAMPs are reported to play a role in the development and integrity of vasculature (Dackor et al., 2006). Despite different tissue distribution of RAMPs isoforms, there are still no pharmacological differences between ADM-1 and -2 receptors to be observed so far. However, large tissue-specific analysis of the human and mouse transcriptomes shows that expression of RAMP2 is among the top 10 genes correlated with the expression pattern of CRLR, suggesting that most CRLR is coupled to RAMP-2 as a functional ADM receptor (Su et al. 2002; Gibbons et al., 2007). CRLR belongs to the super family of seven transmembrane GPCR and undergoes conformational changes resulting in coupling to cholera toxin-sensitive Gs protein, activating adenylate cyclase and thus increasing second messenger cAMP (Mittra et al., 2006; Shimekake et al., 1995).

6.2.1. The cAMP signaling in endothelial barrier function

The intracellular second messenger cAMP is involved in a multitude of biological functions, ranging from metabolism, gene expression, cell division and growth, cell differentiation and apoptosis, as well as secretion and

neurotransmission. A large number of studies extensively document that stimulation of cAMP signaling stabilizes endothelial barrier function (Stelzner et al., 1989). However, several studies show the divergent effect of cAMP in endothelial monolayers of coronary artery origin (e.g. rat, swine, and guine pig) (Hempel et al., 1996; Noll et al., 1996; Watanabe et al., 1992), as well as in microvessels from the coronary system (Huxley et al., 1997), in hamster cheek pouch (Gawlowski & Duran, 1986), and adipose tissue (Sollvei & Fredholm, 1981). In the study of Bindewald and colleagues, using adenosine analogs, beta receptor agonists and FSK the opposite response to cAMP in microvascular coronary endothelial cells (destabilization) and macrovascular aortic endothelial cells (stabilization) are observed and further analyzed (Bindewald et al., 2004). In both endothelial cells, contractile elements have identical response to cAMP, reducing phosphorylation status of MLC via activation of MLCP. However, in coronary endothelial cells, but not in aortic endothelial cells, an additional cAMP-mediated effect, delocalization of VE-cadherin and paxillin from cellular adhesion complexes, overrules cAMP-mediated relaxation effect on contractile elements and provokes a divergent effect on endothelial barrier function. This effect was most likely due to the loss of matrix adhesion rather than to the loss of intercellular barrier integrity and the *in vivo*-relevance is not established yet.

In the present study, the cAMP elevating agent FSK like ADM showed in lung microvessel endothelial cells and umbilical venous endothelial cells concordantly stabilizing effects on barrier function, as reflected by increased electrical resistance, decreased endothelial permeability, and inhibited extravasation of granulocytes. Similar effect on endothelial barrier function was also observed by using unspecific PDE inhibitor IBMX (data not shown). The effects of FSK could be synergistically increased by IBMX (data not shown), underlining the robustness of pulmonary microvascular and umbilical vein endothelial cells as *in vitro*-model for the barrier stabilizing effect of cAMP in endothelial cells of different origins.

6.2.2. Correlation of ADM effects with cAMP signaling

Driven by the fact that FSK, a direct activator of adenylate cyclase, although inducing much higher cAMP levels than ADM was less effective with respect to permeability it has been discussed that ADM may cause its effect also via cAMP-independent signaling (Hippenstiel et al., 2002). However, the precise correlation of increased cAMP levels with their effects on endothelial barrier functions was not established in the studies. For this purpose, the pharmacology of ADM and FSK was re-evaluated, and their effects were quantified by using the lowest effective doses and pEC50 values. Throughout all the tested models, ADM and FSK showed qualitatively identical effects: both of them activated cAMP signaling pathways demonstrated by the activation of PKA and Epac/Rap1. Furthermore, both ADM and FSK were capable of increasing electrical resistance, decreasing macromolecular permeability, and inhibiting transendothelial migration of leukocytes. On a molar basis equivalently active doses (either with respect to pEC50 or minimal effective dose), FSK and ADM differed from each other overall by the same factor (~1000) in different models. This finding points at cAMP as the common signaling pathway in regulating barrier function.

When changes of cAMP (ΔcAMP over baseline) induced by equally effective doses of ADM and FSK were compared it was demonstrated that FSK requires 3-5-fold higher cAMP concentration than ADM to achieve comparable effects on endothelial barrier function and activation of downstream events. The question was raised whether this quantitative difference of ADM and FSK is due to the different distribution of induced cAMP in endothelial cells. In a report by Rich and colleagues, a compartmentalized model of cAMP distribution is proposed that distinguishes between the microdomain and cytosol compartments (Rich et al., 2000). By using the cyclic nucleotide-gated (CNG) channels as cAMP sensors, which allow the real-time localized measurement of cAMP concentration in single cells, it was demonstrated that cAMP produced by transmembrane adenylate cyclase accumulates near membrane surface, and its further diffusion into cytosol is suggested to be hindered by the endoplasmic reticulum (ER) and plasma membrane invaginations such as caveolae (Rich et

al., 2000). The microdomain compartment of cAMP and its restricted diffusional access to the cytosol facilitate rapid and efficient activation of downstream events and also facilitate differential regulation of cellular targets (Rich et al., 2000). Cyclic AMP gradients with decreasing concentrations from the subplasma membrane space toward the cell center have protective effects with respect to endothelial barrier function (Sayner et al., 2011). In contrast, reverse cAMP gradients with increasing concentrations in cytosol alter cytoskeleton and cell shape, leading to cell rounding and thus disruption of endothelial barrier function (Hong et al., 2005; Dal Molin et al., 2006). Edema factor of Bacillus anthracis activates a calcium- and calmodulin-dependent soluble adenylate cyclase, catalyzing the production of cAMP at the peri-nuclear region, which ultimately leads to the formation of transendothelial cell tunnels, barrier break down and edema (Maddugoda et al., 2011). Both FSK and ADM activate transmembrane G-protein coupled adenylate cyclase and induce microdomain compartment of cAMP, protecting endothelial barrier function. However, location of ADM receptor (CRLR and RAMP2/3) might be in close proximity to the target proteins, allowing that induced compartmentalized cAMP more sufficiently activate downstream signaling. This could explain the rather low difference of factor 2 to 3 between the cAMP levels needed for establishing equivalent effects by ADM and FSK, respectively. Notably all effects of ADM could be mimicked by use of FSK and moreover much higher efficacy in most assay systems was obtained upon dose escalation of FSK. This was clearly correlated to the much higher cAMP levels that were induced after FSK dose escalation, while induction of cAMP was saturated on a rather low level after escalation of ADM concentrations. This might be due to the limited number of ADM receptors of the cell surface limiting the signaling input. On the other hand this finding strongly supports the concept that all barrier protective effects of ADM are related to signaling via cAMP.

6.3. Impacts of PKA and Epac/Rap1 on ADM signalling

In eukaryotic cells, cAMP mediates its biological function via two ubiquitously expressed intracellular cAMP receptors, the classic protein kinase A (PKA) as well as the recently discovered exchange protein directly activated by cAMP

(Epac). Data of the present study show that ADM like FSK activates both pathways: activation of PKA pathway demonstrated by phosphorylation status of vasodilator stimulated phosphoprotein (VASP) as well as activation of Epac/Rap1 detected by use of a Rap1-pulldown assay. In order to find out to what extent the individual pathways contribute to the anti-edematous and anti-inflammatory effects of ADM, the pathways were dissected by use of pathway specific cAMP mimetics, "007" for the Epac/Rap1 pathway and Benz-cAMP for the PKA pathway. In the present study, specificity of tool compounds for their corresponding pathways was demonstrated: Benz-cAMP specifically activated PKA pathway demonstrated by phosphorylation status of VASP in HUVECs and phosphorylation status of CREB in luciferase transfected CHO cells, while "007" specifically activated the Epac/Rap1 pathway detected by use of Rap1-pulldown assay but not vice versa.

The coexistence of two cAMP effectors, PKA and Epac, allows a more precise and integrated control of cAMP-mediated signaling in a spatial and temporal manner (reviewed by Cheng et al., 2008). Firstly, PKA and Epac pathways can play distinct roles in a variety of biological processes. Epac but not PKA can mediate the prostanoid-mediated anti-proliferative effects (Haag et al., 2008). Epac/Rap1 pathway is exclusively involved in cAMP-mediated regulation of monocyte adhesion and chemotaxis (Lorenowicz et al., 2006). PKA is exclusively involved in the PGE2-induced inhibition of collagen I expression, while inhibition of fibroblast proliferation is exclusively mediated by Epac1 (Huang et al., 2007). PKA activation but not Epac, has inhibitory effect on contractile activity of lung fibroblasts (Kamio et al., 2007). Secondly, Epac and PKA may play opposing physiological roles in different cell types (Mei et al., 2002). Thirdly and most frequently, PKA and Epac signaling are interconnected in many cellular processes (Bos, 2006). The cAMP-activated signal pathways are interconnected in the regulation of endothelial barrier function. However, the exact crosstalk between both signaling is still not well understood. Particularly, the impacts of PKA and Epac/Rap1 signaling in ADM signaling are unknown and therefore are intensely investigated in the present study.

6.3.1. Impacts of cAMP signaling on anti-edematous effects of ADM

In the present *in vitro*-study, both pathways were demonstrated to be equally involved in effects on regulating permeability, characterized by increased electrical resistance and reduced macromolecular permeability. Consistently, both pathway activators prevented vascular basal permeability and also hyper-permeability induced by histamine *in vivo*. This finding was consistent with the previous studies that both PKA and Epac/Rap1 pathways exhibited permeability stabilized function (Birukova et al., 2010; Aslam et al., 2010). In human pulmonary artery endothelial cells (HPAEC), agents like Prostaglandin E2 (PGE2), prostacyclin, and atrial natriuretic peptide (ANP), are shown to induce cAMP elevation and subsequently stabilize pulmonary endothelial barrier function through both PKA and Epac pathways (Birukova et al., 2007; Birukova et al., 2008). Rac GTPase is further identified as a convergence point of PKA and Epac/Rap1 induced endothelial barrier protection (Birukova et al., 2010). Both PKA and Epac can activate Rac-specific GEFs, Tiam1 and Vav2, and converge on Rac activation, resulting in enhancement of cortical actin and adherens junctions. Down-regulating Epac, Rap1, Tiam1 and Vav2 by using SiRNA technique, as well as inhibiting PKA activity by PKI, all decrease Rac1 activation and cAMP-mediated endothelial barrier enhancement (Birukova et al., 2010). However, in the present study, both pathway activators were shown to synergistically enhance endothelial barrier function *in vitro.* In the Miles assay although both compounds effectively prevented histamine-induced hyperpermeability even no further additive effect was achievable upon combination of the used doses which might be explained by having reached the maximum achievable effect with the doses used. However, the synergistic effect of PKA and Epac/Rap1 activators *in vitro* suggested that both pathways do not regulate barrier function by simply converging in a Rac-dependent mechanisms. Indeed, PKA was reported to reduce endothelial MLC kinase activity, leading to decreased MLC phosphorylation and relaxed cellular contractility in a Rac-independent manner (Birukova et al., 2004a; Yuan et al., 1997). Through phosphorylation on VASP, PKA could cause structural relaxation of the actin cytoskeleton linked to tight junctions via VASP-ZO-1 complex, thus stabilizing endothelial barrier function (Comerford et al., 2002). On the other hand,

Epac/Rap1 might directly enhance barrier function in a way of Rap1-dependent assembly of adherens junction and tight junction complexes in epithelial cell lines (Takai & Nakanishi, 2003; Birukova et al., 2010).

6.3.2. Impacts of cAMP signaling on effects of ADM regulating granulocyte extravasation

In the present study, ADM was demonstrated to inhibit granulocyte extravasation via its receptor activation and accumulation of intracellular cAMP. However, while the PKA activator Benz-cAMP inhibits leukocyte transmigration, which is comparable with the effect of ADM, "007" is shown to have no effect in this process. Even the combination of Benz-cAMP and "007" had no additional inhibitory effects on granulocyte extravasation, as compared to single treatment with Benz-cAMP. In a previous study, activation of Rap1 GTPase was reported to inhibit granulocyte transmigration by improving endothelial barrier function, whereas inhibiting Rap1 activity led to increased leukocyte transmigration (Wittchen et al., 2005). Notably, in the *in vitro*-leukocyte transendothelial migration assay used in the study by Wittchen et al., differentiated HL-60 cell lines instead of freshly isolated human PMNs were used for transmigration through the HUVECs monolayer, which might explain the different results. In line with this finding, a PKA inhibitor abolished the inhibitory effect of ADM on granulocyte transmigration, while the PKA inhibitor alone had no effects on granulocyte transmigration. These data are in support of a crucial role of PKA signaling in ADM-mediated regulation of leukocyte transmigration.

For the paracellular transendothelial migration of neutrophils, the sequential opening and re-annealing of endothelial cell-cell junctions are required. Neutrophils release granular contents containing digestive enzymes and produce cytotoxic agents (e.g. reactive oxygen species and cytokines), inducing junction dissociation triggered by phosphorylation, actin stress fiber formation, and actomyosin contraction, subsequently causing endothelial hyperpermeability (Yuan et al., 2012). This mechanical disruption of endothelial barrier function was initially believed necessary for this process. However, this conventional concept, the coupling between granulocyte transmigration and

endothelial hyperpermeability, has been recently challenged and discussed (reviewed by He, 2010; Yuan et al., 2012). The process of a neutrophil moving through two adjacent endothelial cells was demonstrated not to be accompanied with tracer protein leakage (Lewis and Granger, 1988). Both neutrophil and endothelial cell membranes were observed to remain in close contact during transmigration process using an immunofluorescence microscopic approach (Carman et al., 2007; Carman and Springer, 2004). Recently, granulocyte transmigration and endothelial hyperpermeability were shown to be temporally separated in aseptic cutaneous wounds: hyperpermeability preceded transmigration by several hours, and vascular permeability increased approximately threefold faster as compared to the rate of PMN influx (Kim et al., 2009). Indeed, in the present study, although PKA and Epac/Rap1 pathway differently influence granulocyte transmigration, both pathway activators were shown to attenuate PMN-induced endothelial hyperpermeability in the same manner (detected in ECIS model).

Adherence of neutrophils induces increase of intracellular calcium concentration and activation of MLC kinase in endothelial cells (Saito et al., 1998). Subsequently, the signaling activates endothelial contractile apparatus and causes paracellular gap formation, being a key determinant of leukocyte transendothelial migration in response to inflammation (Garcia et al., 1998). MLC kinase phosphorylates MLC on serine 19, which subsequently facilitates the interaction of myosin with actin, leading to the actomyosin based contractile response. In our study, the MLCK inhibitor (ML-9) and the intracellular calcium chelator (BAPTA/AM) were shown to sufficiently inhibit leukocyte transmigration. In addition to MLCK, Rho kinase on one hand phosphorylates MLC on serine 19, and on the other hand phosphorylates the myosin –binding subunit (MBS) and inactivates MLC phosphatase, being also crucial in regulating the phosphorylation status of MLC (Kawano et al., 1999; Amano et al., 1996). BAY77-7549, a potent and highly selective Rho kinase inhibitor (Kast et al., 2007) was shown to inhibit leukocyte transmigration. These data were consistent with the previous findings, suggesting that neutrophil-dependent activation of cellular contractility, indicated by phosphorylation status of endothelial MLC, could be a key determinant to regulate transendothelial

migration of leukocytes (Saito et al., 2001; Saito et al., 1998). In the present study, PKA activation was shown to reduce the phosphorylation status of MLC, whereas Epac/Rap1 activation was shown to have no effects on the same. However, the different data were reported by Birukova et al: phosphorylation of MLC was decreased by both PKA and Epac/Rap1 pathway activators (Birukova et al., 2010). It is of note that in their study human pulmonary artery endothelial cells instead of HUVECs were used to analyze the contractile apparatus. In another study using HUVECs, PKA activation but not Epac/Rap1 was also demonstrated to inhibit thrombin-induced phosphorylation of MLC and MLCP regulatory subunit MYPT1, partly via inhibition of the RhoA/ROCK pathway (Aslam et al., 2010). It is still unknown why PKA and Epac differently regulate contractile apparatus of endothelial cells from different origins. However, leukocyte adhesion and inflammatory hyperpermeability mainly occur in the postcapillary venules. Therefore, the endothelial contractility in HUVECs might be more predictive for the extravasation of PMN *in vivo*. In summary the data provide evidence that inhibition of leukocyte extravasation after cAMP signaling is linked to the contractile apparatus of the endothelial cell via PKA activation and subsequently reduced phosphorylation of the myosin light chain. Furthermore, these data underscore the concept that endothelial hyperpermeability and PMN transmigration are independently regulated processes and that hyperpermeability is not a prerequisite for transmigration because effective inhibition by activation of the Epac/Rap1 pathway is completely insufficient to inhibit PMN transmigration.

6.4. Role of cortactin in cellular signalling of ADM

Cortactin is one of the most important cytoskeletal components, and is identified as an F-actin binding protein and Src substrate. It is an 80 to 85 kDa actin-binding protein involved in cortical actin assembly and dynamic actin rearrangement (Ammer & Weed, 2008). Cortactin is ubiquitously expressed with the exception that in leukocytes the cortactin-related protein hematopoietic cell-specific Lyn substrate 1 (HS1) is expressed instead (Kitamura et al., 1989). The multidomain scaffold protein structure of cortactin facilitates multiple signals at locations of rapid actin rearrangement, such as sites of leukocyte adhesion and

transmigration. Cortactin stimulates actin polymerization by binding to the Arp2/3 complex in the cortical actin networks. The tyrosine residues 421, 466, and 482 within this proline-rich region of murine cortactin are identified as important targets of Src tyrosine kinases (Huang et al., 1998). Mutation of tyrosine residues with phenylalanine was previously shown to impair endothelial cell migration, which demonstrated the importance of tyrosine phosphorylation of cortactin in cytoskeletal regulation (Huang et al., 1998).

Initially, cortactin was observed as a regulator of dynamic cytoskeletal remodeling involved in cell mobility. Recently, the role of endothelial cortactin in leukocytes transmigration and barrier integrity has been recognized increasingly. Following leukocyte adhesion or upon antibody-induced clustering of E-selectin or ICAM-1, cortactin was previously identified to become tyrosine phosphorylated and associated with adhesion molecules in human endothelial cells (Durieu-Trautmann et al., 1994; Adamson et al., 1999; Tilghman & Hoover, 2002). This study suggested the role of cortactin in leukocyte transmigration by regulating adhesion molecule clustering on endothelial cells. Furthermore, silencing of cortactin by small interfering RNA (siRNA) was observed to inhibit leukocytes transmigration through HUVEC monolayer, accompanied by reduced accumulation of ICAM-1 at sites of neutrophil attachment (Yang et al., 2006 a, b; Schnoor et al., 2011). *In vivo*, neutrophil extravasation into the TNF-stimulated cremaster was inhibited in cortactin-deficient mice, which was caused by enhanced rolling velocity and reduced adhesion in postcapillary venules (Schnoor et al., 2011). More in-depth, cortactin supported neutrophil rolling via β2-integrin ligands instead of endothelial selectins, and cortactin facilicited firm adhesion via reduced ICAM-1 clustering around neutrophils (Schnoor et al., 2011).

In line with the previous reports, silencing of cortactin by SiRNA *in vitro* was shown to increase endothelial permeability and reduce leukocyte transmigration. The cortactin knockdown-induced hyperpermeability could be reversed by ADM, suggesting that the cortactin-independent pathway was partly involved in ADM signaling on regulating endothelial permeability. In contrast to endothelial permeability, down-regulation of cortactin expression decreased

transendothelial migration of human neutrophils and abolished the inhibitory effect of ADM. These data suggest for the first time a crucial role of cortactin in ADM signaling to regulate granulocyte extravasation. Again these findings are in line with the concept that ADM influences endothelial permeability by both actin-dependent and actin independent pathways while its effects on PMN transmigration are solely dependent on actin modulating effects.

6.5.   Therapeutical potential of ADM for inflammatory diseases

ADM is a multifunctional peptide which is able to act as an autocrine, paracrine, or endocrine mediator in many important and interrelated biological functions under normal and pathological conditions. Our present preliminary data evidences the beneficial effects of ADM during inflammatory processes, suggesting its pharmacological potency to treat human inflammatory diseases. Despite the wide expression of ADM throughout different organs and tissues, the receptor of ADM is demonstrated to be highly expressed in microvessels of lungs (Harel et al., 2008). Due to its specific receptor distribution ADM might be in particular of benefit for patients with acute lung inflammatory diseases (e.g. ALI or ARDS). ADM has been tested in several small clinical trials in humans for its potent hypotensive effects (Del Bene et al., 2000; Nagaya et al., 2000; Oya et al., 2000; Lainchbury et al., 1997; Lainchbury et al., 2000; Meeran et al., 1997). All these studies demonstrated the safety of the endogenous peptide ADM in humans, being at significant advantage as compared to the direct adenylate cyclase activator (forskolin) with strong anti-inflammatory effects *in vitro*. The colforsin daropate hydrochloride (water-soluble forskolin derivative) has been approved in Japan as positive inotropic and vasodilatory compound to treat ventricular dysfunction in patients undergoing coronary artery bypass grafting (Kikura et al., 2004). However, due to unspecific effects of cyclic AMP, a number of side effects were observed in clinical trials, including tachycardia/palpitations, premature ventricular constriction, headache, hot flushes, as well as abnormal laboratory results (elevated LDH level, proteinuria, thrombocytopenia). Based on these considerations, the development of ADM as an orphan medicinal product to treat life-threatening ALI is currently supported by the recent positive opinion of the Committee for Orphan Medicinal

Products of the European Medicines Agency (see the report from European Medicines Agency, EU/3/10/744).

.

7. REFERENCES

Aandahl EM, Aukrust P, Skålhegg BS, Müller F, Frøland SS, Hansson V, Taskén K. (**1998**) Protein kinase A type I antagonist restores immune responses of T cells from HIV-infected patients. FASEB J. 1998 Jul;12(10):855-62.

Adamson P, Etienne S, Couraud PO, Calder V, Greenwood J. (**1999**) Lymphocyte migration through brain endothelial cell monolayers involves signaling through endothelial ICAM-1 via a rho-dependent pathway. J Immunol. 1999 Mar 1;162(5):2964-73.

Adamson RH, Ly JC, Sarai RK, Lenz JF, Altangerel A, Drenckhahn D, Curry FE. (**2008**) Epac/Rap1 pathway regulates microvascular hyperpermeability induced by PAF in rat mesentery. Am J Physiol Heart Circ Physiol. 2008 Mar;294(3):H1188-96.

Agorreta J, Zulueta JJ, Montuenga LM, Garayoa M.(**2005**) Adrenomedullin expression in a rat model of acute lung injury induced by hypoxia and LPS. Am J Physiol Lung Cell Mol Physiol 2005; 288: L536-L545.

Allaker RP, Grosvenor PW, McAnerney DC, et al.(**2005**) Mechanisms of adrenomedullin antimicrobial action. Peptides 2005; 27: 661–666.

Amano M, Ito M, Kimura K, Fukata Y, Chihara K, Nakano T, Matsuura Y, Kaibuchi K. (**1996**) Phosphorylation and activation of myosin by Rho-associated kinase (Rho-kinase). J Biol Chem. 1996 Aug 23;271(34):20246-9.

Ammer AG & **Weed** SA. (**2008**) Cortactin branches out: roles in regulating protrusive actin dynamics. Cell Motil Cytoskeleton. 2008 Sep;65(9):687-707.

Angelini DJ, Hyun SW, Grigoryev DN, Garg P, Gong P, Singh IS, Passaniti A, Hasday JD, Goldblum SE. (**2006**). TNF-alpha increases tyrosine phosphorylation of vascular endothelial cadherin and opens the paracellular pathway through fyn activation in human lung endothelia. Am J Physiol Lung Cell Mol Physiol 291, L1232-45.

Arsalane, K., F. Broeckaert, B. Knoops, M. Wiedig, G. Toubeau, and A. Bernard. (**2000**). Clara cell specific protein (CC16) expression after acute lung inflammation induced by intratracheal lipopolysaccharide administration. American Journal of Respiratory and Critical Care Medicine 161: 1624–1630.

Asakawa H, Nishikimi T, Suzuki T, Hara S, Tsubokou Y, Yagi H, Yabe A, Tsuchiya N, Horinaka S, Kangawa K, Matsuoka H. (**2001**) Elevation of two molecular forms of adrenomedullin in plasma and urine in patients with acute myocardial infarction treated with early coronary angioplasty. Clin Sci (Lond). 2001 Jan;100(1):117-26.

Aslam M, Härtel FV, Arshad M, Gündüz D, Abdallah Y, Sauer H, Piper HM, Noll T. (**2010**) cAMP/PKA antagonizes thrombin-induced inactivation of endothelial myosin

light chain phosphatase: role of CPI-17. Cardiovasc Res. 2010 Jul 15;87(2):375-84. Epub 2010 Mar 3.

Baldwin AL & **Thurston** G. (**1995**) Changes in endothelial actin cytoskeleton in venules with time after histamine treatment. Am J Physiol. 1995 Nov;269(5 Pt 2):H1528-37.

Baldwin AL & **Thurston** G. (**2001**) Mechanics of endothelial cell architecture and vascular permeability. Crit Rev Biomed Eng. 2001;29(2):247-78. Review.

Barreiro O, Vicente-Manzanares M, Urzainqui A, Yáñez-Mó M, Sánchez-Madrid F. (**2004**) Inter-active protrusive structures during leukocyte adhesion and transendothelial migration. Front Biosci. 2004 May 1;9:1849-63.

Bazzoni G. (**2006**) Endothelial tight junctions: permeable barriers of the vessel wall. Thromb Haemost. 2006;95:36-42.

Bazzoni, G. & **Dejana**, E. (**2004**). Endothelial Cell-to-Cell Junctions: Molecular Organization and Role in Vascular Homeostasis, vol. 84, pp. 869-901.

Beltowski J, & **Jamroz** A. (**2004**) Adrenomedullin--what do we know 10 years since its discovery? Pol J Pharmacol 2004; 56: 5–27.

Bindewald K, Gündüz D, Härtel F, Peters SC, Rodewald C, Nau S, Schäfer M, Neumann J, Piper HM, Noll T. (**2004**) Opposite effect of cAMP signaling in endothelial barriers of different origin. Am J Physiol Cell Physiol. 2004 Nov;287(5):C1246-55.

Birukova AA, Liu F, Garcia JG, Verin AD. (**2004a**) Protein kinase A attenuates endothelial cell barrier dysfunction induced by microtubule disassembly. Am J Physiol Lung Cell Mol Physiol. 2004 Jul;287(1):L86-93. Epub 2004 Mar 5.

Birukova AA, Smurova K, Birukov KG, Kaibuchi K, Garcia JG, Verin AD. (**2004b**) Role of Rho GTPases in thrombin-induced lung vascular endothelial cells barrier dysfunction. Microvasc Res. 2004 Jan;67(1):64-77.

Birukova AA, Zagranichnaya T, Fu P, Alekseeva E, Chen W, Jacobson JR, Birukov KG. (**2007**)   Prostaglandins PGE(2) and PGI(2) promote endothelial barrier enhancement via PKA- and Epac1/Rap1-dependent Rac activation. Exp Cell Res. 2007 Jul 1;313(11):2504-20.

Birukova AA, Zagranichnaya T, Alekseeva E, Bokoch GM, Birukov KG. (**2008**) Epac/Rap and PKA are novel mechanisms of ANP-induced Rac-mediated pulmonary endothelial barrier protection. J Cell Physiol. 2008 Jun;215(3):715-24.

Birukova AA, Burdette D, Moldobaeva N, Xing J, Fu P, Birukov KG. (**2010**) Rac GTPase is a hub for protein kinase A and Epac signaling in endothelial barrier protection by cAMP. Microvasc Res. 2010 Mar;79(2):128-38.

Bos JL. (**2006**) Epac proteins: multi-purpose cAMP targets. Trends Biochem Sci. 2006 Dec;31(12):680-6.

Brain SD & **Grant** AD (**2004**) Vascular actions of calcitonin gene-related peptide and adrenomedullin. Physiol Rev 84:903–934

Brazil TJ, Rossi AG, Haslett C, McGorum B, Dixon PM, Chilvers ER. (**1998**) Priming induces functional coupling of N-formyl-methionyl-leucyl-phenylalanine receptors in equine neutrophils. J Leukoc Biol. 1998 Mar;63(3):380-8.

Brell B, Temmesfeld-Wollbruck B, Altzschner I, et al. (**2005**) Adrenomedullin reduces Staphylococcus aureus alpha-toxin-induced rat ileum microcirculatory damage. Crit Care Med 33: 819–826.115.

Broermann A, Winderlich M, Block H, Frye M, Rossaint J, Zarbock A, Cagna G, Linnepe R, Schulte D, Nottebaum AF, Vestweber D. (**2011**) Dissociation of VE-PTP from VE-cadherin is required for leukocyte extravasation and for VEGF-induced vascular permeability in vivo. J Exp Med. 2011 Nov 21;208(12):2393-401.

Butt, E., K. Abel, M. Krieger, D. Palm, V. Hoppe, J. Hoppe, and U. Walter. (**1994**) cAMP- and cGMPdependent protein kinase phosphorylation sites of the focal adhesion vasodilator-stimulated phosphoprotein (VASP) in vitro and in intact human platelets. J Biol Chem 269, 14509-17.

Carman CV, Sage PT, Sciuto TE, de la Fuente MA, Geha RS, Ochs HD, Dvorak HF, Dvorak AM, Springer TA. (**2007**) Transcellular diapedesis is initiated by invasive podosomes. Immunity. 2007 Jun;26(6):784-97.

Carman CV, **Springer** TA. (**2004**). A transmigratory cup in leukocyte diapedesis both through individual vascular endothelial cells and between them. J Cell Biol 167, 377-88.

Caron KM & **Smithies** O. (**2001**) Extreme hydrops fetalis and cardiovascular abnormali-ties in mice lacking a functional adrenomedullin gene. Proc Natl Acad Sci USA 98: 615–619.

Chakravarty P, Suthar TP, Coppock HA, Nicholl CG, Bloom SR, Legon S, Smith DM. (**2000**) CGRP and adrenomedullin binding correlates with transcript levels for calcitonin receptor-like receptor (CRLR) and receptor activity modifying proteins (RAMPs) in rat tissues. Br J Pharmacol. 2000 May;130(1):189-95.

Cheng X, Ji Z, Tsalkova T, Mei F. (**2008**) Epac and PKA: a tale of two intracellular cAMP receptors. Acta Biochim Biophys Sin (Shanghai). 2008 Jul;40(7):651-62.

Cheung BM, Hwang IS, Li CY, O WS, Tsang KW, Leung RY, Kumana CR, Tang F. (**2004**) Increased Adrenomedullin expression in lungs in endotoxaemia. J Endocrinol 2004; 181: 339–345.

Chiba T, Yamaguchi A, Yamatani T, Nakamura A, Morishita T, Inui T, Fukase M, Noda T, Fujita T. (**1989**) Calcitonin gene-related peptide receptor antagonist human CGRP-(8-37). Am J Physiol. 1989 Feb;256(2 Pt 1):E331-5.

Comerford KM, Lawrence DW, Synnestvedt K, Levi BP, Colgan SP. (**2002**) Role of vasodilator-stimulated phosphoprotein in PKA-induced changes in endothelial junctional permeability. FASEB J. 2002 Apr;16(6):583-5.

Crone C & **Olesen** SP. (**1982**) Electrical resistance of brain microvascular endothelium. Brain Res. 1982;241:49–55.

Cui X,Wu R,Zhou M, et al. (**2005**) Adrenomedullinand its binding protein attenuatethe pro inflammatory response after hemorrhage. Crit Care Med 2005; 33: 391–398.

Cullere X, Shaw SK, Andersson L, Hirahashi J, Luscinskas FW, Mayadas TN. (**2005**) Regulation of vascular endothelial barrier function by Epac, a cAMP-activated exchange factor for Rap GTPase. Blood. 2005 Mar 1;105(5):1950-5. Epub 2004 Sep 16.

Czyzyk TA, Ning Y, Hsu MS, et al. (**2005**) Deletion of peptide amidation enzymatic activity leads to edema and embryonic lethality in the mouse. Dev Biol 287: 301–313.

Dackor R & **Caron** K. Mice heterozygous for adrenomedullin exhibit a more extreme inflammatory response to endotoxin-induced septic shock. Peptides. 2007 Nov;28(11):2164-70.

Dackor RT, Fritz-Six K, Dunworth WP, et al. (**2006**) Hydrops fetalis, cardiovascular defects, and embryonic lethality in mice lacking the calcitonin receptor-like receptor gene. Mol Cell Biol 26: 2511–2518

Dal Molin F, Tonello F, Ladant D, Zornetta I, Zamparo I, Di Benedetto G, Zaccolo M, Montecucco C. (**2006**) Cell entry and cAMP imaging of anthrax edema toxin. EMBO J. 2006 Nov 15;25(22):5405-13.

de Rooij J, Zwartkruis FJ, Verheijen MH, Cool RH, Nijman SM, Wittinghofer A, Bos JL. (**1998**) Epac is a Rap1 guanine-nucleotide-exchange factor directly activated by cyclic AMP. Nature. 1998 Dec 3; 396 (6710):474-7.

Dejana E. (**2004**) Endothelial cell-cell junctions: happy together. Nature Reviews Molecular Cell Biology. 2004;5:261–270.

Del Bene R, Lazzeri C, Barletta G, Vecchiarino S, Guerra CT, Franchi F, La Villa G (**2000**) Effects of low-dose adrenomedullin on cardiac function and systemic haemodynamics in man. Clin Physiol 20:457–465

Dennis T, Fournier A, Cadieux A, Pomerleau F, Jolicoeur FB, St Pierre S, Quirion R. (**1990**) hCGRP8-37, a calcitonin gene-related peptide antagonist revealing calcitonin

gene-related peptide receptor heterogeneity in brain and periphery. J Pharmacol Exp Ther. 1990 Jul;254(1):123-8.

Derian CK, Santulli RJ, Rao PE, Solomon HF, Barrett JA. (**1995**) Inhibition of chemotactic peptide-induced neutrophil adhesion to vascular endothelium by cAMP modulators. J Immunol. 1995 Jan 1;154(1):308-17.

Dong JM, Leung T, Manser E, Lim L. (**1998**) cAMP-induced morphological changes are counteracted by the activated RhoA small GTPase and the Rho kinase ROKalpha. J Biol Chem. 1998 Aug 28;273(35):22554-62.

Downey, G.P., Fialkow, L. and Fukushima, T., (**1995**). Initial interaction of leukocytes within the microvasculature: deformability, adhesion, and transmigration. New Horizons 3, pp. 219–228.

Dschietzig T, Azad HA, Asswad L, Böhme C, Bartsch C, Baumann G, Stangl K. (**2002**) The adrenomedullin receptor acts as clearance receptor in pulmonary circulation. Biochem Biophys Res Commun. 2002 Jun 7;294(2):315-8.

Dudek SM & **Garcia** JG. (**2001**) Cytoskeletal regulation of pulmonary vascular permeability. J Appl Physiol. 2001 Oct;91(4):1487-500. Review.

Dunworth WP, Fritz-Six KL, Caron KM. (**2008**) Adrenomedullin stabilizes the lymphatic endothelial barrier in vitro and in vivo. Peptides 2008 Dec; 29(12):2243-9.

Dupuis J, Caron A, Ruël N. (**2005**) Biodistribution, plasma kinetics and quantification of single-pass pulmonary clearance of adrenomedullin. Clin Sci (Lond). 2005 Jul;109(1):97-102.

Durieu-Trautmann O, Chaverot N, Cazaubon S, Strosberg AD, Couraud PO. (**1994**) Intercellular adhesion molecule 1 activation induces tyrosine phosphorylation of the cytoskeleton-associated protein cortactin in brain microvessel endothelial cells. J Biol Chem. 1994 Apr 29;269(17):12536-40.

Ebnet K, **Vestweber** D. (**1999**). Molecular mechanisms that control leukocyte extravasation: the selectins and the chemokines. Histochem Cell Biol 112, 1-23.

Eguchi S, Hirata Y, Iwasaki H, et al. (**1994**) Structure-activity relationship of adrenomedullin, a novel vasodilatory peptide, in cultured rat vascular smooth muscle cells. Endocrinology 135: 2454–2458

Elsasser TH, Kahl S, Martinez A, Montuenga LM, Pio R, Cuttitta F (**1999)** Adrenomedullin binding protein in the plasma of multiple species: characterization by radioligand blotting. Endocrinology 140:4908–4911

Ertmer C, Morelli A, Rehberg S, Lange M, Hucklenbruch C, Van Aken H, Booke M, Westphal M. (**2007**) Exogenous adrenomedullin prevents and reverses hypodynamic

circulation and pulmonary hypertension in ovine endotoxaemia. Br J Anaesth. 2007 Dec;99(6):830-6.

Essler M, Staddon JM, Weber PC, Aepfelbacher M. (**2000**) Cyclic AMP blocks bacterial lipopolysaccharide-induced myosin light chain phosphorylation in endothelial cells through inhibition of Rho/Rho kinase signaling. J Immunol. 2000 Jun 15; 164(12):6543-9.

Farmer PJ, Bernier SG, Lepage A, Guillemette G, Regoli D, Sirois P. (**2001**) Permeability of endothelial monolayers to albumin is increased by bradykinin and inhibited by prostaglandins. Am J Physiol Lung Cell Mol Physiol. 2001 Apr;280(4):L732-8.

Franck T, Kohnen S, de la Rebière G, Deby-Dupont G, Deby C, Niesten A, Serteyn D. (**2009**) Activation of equine neutrophils by phorbol myristate acetate or N-formyl-methionyl-leucyl-phenylalanine induces a different response in reactive oxygen species production and release of active myeloperoxidase. Vet Immunol Immunopathol. 2009 Aug 15;130(3-4):243-50.

Friedman GB, Taylor CT, Parkos CA, Colgan SP. (**1998**) Epithelial permeability induced by neutrophil transmigration is potentiated by hypoxia: role of intracellular cAMP. J Cell Physiol. 1998 Jul;176(1):76-84.

Frohman EM, Racke MK, Raine CS. (**2006**) Multiple sclerosis--the plaque and its pathogenesis. N Engl J Med. 2006 Mar 2;354(9):942-55.

Fukuhara S, Sakurai A, Sano H, Yamagishi A, Somekawa S, Takakura N, Saito Y, Kangawa K, Mochizuki N. (**2005**) Cyclic AMP potentiates vascular endothelial cadherin-mediated cell-cell contact to enhance endothelial barrier function through an Epac-Rap1 signaling pathway. Mol Cell Biol. 2005 Jan;25(1):136-46.

Garayoa M, Bodegas E, Cuttitta F, Montuenga LM (**2002**) Adrenomedullin in mammalian embryogenesis. Microsc Res Tech 57:40–54

Garcia JG, Davis HW, Patterson CE. (**1995**). Regulation of endothelial cell gap formation and barrier dysfunction: role of myosin light chain phosphorylation. J Cell Physiol 163, 510-22.

Garcia JG, Verin AD, Herenyiova M, English D. (**1998**) Adherent neutrophils activate endothelial myosin light chain kinase: role in transendothelial migration. J Appl Physiol. 1998 May;84(5):1817-21.

Gavard, J. & **Gutkind**, J. S. (**2006**). VEGF controls endothelial-cell permeability by promoting the beta-arrestin-dependent endocytosis of VE-cadherin. Nat Cell Biol 8, 1223-34.

Gawlowski DM & **Duran** WN. (**1986**) Dose-related effects of adenosin and bradykinin on microvascular permselectivity to macromolecules in hamster cheek pouch. Circ Res 58: 348–355, 1986.

Gibbons C, Dackor R, Dunworth W, Fritz-Six K, Caron KM. (**2007**) Receptor activity-modifying proteins: RAMPing up adrenomedullin signaling. Mol Endocrinol. 2007 Apr;21(4):783-96.

Goeckeler ZM & **Wysolmerski** RB. (**1995**) Myosin light chain kinase-regulated endothelial cell contraction: the relationship between isometric tension, actin polymerization, and myosin phosphorylation. J Cell Biol. 1995 Aug;130(3):613-27.

Goeckeler ZM, Masaracchia RA, Zeng Q, Chew TL, Gallagher P, Wysolmerski RB. (**2000**) Phosphorylation of myosin light chain kinase by p21-activated kinase PAK2. J Biol Chem. 2000 Jun 16;275 (24):18366-74.

Gonzalez-Rey E,Chorny A, Varela N,etal. (**2006**) Urocortin and adrenomedullin prevent lethal endotoxemia by down-regulatingthe inflammatory response. Am J Pathol 2006; 168: 1921–1930.

Gorovoy M, Niu J, Bernard O, Profirovic J, Minshall R, Neamu R, Voyno-Yasenetskaya T. (**2005**) LIM kinase 1 coordinates microtubule stability and actin polymerization in human endothelial cells. J Biol Chem. 2005 Jul 15;280(28):26533-42.

Grant AD, Tam CW, Lazar Z, Shih MK, Brain SD. (**2004**) The calcitonin gene-related peptide (CGRP) receptor antagonist BIBN4096BS blocks CGRP and adrenomedullin vasoactive responses in the microvasculature. Br JPharmacol 2004; 142: 1091–1098.

Haag S, Warnken M, Juergens UR, Racké K. (**2008**) Role of Epac1 in mediating anti-proliferative effects of prostanoid EP(2) receptors and cAMP in human lung fibroblasts. Naunyn Schmiedebergs Arch Pharmacol. 2008 Dec;378(6):617-30.

Hagi-Pavli E, Farthing PM, Henshaw FN, Kapas S. (**2005**) Presentation of ICAM-1 protein at the cell surface of oral keratinocytes in the presence of adrenomedullin and corticotrophin. Cell Physiol Biochem**.** 2005; 15(1-4):167-74.

Hagi-Pavli E, Farthing PM, Kapas S. (**2004**) Stimulation of adhesion molecule expression in human endothelial cells (HUVEC) by adrenomedullin and corticotrophin. Am J Physiol Cell Physiol. 2004 Feb; 286(2): C239-46.

Hagner S, Stahl U, Knoblauch B, McGregor GP, Lang RE. (**2002**) Calcitonin receptor-like receptor: identification and distribution in human peripheral tissues. Cell Tissue Res. 2002 Oct;310(1):41-50.

Hamid SA. & **Baxter** GF. (**2005**) Adrenomedullin: regulator of systemic and cardiac homeostasis in acute myocardial infarction. Pharmacol Ther. 2005 Feb;105(2):95-112.

Hansson GK, Libby P. (**2006**) The immune response in atherosclerosis: a double-edged sword. Nat Rev Immunol. 2006 Jul;6(7):508-19.

Harel F, Fu Y, Nguyen QT, Letourneau M, Perrault LP, Caron A, Fournier A, Dupuis J. (**2008**) Use of adrenomedullin derivatives for molecular imaging of pulmonary circulation. J Nucl Med. 2008 Nov;49(11):1869-74.

Hawkins BT & **Davis** TP. (**2005**) The blood-brain barrier/neurovascular unit in health and disease. Pharmacol Rev. 2005; 57: 173–185.

He P. (**2010**) Leucocyte/endothelium interactions and microvessel permeability: coupled or uncoupled? Cardiovasc Res. 2010 Jul 15;87(2):281-90. Review.

Hempel A, Noll T, Muhs A, and Piper HM. (**1996**) Functional antagonism between cAMP and cGMP on permeability of coronary endothelial monolayers. Am J Physiol Heart Circ Physiol 270: H1264–H1271, 1996.

Hinson JP, Kapas S, Smith DM (**2000**) Adrenomedullin, a multifunctional regulatory peptide. Endocr Rev 21:138–167

Hippenstiel S, Witzenrath M, Schmeck B, et al. (**2002**) Adrenomedullin reduces endothelial hyperpermeability. Circ Res 91: 618–625.

Hixenbaugh EA, Goeckeler ZM, Papaiya NN, Wysolmerski RB, Silverstein SC, Huang AJ. (**1997**) Stimulated neutrophils induce myosin light chain phosphorylation and isometric tension in endothelial cells. Am J Physiol. 1997 Aug;273(2 Pt 2):H981-8.

Hocke AC, Temmesfeld-Wollbrueck B, SchmeckB, et al. (**2006**) Perturbation of endothelial junction proteins by Staphylococcus aureus alpha-toxin: inhibition of endothelial gap formation by adrenomedullin. Histochem Cell Biol 126: 305–316

Holz GG, Kang G, Harbeck M, Roe MW, Chepurny OG. (**2006**) Cell physiology of cAMP sensor Epac. J Physiol. 2006 Nov 15;577(Pt 1):5-15.

Honda M, Nakagawa S, Hayashi K, Kitagawa N, Tsutsumi K, Nagata I, Niwa M. (**2006**) Adrenomedullin improves the blood-brain barrier function through the expression of claudin-5. Cell Mol Neurobiol 2006; 26: 109–118.

Hong J, Beeler J, Zhukovskaya NL, He W, Tang WJ, Rosner MR. (**2005**) Anthrax edema factor potency depends on mode of cell entry. Biochem Biophys Res Commun. 2005 Sep 30;335(3):850-7.

Huang C, Liu J, Haudenschild CC, Zhan X. (**1998**) The role of tyrosine phosphorylation of cortactin in the locomotion of endothelial cells. J Biol Chem. 1998 Oct 2;273(40):25770-6.

Huang S, Wettlaufer SH, Hogaboam C, Aronoff DM, Peters-Golden M. (**2007**) Prostaglandin E(2) inhibits collagen expression and proliferation in patient-derived

normal lung fibroblasts via E prostanoid 2 receptor and cAMP signaling. Am J Physiol Lung Cell Mol Physiol. 2007 Feb;292(2):L405-13.

Huxley VH & **Williams** DA. (**2000**) Role of a glycocalyx on coronary arteriole permeability to proteins: evidence from enzyme treatments. Am J Physiol Heart Circ Physiol 278: H1177–H1185, 2000.

Huxley VH, Williams DA, Meyer DJ Jr, Laughlin MH. (**1997**) Altered basal and adenosine-mediated protein flux from coronary arterioles isolated from exercise-trained pigs. Acta Physiol Scand. 1997 Aug;160(4):315-25.

Ishimitsu T, Ono H, Minami J, Matsuoka H. (**2006**) Pathophysiologic and therapeutic implications of adrenomedullin in cardiovascular disorders. Pharmacol Ther. 2006 Sep;111(3):909-27.

Itoh T, Obata H, Murakami S, Hamada K, Kangawa K, Kimura H, Nagaya N. (**2007**) Adrenomedullin ameliorates lipopolysaccharide-induced acute lung injury in rats. Am J Physiol Lung Cell Mol Physiol. 2007 Aug;293(2):L446-52.

Jin D, Otani K, Yamahara K, Ikeda T, Nagaya N, Kangawa K. (**2011**) Adrenomedullin reduces expression of adhesion molecules on lymphatic endothelial cells. Regul Pept. 2011 Jan 17;166(1-3):21-7.

Kamio K, Liu X, Sugiura H, Togo S, Kobayashi T, Kawasaki S, Wang X, Mao L, Ahn Y, Hogaboam C, Toews ML, Rennard SI. (**2007**) Prostacyclin analogs inhibit fibroblast contraction of collagen gels through the cAMP-PKA pathway. Am J Respir Cell Mol Biol. 2007 Jul;37(1):113-20.

Kang, J.L., H.W. Lee, H.S. Lee, I.S. Pack, Y. Chong, and V. Castranova. (**2001**). Genistein prevents nuclear factor-kappa B activation and acute lung injury induced by lipopolysaccharide. American Journal of Respiratory and Critical Care Medicine 164: 2206–2212.

Kast R, Schirok H, Figueroa-Pérez S, Mittendorf J, Gnoth MJ, Apeler H, Lenz J, Franz JK, Knorr A, Hütter J, Lobell M, Zimmermann K, Münter K, Augstein KH, Ehmke H, Stasch JP. (**2007**) Cardiovascular effects of a novel potent and highly selective azaindole-based inhibitor of Rho-kinase. Br J Pharmacol. 2007 Dec;152(7):1070-80.

Kawano Y, Fukata Y, Oshiro N, Amano M, Nakamura T, Ito M, Matsumura F, Inagaki M, Kaibuchi K. (**1999**) Phosphorylation of myosin-binding subunit (MBS) of myosin phosphatase by Rho-kinase in vivo. J Cell Biol. 1999 Nov 29;147(5):1023-38.

Kikura M, Morita K, Sato S. (**2004**) Pharmacokinetics and a simulation model of colforsin daropate, new forskolin derivative inotropic vasodilator, in patients undergoing coronary artery bypass grafting. Pharmacol Res. 2004 Mar;49(3):275-81.

Kim W, Moon SO, Lee S, Sung MJ, Kim SH, Park SK. (**2003**) Adrenomedullin reduces VEGF-induced endothelial adhesion molecules and adhesiveness through a

phosphatidylinositol 3'-kinase pathway. Arterioscler Thromb Vasc Biol**.** 2003 Aug 1;23(8):1377-83.

Kim MH, Curry FR, Simon SI. (**2009**) Dynamics of neutrophil extravasation and vascular permeability are uncoupled during aseptic cutaneous wounding. Am J Physiol Cell Physiol. 2009 Apr;296(4):C848-56.

Kis B, Deli MA, Kobayashi H, Abrahám CS, Yanagita T, Kaiya H, Isse T, Nishi R, Gotoh S, Kangawa K, Wada A, Greenwood J, Niwa M, Yamashita H, Ueta Y. (**2001**) Adrenomedullin regulates blood-brain bar-rier functions in vitro. Neuroreport 12: 4139–4142.

Kis B, Snipes JA, Deli MA, Abrahám CS, Yamashita H, Ueta Y, Busija DW. (**2003**) Chronic Adrenomedullin treatment improves blood-brain barrier function but has no effects on expression of tight junction proteins. Acta Neurochir Suppl 2003; 86: 565–568.

Kitamura D, Kaneko H, Miyagoe Y, Ariyasu T, Watanabe T. (**1989**) Isolation and characterization of a novel human gene expressed specifically in the cells of hematopoietic lineage. Nucleic Acids Res. 1989 Nov 25;17(22):9367-79.

Kitamura K, Ichiki Y, Tanaka M, Kawamoto M, Emura J, Sakakibara S, Kangawa K, Matsuo H, Eto T. (**1994**) Immunoreactive adrenomedullin in human plasma. FEBS Lett. 1994 Mar 21;341(2-3):288-90.

Kitamura K, Kangawa K, Eto T. (**2002**) Adrenomedullin and PAMP: discovery, structures, and cardiovascular functions. Microsc Res Tech 2002; 57: 3–13.

Kitamura K, Kangawa K, Kawamoto M, Ichiki Y, Nakamura S, Matsuo H, Eto T (**1993**) Adrenomedullin: a novel hypotensive peptide isolated from human pheochromocytoma. Biochem Biophys Res Commun 192:553–560

Kitamura K, Kato J, Kawamoto M, Tanaka M, Chino N, Kangawa K, Eto T. (**1998**) The intermediate form of glycine-extended adrenomedullin is the major circulating molecular form in human plasma. Biochem Biophys Res Commun. 1998 Mar 17;244(2):551-5.

Komarova Y & **Malik** AB. (**2010**) Regulation of endothelial permeability via paracellular and transcellular transport pathways. Annu Rev Physiol. 2010 Mar 17;72:463-93.

Konstantoulaki M, Kouklis P, Malik AB. (**2003**) Protein kinase C modifications of VE-cadherin, p120, and beta-catenin contribute to endothelial barrier dysregulation induced by thrombin. Am J Physiol Lung Cell Mol Physiol. 2003 Aug;285(2):L434-42.

Kooistra MR, Corada M, Dejana E, Bos JL. (**2005**) Epac1 regulates integrity of endothelial cell junctions through VE-cadherin. FEBS Lett. 2005 Sep 12;579(22):4966-72.

Korthuis RJ, Carden DL, Kvietys PR, Shepro D, Fuseler J. (**1991**) Phalloidin attenuates postischemic neutrophil infiltration and increased microvascular permeability. J Appl Physiol. 1991 Oct;71(4):1261-9.

Kumar P, Shen Q, Pivetti CD, Lee ES, Wu MH, Yuan SY. (**2009**) Molecular mechanisms of endothelial hyperpermeability: implications in inflammation. Expert Rev Mol Med. 2009 Jun 30;11:e19.

Lainchbury JG, Cooper GJ, Coy DH, Jiang NY, Lewis LK, Yandle TG, Richards AM, Nicholls MG (**1997**) Adrenomedullin: a hypotensive hormone in man. Clin Sci (Lond) 92:467–472

Lainchbury JG, Troughton RW, Lewis LK, Yandle TG, Richards AM, Nicholls MG. (**2000**) Hemodynamic, hormonal, and renal effects of short-term adrenomedullin infusion in healthy volunteers. J Clin Endocrinol Metab. 2000 Mar;85(3):1016-20.

Lampugnani MG, Corada M, Caveda L, Breviario F, Ayalon O, Geiger B, Dejana E. (**1995**). The molecular organization of endothelial cell to cell junctions: differential association of plakoglobin, beta-catenin, and alpha-catenin with vascular endothelial cadherin (VE-cadherin). J Cell Biol 129, 203-17.

Lampugnani MG, Corada M, Andriopoulou P, Esser S, Risau W, Dejana E. (**1997**). Cell confluence regulates tyrosine phosphorylation of adherens junction components in endothelial cells. J Cell Sci 110 (Pt 17), 2065-77.

Lang P, Gesbert F, Delespine-Carmagnat M, Stancou R, Pouchelet M, Bertoglio J. (**1996**) Protein kinase A phosphorylation of RhoA mediates the morphological and functional effects of cyclic AMP in cytotoxic lymphocytes. EMBO J. 1996 Feb 1;15(3):510-9.

Laudanna C, Campbell JJ, Butcher EC. (**1997**) Elevation of intracellular cAMP inhibits RhoA activation and integrin-dependent leukocyte adhesion induced by chemoattractants. J Biol Chem. 1997 Sep 26;272(39):24141-4.

Lewis RE & **Granger** HJ. (**1988**) Diapedesis and the permeability of venous microvessels to protein macromolecules: the impact of leukotriene B4 (LTB4). Microvasc Res. 1988 Jan;35(1):27-47.

Ley K, Laudanna C, Cybulsky MI, Nourshargh S. (**2007**) Getting to the site of inflammation: the leukocyte adhesion cascade updated. Nat.Rev.Immunol. 7,678–689

Lisy O, Jougasaki M, Schirger JA, Chen HH, Barclay PT, Burnett Jr JC. (**1998**) Neutral endopeptidase inhibition potentiates the natriuretic actions of adrenomedullin. Am J Physiol 275:F410–F414

Liu F, Verin AD, Borbiev T, Garcia JG. (**2001**) Role of cAMP-dependent protein kinase A activity in endothelial cell cytoskeleton rearrangement. Am J Physiol Lung Cell Mol Physiol. 2001 Jun;280(6):L1309-17.

Lopez J & **Martinez** A. (**2002**) Cell and molecular biology of the multifunctional peptide, adrenomedullin. Int Rev Cytol 221:1–92

Lorenowicz MJ, van Gils J, de Boer M, Hordijk PL, Fernandez-Borja M. (**2006**) Epac1-Rap1 signaling regulates monocyte adhesion and chemotaxis. J Leukoc Biol. 2006 Dec;80(6):1542-52.

Maddugoda MP, Stefani C, Gonzalez-Rodriguez D, Saarikangas J, Torrino S, Janel S, Munro P, Doye A, Prodon F, Aurrand-Lions M, Goossens PL, Lafont F, Bassereau P, Lappalainen P, Brochard F, Lemichez E. (**2011**) cAMP signaling by anthrax edema toxin induces transendothelial cell tunnels, which are resealed by MIM via Arp2/3-driven actin polymerization. Cell Host Microbe. 2011 Nov 17;10(5):464-74.

Matthay MA & **Zemans** RL. (**2011**) The acute respiratory distress syndrome: pathogenesis and treatment. Annu Rev Pathol. 2011;6:147-63.

McLatchie LM, Fraser NJ, Main MJ, Wise A, Brown J, Thompson N, Solari R, Lee MG, Foord SM (**1998**) RAMPs regulate the transport and ligand specificity of the calcitonin-receptor-like receptor. Nature 393:333–339

Meeran K, O'Shea D, Upton PD, Small CJ, Ghatei MA, Byfield PH, Bloom SR. (**1997**) Circulating adrenomedullin does not regulate systemic blood pressure but increases plasma prolactin after intravenous infusion in humans: a pharmacokinetic study. J Clin Endocrinol Metab. 1997 Jan;82(1):95-100.

Mehta D & **Malik** AB. (**2006**) Signaling mechanisms regulating endothelial permeability. Physiol Rev. 2006; 86: 279–367.

Mei FC, Cheng X. (**2005**) Interplay between exchange protein directly activated by cAMP (Epac) and microtubule cytoskeleton. Mol Biosyst. 2005 Oct;1(4):325-31.

Mei FC, Qiao J, Tsygankova OM, Meinkoth JL, Quilliam LA, Cheng X. (**2002**) Differential signaling of cyclic AMP: opposing effects of exchange protein directly activated by cyclic AMP and cAMP-dependent protein kinase on protein kinase B activation. J Biol Chem. 2002 Mar 29;277(13):11497-504.

Mittra S, Bourreau JP. (**2006**) Gs and Gi coupling of adrenomedullin in adult rat ventricular myocytes. Am J Physiol Heart Circ Physiol. 2006 May;290(5):H1842-7.

Moll T, Dejana E, Vestweber D. (**1998**) In vitro degradation of endothelial catenins by a neutrophil protease. J Cell Biol. 1998 Jan 26;140(2):403-7.

Moy AB, Van Engelenhoven J, Bodmer J, Kamath J, Keese C, Giaever I, Shasby S, Shasby DM. (**1996**) Histamine and thrombin modulate endothelial focal adhesion through centripetal and centrifugal forces. J Clin Invest. 1996 Feb 15;97(4):1020-7.

Muff R, Born W, Fischer JA (**1995)** Calcitonin, calcitonin gene-related peptide, adrenomedullin and amylin: homologous peptides, separate receptors and overlapping biological actions. Eur J Endocrinol 133:17–20

Müller HC, Witzenrath M, Tschernig T, Gutbier B, Hippenstiel S, Santel A, Suttorp N, Rosseau S. (**2010**) Adrenomedullin attenuates ventilator-induced lung injury in mice. Thorax. 2010 Dec;65(12):1077-84.

Nagaya N, Satoh T, Nishikimi T, Uematsu M, Furuichi S, Sakamaki F, Oya H, Kyotani S, Nakanishi N, Goto Y, Masuda Y, Miyatake K, Kangawa K (**2000**) Hemodynamic, renal, and hormonal effects of adrenomedullin infusion in patients with congestive heart failure.Circulation 101:498–503

Nishikimi T. (**2007**) Adrenomedullin in the kidney-renal physiological and pathophysiological roles. Curr Med Chem. 2007;14(15):1689-99.

Noda M, Yasuda-Fukazawa C, Moriishi K, Kato T, Okuda T, Kurokawa K, Takuwa Y. (**1995**) Involvement of rho in GTP gamma S-induced enhancement of phosphorylation of 20 kDa myosin light chain in vascular smooth muscle cells: inhibition of phosphatase activity. FEBS Lett. 1995 Jul 3;367(3):246-50.

Noll T, Hempel A, and Piper HM. (**1996**) Neuropeptide Y reduces macromolecule permeability of coronary endothelial monolayers. Am J Physiol Heart Circ Physiol 271: H1878–H1883, 1996.

Nottebaum AF, Cagna G, Winderlich M, Gamp AC, Linnepe R, Polaschegg C, Filip-pova K, Lyck R, Engelhardt B, Kamenyeva O, Bixel MG, Butz S, Vestweber D. (**2008**) VE-PTP maintains the endothelial barrier via plakoglobin and becomes dissociated from VE-cadherin by leukocytes and by VEGF. J Exp Med. 205(12):2929-45.

Ohbayashi H, Suito H, Yoshida N, et al. (**1999**) Adrenomedullin inhibits ovalbuminin-duced bronchoconstriction and airway microvascular leakage in guinea-pigs. Eur Respir J 14: 1076–1081.

Oya H, Nagaya N, Furuichi S, Nishikimi T, Ueno K, Nakanishi N, Yamagishi M, Kan-gawa K, Miyatake K (**2000**) Comparison of intravenous adrenomedullin with atrial natriuretic peptide in patients with congestive heart failure. Am J Cardiol 86:94–98

Panés J & **Granger** DN. (**1998**) Leukocyte-endothelial cell interactions: molecular mechanisms and implications in gastrointestinal disease. Gastroenterology 114, 1066-90.

Partrick D.A., Moore F.A., Moore E.E., Barnett Jr. C.C., Silliman C.C. (**1996**) Neutrophil priming and activation in the pathogenesis of postinjury multiple organ failure New Horiz., 4 1996, pp. 194–210

Paczkowski NJ, Finch AM, Whitmore JB, Short AJ, Wong AK, Monk PN, Cain SA, Fairlie DP, Taylor SM. (**1999**) Pharmacological characterization of antagonists of the C5a receptor. Br J Pharmacol. 1999 Dec;128(7):1461-6.

Petrache I, Birukova A, Ramirez SI, Garcia JG, Verin AD. (**2003**) The role of the microtubules in tumor necrosis factor-alpha-induced endothelial cell permeability. Am J Respir Cell Mol Biol. 2003 May;28(5):574-81.

Pio R, Martinez A, Unsworth EJ, Kowalak JA, Bengoechea JA, Zipfel PF, Elsasser TH, Cuttitta F (**2001)** Complement factor H is a serum-binding protein for adrenomedullin, and the resulting complex modulates the bioactivities of both partners. J Biol Chem 276:12292–12300

Qiao J, Huang F, Lum H. (**2003**) PKA inhibits RhoA activation: a protection mechanism against endothelial barrier dysfunction. Am J Physiol Lung Cell Mol Physiol. 2003 Jun;284(6):L972-80.

Rich TC, Fagan KA, Nakata H, Schaack J, Cooper DM, Karpen JW. (**2000**) Cyclic nucleotide-gated channels colocalize with adenylyl cyclase in regions of restricted cAMP diffusion. J Gen Physiol. 2000 Aug;116(2):147-61.

Saitoh M, Ishikawa T, Matsushima S, Naka M, Hidaka H. (**1987**) Selective inhibition of catalytic activity of smooth muscle myosin light chain kinase. J Biol Chem. 1987 Jun 5;262(16):7796-801

Sandoval R, Malik AB, Naqvi T, Mehta D, Tiruppathi C. (**2001**) Requirement for Ca2+ signaling in the mechanism of thrombin-induced increase in endothelial permeability. Am J Physiol Lung Cell Mol Physiol. 2001 Feb;280(2):L239-47.

Sato K, Hirata Y, Imai T, Iwashina M, Marumo F. (**1995**) Characterization of immunoreactive adrenomedullin in human plasma and urine. Life Sci. 1995;57(2):189-94.

Saito H, Minamiya Y, Kitamura M, Saito S, Enomoto K, Terada K, Ogawa J. (**1998**) Endothelial myosin light chain kinase regulates neutrophil migration across human umbilical vein endothelial cell monolayer. J Immunol. 1998 Aug 1;161(3):1533-40.

Saito Y, Nakagawa C, Uchida H, Sasaki F, Sakakibara H. (**2001**) Adrenomedullin suppresses fMLP-induced upregulation of CD11b of human neutrophils. Inflammation. 2001 Jun;25(3):197-201.

Sayner SL. (**2011**) Emerging themes of cAMP regulation of the pulmonary endothelial barrier. Am J Physiol Lung Cell Mol Physiol. 2011 May;300(5):L667-78.

Schnittler HJ, Wilke A, Gress T, Suttorp N, Drenckhahn D. (**1990**) Role of actin and myosin in the control of paracellular permeability in pig, rat and human vascular endothelium. J Physiol. 1990 Dec;431:379-401.

Schnoor M, Lai FP, Zarbock A, Kläver R, Polaschegg C, Schulte D, Weich HA, Oelkers JM, Rottner K, Vestweber D. (**2011**) Cortactin deficiency is associated with reduced neutrophil recruitment but increased vascular permeability in vivo. J Exp Med. 2011 Aug 1;208(8):1721-35.

Sehrawat S, Cullere X, Patel S, Italiano J Jr, Mayadas TN. (**2008**) Role of Epac1, an exchange factor for Rap GTPases, in endothelial microtubule dynamics and barrier function. Mol Biol Cell. 2008 Mar;19(3):1261-70.

Seybold J, Thomas D, Witzenrath M, Boral S, Hocke AC, Bürger A, Hatzelmann A, Tenor H, Schudt C, Krüll M, Schütte H, Hippenstiel S, Suttorp N. (**2005**) Tumor necrosis factor-alpha-dependent expression of phosphodiesterase 2: role in endothelial hyperpermeability. Blood. 2005 May 1;105(9):3569-76.

Shasby DM, Shasby SS, Sullivan JM, Peach MJ. (**1982**) Role of endothelial cell cytoskeleton in control of endothelial permeability. Circ Res. 1982 Nov;51(5):657-61.

Sheppard FR, Kelher MR, Moore EE, McLaughlin NJ, Banerjee A, Silliman CC. (**2005**) Structural organization of the neutrophil NADPH oxidase: phosphorylation and translocation during priming and activation. J Leukoc Biol. 2005 Nov;78(5):1025-42.

Shimekake Y, Nagata K, Ohta S, Kambayashi Y, Teraoka H, Kitamura K, Eto T, Kangawa K, Matsuo H. (**1995**) Adrenomedullin stimulates two signal transduction pathways, cAMP accumulation and Ca2+ mobilization, in bovine aortic endothelial cells. J Biol Chem. 1995 Mar 3;270(9):4412-7.

Shindo T, Kurihara H, Maemura K, Kurihara Y, Kuwaki T, Izumida T, Minamino N, Ju KH, Morita H, Oh-hashi Y, Kumada M, Kangawa K, Nagai R, Yazaki Y. (**2000**) Hypotension and resistance to lipopolysaccharide-induced shock in transgenic mice overexpressing adrenomedullin in their vasculature. Circulation 101(19):2309-16.

Smith CW. (**1993**) Endothelial adhesion molecules and their role in inflammation. Can J Physiol Pharmacol. 1993 Jan;71(1):76-87. Review.

Sollevi A & **Fredholm** BB. (**1981**) Role of adenosine in adipose tissue circulation. Acta Physiol Scand. 1981 Jul;112(3):293-8.

Springer TA. (**1994**) Traffic signals for lymphocyte recirculation and leukocyte emigration: the multistep paradigm. Cell. 1994 Jan 28;76(2):301-14.

Stelzner TJ, Weil JV, O'Brien RF. (**1989**) Role of cyclic adenosine monophosphate in the induction of endothelial barrier properties. J Cell Physiol. 1989 Apr;139(1):157-66.

Su AI, Cooke MP, Ching KA, Hakak Y, Walker JR, Wiltshire T, Orth AP, Vega RG, Sapinoso RM, Mogrich A, Patapoutian A, Hampton GM, Schultz PG, Hogenesch JB (**2002**) Large-scale analysis of the human and mouse transcriptomes. Proc Natl Acad Sci USA 99:4465–4470

Suzuki Y, Horio T, Hayashi T, Nonogi H, Kitamura K, Eto T, Kangawa K, Kawano Y. (**2004**) Plasma adrenomedullin concentration is increased in patients with peripheral arterial occlusive disease associated with vascular inflammation. Regul Pept. 2004 Apr 15;118(1-2):99-104.

Szokodi I, Kinnunen P, Tavi P, Weckström M, Tóth M, Ruskoaho H. (**1998**) Evidence for cAMP-independent mechanisms mediatingthe effects of adrenomedullin,anew inotropic peptide. Circulation 1998; 97: 1062–1070.

Takai Y & **Nakanishi** H. (**2003**) Nectin and afadin: novel organizers of intercellular junctions. J Cell Sci. 2003 Jan 1;116(Pt 1):17-27. Review.

Tam C, Brain SD. (**2004**) The assessment of vasoactive properties of CGRP and adrenomedullin in the microvasculature: a study using in vivo and in vitro assays in the mouse. JMol Neurosci 2004; 22: 117–124.

Tao W, Shu YS, Miao QB, Zhu YB. (**2012**) Attenuation of hyperoxia-induced lung injury in rats by adrenomedullin. Inflammation. 2012 Feb;35(1):150-7.

Temmesfeld-Wollbruck B, Brell B, Davidl,etal. (**2007**) Adrenomedullin reduces vascularhyperperme ability and improvessurvivalinrat septicshock. Intensive CareMed 2007; 33: 703–710.

Tilghman RW & **Hoover** RL. (**2002**) The Src-cortactin pathway is required for clustering of E-selectin and ICAM-1 in endothelial cells. FASEB J. 2002 Aug;16(10):1257-9.

Tiruppathi C, Minshall RD, Paria BC, Vogel SM, Malik AB. (**2002**) Role of Ca2+ signaling in the regulation of endothelial permeability. Vascul Pharmacol. 2002 Nov;39(4-5):173-85.

van Nieuw Amerongen GP & **van Hinsbergh** VW. (**2001**) Cytoskeletal effects of rho-like small guanine nucleotide-binding proteins in the vascular system. Arterioscler Thromb Vasc Biol. 2001 Mar;21(3):300-11.

Vandenbroucke E, Mehta D, Minshall R, Malik AB. (**2008**) Regulation of endothelial junctional permeability. Ann N Y Acad Sci. 2008 Mar;1123:134-45.

Verin AD, Birukova A, Wang P, Liu F, Becker P, Birukov K, Garcia JG. (**2001**) Microtubule disassembly increases endothelial cell barrier dysfunction: role of MLC phosphorylation. Am J Physiol Lung Cell Mol Physiol. 2001 Sep;281(3):L565-74.

Verin AD, Patterson CE, Day MA, Garcia JG. (**1995**) Regulation of endothelial cell gap formation and barrier function by myosin-associated phosphatase activities. Am J Physiol. 1995 Jul;269(1 Pt 1):L99-108.

Vestweber D & **Blanks** JE. (**1999**) Mechanisms that regulate the function of the selectins and their ligands. Physiol Rev 79, 181-213.

Vestweber D. (**2007**) Adhesion and signaling molecules controlling the transmigration of leukocytes through endothelium. Immunol Rev. 2007 Aug;218:178-96.

Vestweber, D. (**2008**) VE-Cadherin: The Major Endothelial Adhesion Molecule Controlling Cellular Junctions and Blood Vessel Formation, vol. 28, pp. 223-232.

Vestweber D, Winderlich M, Cagna G, Nottebaum AF. (**2009**) Cell adhesion dynam-ics at endothelial junctions: VE-cadherin as a major player. Trends Cell Biol. 19(1):8-15.

Vouret-Craviari V, Bourcier C, Boulter E, van Obberghen-Schilling E. (**2002**) Distinct signals via Rho GTPases and Src drive shape changes by thrombin and sphingosine-1-phosphate in endothelial cells. J Cell Sci. 2002 Jun 15;115(Pt 12):2475-84.

Wallez Y & **Huber** P. (**2008**) Endothelial adherens and tight junctions in vascular homeostasis, inflammation and angiogenesis. Biochim Biophys Acta. 2008 Mar;1778(3):794-809.

Wang P. (**2001**) Andrenomedullin and cardiovascularresponses in sepsis. Peptides 2001; 22: 1835–1840.

Wang S, Voisin MB, Larbi KY, Dangerfield J, Scheiermann C, Tran M, Maxwell PH, So-rokin L, Nourshargh S. (**2006**) Venular basement membranes contain specific matrix protein low expression regions that act as exit points for emigrating neutrophils. J Exp Med. 2006 Jun 12;203(6):1519-32.

Watanabe H, Kuhne W, Schwartz P, and Piper HM. (**1992**) A2-adenosine receptor stimulation increases macromolecule permeability of coronary endothelial cells. Am J Physiol Heart Circ Physiol 262: H1174–H1181, 1992.

Westphal M, Sander J, Van Aken H, Ertmer C, Stubbe HD, Booke M. (**2006**) Role of adrenomedullin in the pathogenesis and treatment of cardiovascular dysfunctions and sepsis. Anaesthesist. 2006 Feb;55(2):171-8.

Wimalawansa SJ (**1997**) Amylin, calcitonin gene-related peptide, calcitonin, and adrenomedullin: a peptide superfamily. Crit Rev Neurobiol 11:167–239

Wittchen ES, Worthylake RA, Kelly P, Casey PJ, Quilliam LA, Burridge K. (**2005**) Rap1 GTPase inhibits leukocyte transmigration by promoting endothelial barrier function. J Biol Chem. 2005 Mar 25;280(12):11675-82.

Wittchen ES. (**2009**) Endothelial signaling in paracellular and transcellular leukocyte transmigration. Front Biosci. 2009 Jan 1;14:2522-45. Review.

Wojciak-Stothard B & **Ridley** AJ. (**2002**). Rho GTPases and the regulation of endothelial permeability. Vascular Pharmacology 39, 187-199.

Wu R, Dong W, Qiang X, Ji Y, Cui T, Yang J, Zhou M, Blau S, Marini CP, Ravikumar TS, Wang P. (**2008**) Human vasoactive hormone adrenomedullin and its binding protein rescue experimental animals from shock. Peptides. 2008 Jul;29(7):1223-30.

Wunder F, Rebmann A, Geerts A, Kalthof B. (**2008**) Pharmacological and kinetic characterization of adrenomedullin 1 and calcitonin gene-related peptide 1 receptor reporter cell lines. Mol Pharmacol. 2008 Apr;73(4):1235-43.

Xing J & **Birukova** AA. (**2010**) ANP attenuates inflammatory signaling and Rho pathway of lung endothelial permeability induced by LPS and TNFalpha. Microvasc Res. 2010 Jan;79(1):56-62.

Yamaga J, Hashida S, Kitamura K, Tokashiki M, Aoki T, Inatsu H, Ishikawa N, Kangawa K, Morishita K, Eto T. (**2003**) Direct measurement of glycine-extended adrenomedullin in plasma and tissue using an ultrasensitive immune complex transfer enzyme immunoassay in rats. Hypertens Res. 2003 Feb;26 Suppl:S45-53.

Yang S, Zhou M, Chaudry IH, Wang P. (**2002**) Novel approach to prevent the transition from the hyperdynamic phase to the hypodynamic phase of sepsis: role of adrenomedullin and adrenomedullin binding protein-1. Ann Surg. 2002 Nov;236(5):625-33.

Yang L, Kowalski JR, Yacono P, Bajmoczi M, Shaw SK, Froio RM, Golan DE, Thomas SM, Luscinskas FW. (**2006a**) Endothelial cell cortactin coordinates intercellular adhesion molecule-1 clustering and actin cytoskeleton remodeling during polymorphonuclear leukocyte adhesion and transmigration. J Immunol. 2006 Nov 1;177(9):6440-9.

Yang L, Kowalski JR, Zhan X, Thomas SM, Luscinskas FW. (**2006b**) Endothelial cell cortactin phosphorylation by Src contributes to polymorphonuclear leukocyte transmigration in vitro. Circ Res. 2006 Feb 17;98(3):394-402.

Yang J, Wu R, Zhou M, Wang P. (**2010**) Human adrenomedullin and its binding protein ameliorate sepsis-induced organ injury and mortality in jaundiced rats. Peptides. 31(5):872-7.

Yoshioka K, Sugimoto N, Takuwa N, Takuwa Y. (**2007**) Essential role for class II phosphoinositide 3-kinase alpha-isoform in Ca2+-induced, Rho- and Rho kinase-dependent regulation of myosin phosphatase and contraction in isolated vascular smooth muscle cells. Mol Pharmacol. 2007 Mar;71(3):912-20.

Yuan Y, Huang Q, Wu HM. (**1997**) Myosin light chain phosphorylation: modulation of basal and agonist-stimulated venular permeability. Am J Physiol. 1997 Mar;272(3 Pt 2):H1437-43.

Yuan SY. (**2002**) Protein kinase signaling in the modulation of microvascular permeability. Vascul Pharmacol. 2002 Nov;39(4-5):213-23
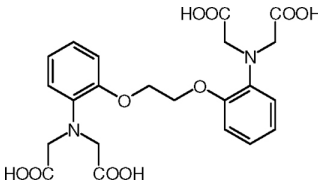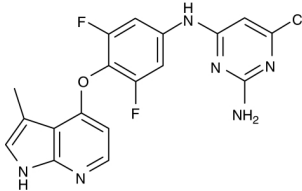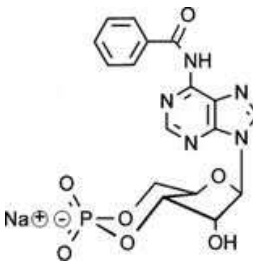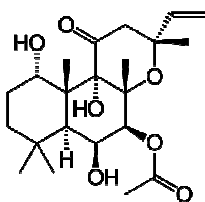
Yuan SY, Shen Q, Rigor RR, Wu MH. (**2012**) Neutrophil transmigration, focal adhesion kinase and endothelial barrier function. Microvasc Res. 2012 Jan;83(1):82-8.

Zhou M, Chaudry IH, Wang P. (**2001**) The small intestine is an important source of adrenomedullin release during polymicrobial sepsis. Am J Physiol Regul Integr Comp Physiol 2001; 281: R654-R660.

Zudaire E, Portal-Nunez S, Cuttitta F. (**2006**) The central role of adrenomedullin in host defense. J Leukoc Biol 2006; 80: 237–244.

Zufall F, Shepherd GM, Barnstable CJ. (**1997**) Cyclic nucleotide gated channels as regulators of CNS development and plasticity. Curr Opin Neurobiol. 1997 Jun;7(3):404-12.

8. APPENDIX

Compounds	Function	Structure
BAPTA/AM	*Intracellular calcium chelator*	[1,2-Bis(2-aminophenoxy)ethane-N,N,N,N'-tetraacetic acid tetrakis(acetoxymethyl ester)]
BAY77-7549	*Rho kinase inhibitor*	[6-chloro-N4-{3,5-difluoro-4-[(3-methyl-1H-pyrrolo[2,3-b]pyridin-4-yl)oxy]-phenyl}pyrimidine-2,4-diamine]
Benz-cAMP	*PKA activator*	[N(6)-benzoyl-adenosine-3',5'-cyclic monophosphate]
FSK (forskolin)	*Adenylate cyclase*	[(3*R*, 4a*R*, 5*S*, 6*S*, 6a*S*, 10*S*, 10a*R*, 10b*S*)-6,10,10b-trihydroxy-3,4a,7,7,10a-pentamethyl-1-oxo-3-vinyldodecahydro-1*H*-benzo[*f*]chromen-5-yl acetate]

IBMX	*Unspecific PDE inhibitor*	[3-Isobutyl-1-methylxanthine]
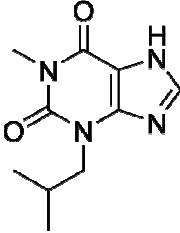
ML-9	*MLCK inhibitor*	[1-(5-Chloronaphthalene-1-sulfonyl)-1H-hexahydro-1,4-diazepine hydrochloride]
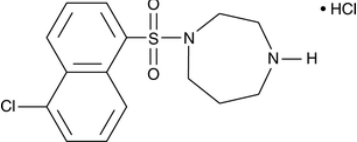
Rp-8-Br-cAMP	*PKA-inhibitor*	[8- Bromoadenosine- 3', 5'- cyclic monophosphorothioate, Rp- isomer]
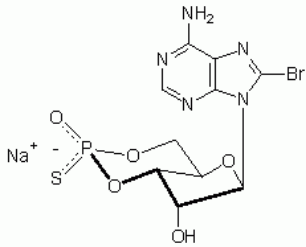
W54011	*C5a antagonist*	[N-((4-Dimethylaminophenyl)methyl)-N-(4-isopropylphenyl)-7-methoxy-1,2,3,4-tetrahydronaphthalen-1-carboxamide, HCl]
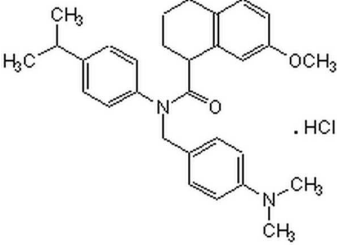
"007"	*Epac/Rap1 activator*	[8-(4-Chlorophenylthio)- 2'- O- methyladenosine-3',5'- cyclic phonophosphate]
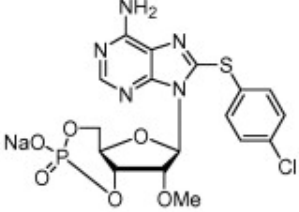
9. ACKNOWLEDGMENTS

First and foremost I would like to express my deepest gratitude to my supervisor PD Dr. Ingo Flamme, for allowing me to pursue my ambitions in the research area and his continuous support and encouragement during my Ph.D. studies. It has been my honor to be his Ph.D. student. I appreciate all of his valuable time and great ideas to make my Ph.D. experience both productive and stimulating. The enthusiasm PD Dr. Flamme exhibited in his research has been a high motivational factor which furthermore made me more embrace the challenging demands and rewarding outcomes of our research work, even during difficult times in finalizing my Ph.D. report.

In addition, I would like to mention that Prof. Dr. Dietmar Vestweber at the Max-Planck institute for biomedicine in Münster, has shown a strong belief in my capabilities and has further been a major motivator by exposing me to the many valuable opportunities working in his lab where I learned the skills and techniques, and his much appreciated guidance towards a successful conclusion of my project.

I would further like to thank the team members of Dr. Flamme, for their much helpful advice in the practical laboratory work.

Last but surely not least, a grateful acknowledgement goes out to Bayer Healthcare without which the funding of my Ph.D. work would not have been possible.

10. ERKLÄRUNG

Ich versichere, dass ich die von mir vorgelegte Dissertation selbständig angefertigt, die benutzten Quellen und Hilfsmittel vollständig angegeben und die Stellen der Arbeit – einschließlich Tabellen, Karten und Abbildungen –, die anderen Werken im Wortlaut oder dem Sinn nach entnommen sind, in jedem Einzelfall als Entlehnung kenntlich gemacht habe; dass diese Dissertation noch keiner anderen Fakultät oder Universität zur Prüfung vorgelegen hat; dass sie – abgesehen von unten angegebenen Teilpublikationen – noch nicht veröffentlicht worden ist sowie, dass ich eine solche Veröffentlichung vor Abschluss des Promotionsverfahrens nicht vornehmen werde. Die Bestimmungen der Promotionsordnung sind mir bekannt. Die von mir vorgelegte Dissertation ist von Priv-Doz. Dr. med. Ingo Flamme betreut worden.

Düsseldorf, den